UNIVERSITY OF CALIFORNIA, SAN DIEGO

Cellular and Molecular Mechanisms for Acid/Base Sensing and Calcification in Corals

A dissertation submitted in partial satisfaction of the requirements for the degree Doctor of Philosophy

in

Marine Biology

by

Megan Elizabeth Barron

Committee in charge:

Martin Tresguerres, Chair
Ronald S. Burton
Lena G. Gerwick
Amro M. Hamdoun
Susan S. Taylor

2018

The Dissertation of Megan Elizabeth Barron is approved, and it is acceptable in quality and form for publication on microfilm and electronically:

_____

_____

_____

_____

_____

Chair

University of California, San Diego

2018

DEDICATION

In recognition of their endless encouragement, love, and support, this dissertation is dedicated to Patricia Barron, Jeffrey Barron, John Barron, Lisa Barron, and Justin Liu.

TABLE OF CONTENTS

Signature Page……..... iii

Dedication……..... iv

Table of Contents……..... v

List of Figures…….. vi

List of Tables……..... viii

Acknowledgements…….. ix

Vita.…….. xi

Abstract of the Dissertation…….. xii

Introduction…….. 1

Introduction: References..... 14

Chapter 1: Soluble adenylyl cyclase in the coral, *Pocillopora damicornis*……..... 20

Chapter 1: References..... 43

Chapter 2: Identification, characterization, and localization of soluble adenylyl cyclase in *Acropora yongei*…….. 46

Chapter 2: References..... 84

Chapter 3: A Na^{+}/Ca^{2+} exchanger in vesicles in coral calcifying cells: revisiting calcification mechanisms……..... 88

Chapter 3: References..... 128

Discussion……..... 134

Discussion: References..... 138

LIST OF FIGURES

Figure 0.1: The four tissue layers in corals surround the coelenteron cavity……. 2

Figure 1.1: Phylogenetic tree of sAC proteins…… 34

Figure 1.2: Alignment of 5'RACE PCR products…….. 35

Figure 1.3: Conserved domains in *P. damicornis* sAC…….. 36

Figure 1.4: Specificity of anti-coral sAC antibodies…….. 39

Figure 1.5: Immunolocalization of sAC in *P. damicornis* tissue……... 40

Figure 1.6: Validation of anti-coral sAC antibodies in *P. damicornis* tissues……... 41

Figure 2.1: 5'RACE products aligned with the *A. digitifera* sAC gene……. 68

Figure 2.2: Alignment of *A. yongei* and *A. digitifera* sAC sequences…… 69

Figure 2.3: Western blot validation of the sAC antibody……. 74

Figure 2.4: cAMP production by coral tissue and aysAC$_{60}$…….. 75

Figure 2.5: Immunofluorescence microscopy…… 76

Figure 2.6: Immunofluorescence microscopy controls indicate the sAC antibody (red fluorescence) is specific…….. 78

Figure 2.7: Immunofluorescence microscopy shows sAC staining (red fluorescence) in the nuclei (Hoechst- blue fluorescence) of *A. yongei* cells……. 79

Figure 2.8: Western blot confirmation of fractionation protocol……... 80

Figure 3.1: Phylogenetic tree of ayNCX$_A$ (A.yongeiNCXA) (highlighted blue) and ayNCX$_{B1-4}$ (A.yongeiNCXB1-4)(highlighted green) with other NCX and NCX-like proteins…… 106

Figure 3.2: Alignment of ayNCX$_B$ sequences…… 108

Figure 3.3: Validation of coral NCX antibody……... 113

Figure 3.4: Immunofluorescence microscopy of *A. yongei* tissue…….. 114

Figure 3.5: Immunofluorescence microscopy controls indicate the NCX antibody (red fluorescence) is specific…….. 115

Figure 3.6: Transmission electron microscopy (TEM) of the calicoblastic epithelium in *A. yongei*…….

Figure 3.7: Sea urchin embryos expressing coral ayNCX$_A$ tagged with fluorescent protein…… 116

Figure 3.8: Sea urchin embryo expressing C-mCherry-ayNCX$_A$ (red fluorescence) ……..... 117

Figure 3.9: Sea urchin embryo expressing C-CFP-ayNCX$_A$ and C-mCherry-ABCC9, an urchin protein localized in vesicles…….... 119

Figure 3.10: Sea urchin embryo expressing C-CFP-ayNCX$_A$ and C-mCherry-ABCB6, an urchin protein localized in the mitochondria……..... 121

Figure 3.11: Mechanism of Ca^{2+} through a cell from the calicoblastic epithelium…… 123

125

LIST OF TABLES

Table 1.1: PCR primers..... 42

Table 1.2: PCR protocols..... 42

Table 2.1: Primers used in RT-PCR, 5'RACE PCR, and sequencing of *A. yongei* sAC.. 81

Table 2.2: Combinations of cofactors tested for HCO_3^- stimulation of recombinant aysAC$_{60}$ 82

Table 2.3: Summary of currently described properties of sAC in marine organisms..... 83

Table 3.1: NCX$_{A/B}$: PCR primers..... 126

Table 3.2: NCX$_{A/B}$: PCR protocols..... 126

Table 3.3: NCX$_A$ cloning with fluorescent protein: PCR primers..... 127

Table 3.4: NCX$_A$ cloning with fluorescent protein: PCR protocol..... 127

ACKNOWLEDGEMENTS

I would like to thank Dr. Martin Tresguerres for his support as the chair of my committee. I could not have asked for a more encouraging and patient advisor. His guidance and revisions have made this dissertation possible. Martin, you have been an amazing mentor and an even better friend these past six years.

I would like to recognize the past and present members of the Tresguerres lab, who have made this journey fun and sometimes a little bit crazy. I am also thankful for the 2011 PhD cohort at Scripps Institution of Oceanography. Without exaggeration, it has been a pleasure getting to know each and every one of you.

I would like to thank Phil Zerofski for his assistance in maintaining healthy corals and urchins in the aquariums in Hubbs Hall at SIO. You saved the corals (and my experiments) on more than one occasion.

The introduction, in part, is a reprint of material as it appears in the following citation: Tresguerres, M., Barott, K. L., Barron, M. E., Deheyn, D. D., Kline, D. I., & Linsmayer, L. B. (2017). Cell Biology of Reef-Building Corals: Ion Transport, Acid / Base Regulation, and Energy Metabolism. *Acid-Base Balance and Nitrogen Excretion in Invertebrates*, 193–218. https://doi.org/10.1007/978-3-319-39617-0. The dissertation author was a coauthor of this book chapter.

Chapter 1, in part, is a reprint of material as it may appear in the following citation: Barott, K. L., Barron, M. E., & Tresguerres, M. (2017). Identification of a molecular pH sensor in coral. *Proceedings of the Royal Society B,* 284, 1–8.201 The dissertation author was a coauthor of this paper.

Chapter 2, in part, is a reprint of material as it may appear in the following citation: Barott, K. L., Helman, Y., Haramaty, L., Barron, M. E., Hess, K. C., Buck, J., Levin, L. R.,

Tresguerres, M. (2013). High adenylyl cyclase activity and in vivo cAMP fluctuations in corals suggest central physiological role. *Scientific Reports, 3* (1379). https://doi.org/10.1038/srep01379. The dissertation author was a coauthor on this paper. Chapter 2, in part, also contains material as it may appear in the following citation: Tresguerres, M., Barott, K. L., Barron, M. E., & Roa, J. N. (2014). Established and potential physiological roles of bicarbonate-sensing soluble adenylyl cyclase (sAC) in aquatic animals. *The Journal of Experimental Biology*, *217*, 663–72. https://doi.org/10.1242/jeb.086157. The dissertation author was a coauthor on this publication.

Chapter 3, in part, is currently being prepared for submission for publication of the material, as it may appear in the following citation: Barron, M. E., Thies, A. B., Espinosa, J. A., Barott, K. L., Hamdoun, A., Tresguerres, M. A Na^{+}/Ca^{2+} exchanger in vesicles in coral calcifying cells: revisiting calcification mechanisms. The dissertation author was the primary investigator and primary author of this material.

This work was supported by the National Science Foundation (NSF) EF-1220641 to Martin Tresguerres, the NSF Graduate Research Fellowship to Megan Barron, and the University of California Regents Fellowship to Megan Barron.

VITA

Education

Scripps Institution of Oceanography, University of California San Diego 2011-2018
PhD, Marine Biology

Scripps Institution of Oceanography, University of California San Diego 2014
MS, Oceanography

University of Virginia 2011
BS, Biology; Minor in French Language and Literature

Awards & Fellowships

Scripps Institution of Oceanography: Outstanding Teaching Assistant 2016-2017
National Science Foundation Graduate Research Fellowship (GRFP) 2012-2015
University of California Regents Graduate Fellowship 2011

Publications

Barron, M.E., Thies, A.B., Espinoza, J.A., Barott, K.L., Hamdoun, A., Tresguerres, M. (in review). A Na^+/Ca^{2+} exchanger in vesicles in coral calcifying cells suggests an intracellular calcification mechanism.

Barott, K.L., **Barron, M.E.**, & Tresguerres, M. (2017). Identification of a molecular pH sensor in coral. Proceedings of the Royal Society B, 284, 1–8.

Tresguerres, M., Barott, K.L., **Barron, M.E.**, Deheyn, D.D., Kline, D.I., and Linsmayer, L.B. (2017) Cell biology of reef-building corals. Ion transport, acid/base regulation, and energy metabolism. In "Acid-base balance and nitrogen excretion in invertebrates - Mechanisms and strategies in various invertebrate groups with considerations of challenges caused by ocean acidification" M O'Donnell and D Weihrauch (eds), Springer, Germany.

Tresguerres, M., Barott, K.L., **Barron, M.E.** and Roa, J.B. (2014). Established and potential physiological roles of bicarbonate-sensing soluble adenylyl cyclase (sAC) in aquatic animals. Journal of Experimental Biology. 217:663-672. 10.1242/jeb.086157

Barott, K.L., Helman, Y., Haramaty, L., **Barron, M.E.**, Hess, K.C., Buck, J., Levin, L.R. and Tresguerres, M. (2013). High adenylyl cyclase activity and in vivo cAMP fluctuations in corals suggests central physiological role. Sci Rep 3, 1379.

ABSTRACT OF THE DISSERTATION

Cellular and Molecular Mechanisms for Acid/Base Sensing and Calcification in Corals

by

Megan Elizabeth Barron

Doctor of Philosophy in Marine Biology

University of California, San Diego, 2018

Professor Martin Tresguerres, Chair

Coral reefs are highly diverse marine ecosystems that are built upon the calcium carbonate skeletons of coral colonies. Despite their great ecological importance, very little is known about corals at the cellular and molecular level. More specifically, the mechanisms behind acid/base sensing and calcification in corals have yet to be determined. Therefore, for my dissertation research I identified and investigated an enzyme and an ion transporter potentially involved in these processes.

Chapters 1 and 2 of my dissertation focus on the acid/base sensor soluble adenylyl cyclase (sAC) in the corals *Pocillopora damicornis* and *Acropora yongei*. sAC is stimulated by HCO_3^- to produce the ubiquitous second messenger, cyclic adenosine monophosphate (cAMP),

which may play a role in regulating internal pH through a number of signaling pathways. I have identified multiple sAC transcripts, which undergo alternative splicing, in both species, and have localized sAC protein to all four tissue layers in corals. These findings represent the first molecular evidence for sAC in a coral species.

Chapter 3 of my dissertation focuses on the sodium calcium exchanger (NCX), an ion transporter that typically exports one Ca^{2+} ion from the cell for every three Na^{+} ions that it imports. NCX has been implicated in bone calcification in some mammals and birds. I identified a potential NCX protein in *Acropora yongei* and cloned five distinct splice variants. Immunofluorescence microscopy indicated NCX protein is found in intracellular vesicles within the calicoblastic epithelium, the thin tissue directly involved in calcification of the coral skeleton. This vesicular localization was confirmed by expression of recombinant, fluorescently-tagged coral NCX protein in sea urchin embryos. Based on my findings, I have proposed a new model for coral calcification in which NCX in the membranes of vesicles sequesters Ca^{2+} ions from the cytoplasm, preventing negative impacts on Ca^{2+} signaling, and delivers Ca^{2+} to the site of calcification.

Together, this research helps us better understand the basic cell biology and physiology of marine organisms, improving current models for acid/base sensing and calcification in marine calcifiers such as corals.

INTRODUCTION

Coral cell biology

Corals reefs are biodiverse ecosystems that are economically and ecologically important on a global scale (Knowlton et al., 2006; Moberg & Folke, 1999; Spurgeon, 1992). At the core of these ecosystems are the reef-building corals, or hermatypic corals, which deposit calcium carbonate in the form of aragonite to build skeletons forming the foundation of the reef (Schuhmacher & Zibrowius, 1985). The research contained in this dissertation focuses on two zooxanthellate, or symbiont-containing, hermatypic coral species: *Pocillopora damicornis* and *Acropora yongei*. Both species are considered "stony corals" and are taxonomically classified within the order *Scleractinia*; however, the two species belong to different families: *Pocilloporidae* and *Acroporidae*, respectively. These families are members of two distinct clades of corals, the Robust (includes *P. damicornis*) and Complex (includes *A. yongei*), which are predicted to have diverged from one another approximately 300-450 million years ago (Romano & Cairns, 2000; Romano & Palumbi, 1996; Stolarski et al., 2011). These two clades exhibit different characteristics in their method of asexual reproduction and the properties of their skeletons. Robust corals demonstrate intratentacular budding when they asexually reproduce and have more heavily calcified skeletons, while Complex corals exhibit extratentacular budding during asexual reproduction and have skeletons that are less calcified and more porous (Wijsman-Best 1975; Veron, 1993).

Despite their differences in evolutionary history, *P. damicornis* and *A. yongei* have the same basic tissue structure which is shared among all coral species. Like all *Cnidarians*, corals are diploblastic, containing an ectodermis and endodermis (in this dissertation, also referred to as gastrodermis) tissue surrounding a body cavity called the coelenteron. From the seawater and

moving in the direction of the skeleton, the tissues/cavity are organized in the following order: the oral ectodermis, oral endodermis (gastrodermis), coelenteron, aboral endodermis (gastrodermis) and the aboral ectodermis (commonly called the calicoblastic epithelium). A diagram of these tissue layers is shown here as Figure 0.1.

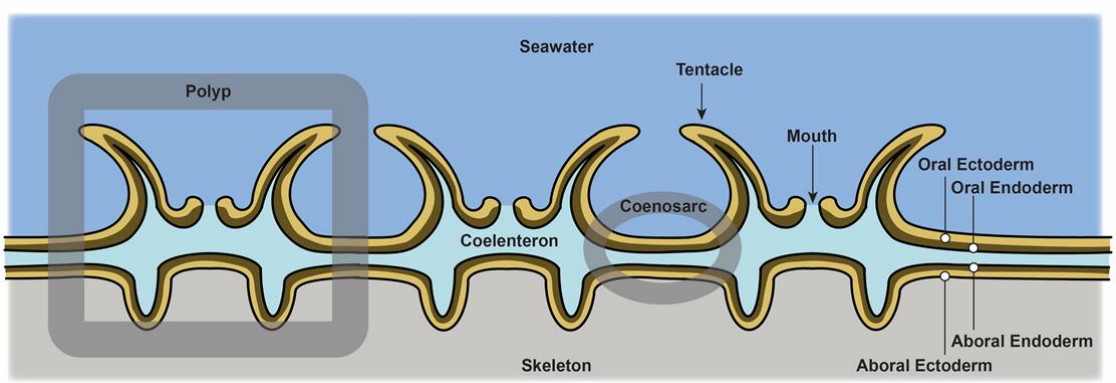

Figure 0.1: The four tissue layers in corals surround the coelenteron cavity (Tresguerres et al., 2017).

Each coral tissue layer accomplishes distinct physiological roles. The oral ectodermis is the interface with the environment and exchanges ions and other molecules with seawater. This tissue also contains specialized cells called nematocysts, which are involved in protection and predation for heterotrophic nutrition. The oral and aboral gastrodermis tissue is unique in its ability to host endosymbiotic dinoflagellates from the genus *Symbiodinium*. These photosynthetic algae are capable of producing sugars that supply the coral with an additional source of energy. Depending on the coral species, depth, and even on the time of year, corals may rely minimally or almost entirely on zooxanthellae for their nutritional needs (Goreau et al., 1971). An important aspect of this symbiotic relationship is the effect it has on intracellular pH (pHi) in gastrodermal cells and the surrounding tissues and cavity. pHi within coral tissues is described below and the identification and characterization of an acid/base sensor called soluble adenylyl cyclase (sAC) is the main subject of Chapter 1 and Chapter 2 in this dissertation. Finally, the calicoblastic epithelium, a thin tissue layer composed of overlayed calicoblastic cells containing abundant

vesicles (Johnston, 1980), is located above the skeleton and is responsible for ion transport and regulation of the subcalicoblastic media (SCM) where calcification occurs. The SCM is tightly regulated, although the exact mechanisms for the delivery of the two major components of the skeleton: Ca^{2+} and CO_3^{2-} (or related form of DIC) are unknown. Ca^{2+} transport within coral tissues is also introduced below, and the identification and localization of a Na^+/Ca^{2+} Exchanger (NCX) in coral is the topic of Chapter 3. For a comprehensive review on coral cell biology, please refer to Tresguerres et al., 2017.

pHi in coral tissues

Many cells in the gastrodermal tissue face pH challenges related to hosting one or more photosynthetic algal cells within their membranes, and there are observable differences in pHi regulation for gastrodermal cells containing zooxanthellae versus those without symbionts. In the coral *Stylophora pistillata,* gastrodermal cells containing zooxanthellae have a significantly higher pHi after a 20 minute long "light" exposure (~7.41) compared with those incubated in the dark for the same amount of time (~7.13) (Venn et al., 2009). Furthermore, inhibition of photosynthesis using the pharmacological drug DCMU prevents such light-induced increases of pHi from occurring in isolated symbiocytes from *S. pistillata* (Laurent et al., 2013). A proposed explanation is that at increased irradiance, when photosynthesis is occurring near its maximum rate, the depletion of CO_2 occurs more rapidly within the zooxanthellae. As CO_2 is removed from the host cytoplasm the DIC equilibrium adjusts by converting HCO_3^- to CO_2 and H_2O, removing H^+ ions from the cytoplasm and leading to the alkalization of the host coral cell (Allemand et al., 1998; Laurent et al., 2013). This photosynthesis-driven cell alkalization may also help counteract cellular acidosis caused by exposure to high CO_2 / low external pH (pHe) conditions (Gibbin et al., 2014). The photosynthetic consumption of CO_2 by zooxanthellae and coral host cells, and the

subsequent alkalization of coral pHi does not continue indefinitely. In irradiated cells from *S. pistillata*, mechanisms for counteracting alkalization occur within 20 minutes (Laurent et al., 2013), but the mechanisms behind maintaining homeostasis are unknown. Potentially, to prevent pHi from rising further, coral cells could increase the excretion of OH^- ions and/or increase the uptake H^+ ions. In anemone, light-incubated endoderm cell layers excrete OH^- into the coelenteron (Furla et al., 1998). Similarly, in the coral *Galaxea fascicularis* the coelenteron is more alkaline (~8.19) during light conditions compared with during the dark (~7.61) (Al-Horani et al., 2003). However, before we can determine the putative ion transportation involved, we must first ask: how do coral sense these dark/light induced changes in pH, which occur daily, at the molecular level?

pHi in the calicoblastic epithelium is more resistant to light/dark fluctuation. A study using the intracellular pH dye SNARF-1 AM measured pHi in *S. pistillata* calicoblastic cells grown on glass coverslips. The pHi in calicoblastic cells, regardless of whether they were incubated in light or dark conditions, was determined to be ~7.4 (Venn et al., 2011; Venn et al., 2009). Interestingly, pHe of the subcalicoblastic media does vary with the day/night cycle. Using a pH microsensor, pHe was measured in the subcalicoblastic fluid of the coral *G. fascicularis* during both light and dark conditions. The calcifying fluid was found to alkalize up to ~pH 9.28 under light conditions, compared with ~8.13 in the dark (seawater pH was 8.2) (Al-Horani et al., 2003). Similarly, pHe of the subcalicoblastic fluid measured using SNARF-1 in *S. pistillata*, was elevated in both light (8.69) and dark (8.36) conditions when compared to seawater (pH 8.15) (Venn et al., 2011). Once again, we must ask, how do corals sense and maintain stable pH in the calicoblastic epithelium? How do calicoblastic cells modify the pH of the subcalicoblastic epithelium to create basic conditions that facilitate calcification?

This dissertation proposes that soluble adenylyl cyclase (sAC) acts as a pH sensor in coral tissues. To facilitate understanding in the research chapters, this introduction includes a section specifically on sAC (below).

Soluble adenylyl cyclase: a conserved pH sensor

Cellular mechanisms for maintaining an optimal intracellular pH are ubiquitous among biological systems, as pH regulation at the cellular level is vital to an organism's overall health and survival. The acid/base status depends not only on the concentration of protons (H^+ ions, pH) in intra- and extracellular fluids, but on the concentrations of carbon dioxide (CO_2) and bicarbonate (HCO_3^-) as well. These three molecules exist in constant equilibrium with one another, and as a result, H^+, CO_2, and HCO_3^- can all act as a proxy for pH sensing in homoeostatic mechanisms regulating pHi (revewied in Tresguerres et al., 2010a).

Soluble adenylyl cyclase (sAC) is a source of the ubiquitous second messenger, cyclic adenosine monophosphate (cAMP); sAC activity is stimulated by HCO_3^-, rendering sAC a physiological sensor of CO_2/pH/HCO_3^- in cells (Buck et al., 1999; Chen et al., 2000). The mammalian gene encoding sAC contains two heterologous, catalytic domains (designated "C1" and "C2") that are highly homologous to sAC-like genes found in cyanobacteria, supporting the hypothesis that sAC is an evolutionarily conserved CO_2/pH/HCO_3^- sensor (Buck et al., 1999; Chen et al., 2000; Steegborn et al., 2005b). Indeed, sAC- regulated responses to acid/base disturbances have been discovered in diverse organisms such as sea urchins, oysters, sharks, rays and humans (Beltran et al., 2007; Pastor-Soler et al., 2003; Roa & Tresguerres, 2016; Tresguerres et al., 2010b; Wang et al., 2016). Moreover, sAC sequences/orthologs are found in the genomes and transcriptomes of organisms representing an even greater diversity of phyla: poriferans,

placozoans, hemichordates, molluscs, cnidarians, tunicates, vertebrates (including bony and cartilaginous fishes and reptiles) (Tresguerres et al., 2014).

HCO_3^--stimulated activation of sAC requires a combination of divalent cation cofactors including Mg^{2+}, Mn^{2+} and Ca^{2+}. All sAC proteins are stimulated by Mg^{2+} but the second cofactor responsible for stimulation is variable (Tresguerres et al., 2014). For example, while Ca^{2+} acts as a cofactor for mammalian sAC (Chen et al., 2000; Zippin et al., 2001; Litvin et al., 2003; reviewed in Tresguerres et al., 2014), dogfish sAC seems to require Mn^{2+} in micromolar amounts (Tresguerres et al., 2010b). In addition, millimolar Mn^{2+} has a large stimulatory effect by itself on sACs from all organisms studied thus far, and in fact it was Mn^{2+}-stimulated cAMP activity in rat testes that lead to the discovery of sAC in the first place (Braun & Dods, 1975). The mechanism behind HCO_3^- stimulation of sAC has been determined using the related cyanobacteria adenylyl cyclase, CyaC, as a model (Steegborn et al., 2005b). In CyaC, an open adenylyl cyclase state has Ca^{2+} bound to the first ion-binding site, which mediates the binding of ATP. HCO_3^- increases the catalytic rate by inducing the active site to close and by recruiting a second catalytic ion. This recruitment causes the phosphates of the bound substrate (ATP) to rearrange, facilitating the formation and release of cAMP (Steegborn et al., 2005b). This mechanism was confirmed and elaborated upon more recently from the crystal structure of human sAC, which determined that HCO_3^- binds adjacent to the amino acid Arg176, which acts as a switch to enable the formation of the catalytic cation sites (Kleinboelting et al., 2014).

An additional source of cAMP in cells are the transmembrane adenylyl cyclases (tmACs), which as their name suggests, span the plasma membrane to respond to extracellular signals (Hanoune & Defer, 2001). Although tmACs and sAC are similar in their general structures- tmACs also have C1/C2 domains that form their catalytically active center- they are encoded by unrelated genes and regulated by different signals (Linder, 2006). tmACs are

regulated by G-protein coupled receptors, allowing them to mediate responses to extern al stimuli such as neurotransmitters, hormones, autacoids, and light (Taussig & Gilman, 1995). tmACs are not stimulated by HCO_3^- and conversely, sAC is insensitive to activity by G-proteins (Buck et al., 1999). Comparing the sequences of sAC and tmACs can help identify the genetic basis behind the unique features of sAC; for example, a threonine or serine residue that is conserved in HCO_3^--responsive sACs is replaced by a conserved aspartate in HCO_3^--insensitive bacterial ACs and tmACs, suggesting this amino acid plays an important role in determining HCO_3^- -stimulation (Cann et al., 2003; Steegborn et al., 2005b).

Even among sAC proteins, amino acid differences are reflected biochemically. Recent crystallization of the human sAC protein indicates HCO_3^- binds between lysine 95 and arginine 175; mutagenesis of the lysine for an alanine eliminates HCO_3^--stimulated activity, suggesting this lysine is another key residue in determining HCO_3^- sensitivity (Kleinboelting et al., 2014) . Such findings could account for the differences in half maximal (EC_{50}) values for HCO_3^- observed between mammalian sAC (~20 mM) and dogfish sAC (~5 mM), where an asparagine replaces lysine at this position (Chen et al., 2000; Litvin et al., 2003; Tresguerres, 2014).

Methods for distinguishing between cAMP produced by tmACs and cAMP produced by sAC are invaluable to identifying and describing physiological proceses involving either protein. Such tools include pharmacological drugs that stimulate or inhibit one or both of types of ACs. For example, production of cAMP by mammalian sAC is inihibited by the small molecule KH7 (Hess et al., 2005), which later was confirmed to also inhibit sAC from sea urchin, dogfish shark, and ray (Beltran et al., 2007; Roa & Tresguerres, 2016; Tresguerres et al., 2010b). Other pharmacological drugs include sAC-selective inhibitors that are derivatives of catechol estrogen (e.g. 2CE, 4CE) and LRE1 (Ramos-Espiritu et al., 2016), and a tmAC-specific inhibitor 2',5'-dideoxyadenosine (or 'P-sites', named after the site it blocks) (Steegborn et al., 2005a; reviewed

in Tresguerres et al., 2011). There are no identified pharmacological stimulators of sAC, and one known tmAC-specific sitmulator in vertebrates, Forskolin, has been confirmed to not affect mammalian sAC activity (Buck et al., 1999; Seamon et al., 1981). Recent experimental findings showed forskolin does not affect cAMP production in coral homogenates (Barott et al., 2013), and previous studies have reported that Forskolin is not a reliable tmAC-stimulator in invertebrates (Awad & Anctil, 1993; Galliot et al., 1995; Garbers & Kopf, 1980).

cAMP activates Protein Kinase A (PKA)-dependent phosphorylation in target proteins, giving cAMP and potentially sAC control over a number of diverse cellular processes (Wong & Scott, 2004). Additional targets of cAMP include nucleotide-gated channels and exchange protein activated by cAMP (EPACs) (reviewed in Cooper, 2003; Zaccolo et al., 2006; Tresguerres et al., 2011). sAC is able to effect control over multiple physiological process concurrently due to the creation of "microdomains" containing PKA and phosphodiesterases (PDEs), which break down cAMP and help regulate the longevity of cAMP signals, anchored to a specific subcellular localization by A-Kinase Anchoring Proteins (AKAPs) (Cooper, 2003; Tresguerres et al., 2011; Wong & Scott, 2004; Zaccolo et al., 2006; Zippin et al., 2003). sAC proteins and activity have been found in the cytoplasm as well as in subcellular compartments such as mitochondria, centrioles, mitotic spindles, mid-bodies, and nuclei; sAC in the mitochondria could respond to unique acid/base conditions created by metabolism, and sAC in the nuclei could potentially help regulate gene expression (reviewed in Cooper, 2003; Zippin et al., 2003; Zippin et al., 2004; Tresguerres et al., 2011). These microdomains are not necessarily mutually exclusive for each type of adenylyl cyclase either; as an example, sAC in sea urchin has been found associated with membrane-bound proteins, indicating HCO_3^-- sensitive cAMP production may also contribute to microdomains near the plasma membrane (Nomura & Vacquier, 2006).

As a result of intracellular cAMP-signaling microdomains, cAMP signal transduction pathways are involved in a wide range of cellular processes including cell growth, movement, metabolism, and ion transport (reviewed in Tresguerres et al., 2011). In the first and best characterized physiological role of sAC, sAC-generated cAMP was proven both pharmacologically and genetically to be responsible for motility and capacitation in mammalian sperm (Esposito et al., 2004; Hess et al., 2005; Xie et al., 2006; Schuh et al., 2006; reviewed in Tresguerres et al., 2010a). Physiological processeses involving sAC have also been proposed in purple sea urchins and elasmobranchs. In purple sea urchin, sAC is concentrated in the proximal half of the sperm flagellum near the mitochondrial midpiece (Bookbinder et al., 1990), suggesting that sAC plays a role in triggering the initiation of sperm motility, a process that is dependent on cAMP-dependent phosphorylation of flagella-associated proteins in response to changes in pH (Bracho et al., 1998; Nomura & Vacquier, 2006). In dogfish sharks, sAC triggers the translocation of Vacuolar H^+-ATPase (VHA) to the basolateral membrane in gill epithelium to counteract blood alkalosis post-feeding (Tresguerres, et al., 2010). A similar mechanism has been described in isolated gill cells from stingray (Roa & Tresguerres, 2016). pH regulation by sAC has been proposed to occur in a number of other marine organsisms, but many of the mechanisms have yet to be confirmed (Tresguerres et al., 2014).

Intracellular [Ca^{2+}]

The concentration of Ca^{2+} within coral tissues is primary determined by two factors: the proximity to the skeleton and the time of day (day/light vs night/dark conditions) when [Ca^{2+}] is measured. Using x-ray microanalysis in freeze-substituted sections of *G. fascicularis*, [Ca^{2+}] was measured in all four tissue layers, in seawater, and within the coelenteron. Generally, the [Ca^{2+}] increases within tissues when moving inwards from the oral ectodermis (21 mmol kg^{-1}), through

the oral gastrodermis (13 mmol kg^{-1}) and aboral gastrodermis (17 mmol kg^{-1}) to the calicoblastic epithelium (19 mmol kg^{-1}) above the skeleton (Marshall et al., 2007). This gradient suggests a concentrating mechanism for Ca^{2+} related to calcification of the skeleton.

Ca^{2+} has also been observed to vary by light conditions. Measurements taken by microsensors indicate that at the surface (seawater) of G. *fascicularis* and within the coelenteron, [Ca^{2+}] decreases during the day and is replenished during the night; in contrast, the [Ca^{2+}] in the SCM increases during the day and decreases during the night (Al-Horani et al., 2003). This increase in Ca^{2+} to the site of calcification during the day matches expectations, based on the ~3x increase in calcification rates observed in corals during light conditions, called light enhanced calcification (reviewed in Allemand et al, 2011). These observations about [Ca^{2+}] in coral tissues raise the following questions: how does Ca^{2+} travel through the four tissue layers and eventually arrive at the site of calcification? And how do corals avoid the toxic effects related to high intracellular [Ca^{2+}]?

These are the questions I set out to answer in Chapter 3 of my thesis, in which I identify and localize a Na^{+}/Ca^{2+} Exchanger (NCX) protein in coral tissues. I have included a section in this introduction chapter to review what is known about the SLC8 protein family (NCX proteins).

Sodium calcium exchanger: calcium transport for homeostasis

NCX is a transmembrane protein that uses the electrochemical gradient of Na^{+} to export Ca^{2+} ions from cells in a 3:1 ratio (Philipson & Nicoll, 2000). NCX belongs to the SLC8 family, which is included in a larger family called the Ca^{2+}/Cation superfamily, and includes other ion tansporters such as $Na^{+}/Ca^{2+}/K^{+}$ Exchangers called NCKXs (Khananshvili, 2013). There are four NCX isoforms in the mammalian SLC8 family: SLC8A1 (NCX1)(Nicoll et al., 1990), SLC8A2

(NCX2)(Li et al., 1994), SLC8A3 (NCX3)(Nicoll et al., 1996), as well as a more recently identified NCX protein called SLC8B1 that is $Na^+/Ca^{2+}/Li^+$ Exchanger (NCLX) found in the mitochondria (Palty et al., 2010).

The evolution of NCX genes most likely occurred as a result of two whole genome duplication events; based on the lack of additional NCX genes in tunicate (*Ciona*), the first NCX duplication is predicted to have occurred after the divergence of chordates from invertebrates (On et al., 2008). A second gene duplication event that occurred in an ancestor of tetrapods resulted in a fourth NCX gene, however this isoform has been lost in mammals and birds and is only present in amphibians and fish (Marshall et al., 2005; On et al., 2008). At the time when these phylogenetic determinations were made, there was little evidence for any non NCX1-like proteins in invertebrates, but recent advances in genomics and transcriptomics has led to an explosion of gene models and predicted NCX2-like and NCX3-like proteins in invertebrate species. However, the relationship and relatedness of these proteins to their similarly named mammalian counterparts has yet to be determined, since there are very few NCX1 proteins that have been studied in invertebrate systems (Philipson & Nicoll, 2000). Therefore, the characterization of NCX1 and other NCX proteins in invertebrates, including corals, is severely lacking.

An interesting aspect of NCX regulation in vertebrate species is the use of alternative splicing to generate multiple potential isoforms. While the physiological significance is unclear, alternative splicing of NCX might be related to differential expression in different cell types, Ca^{2+} transport kinetics, or regulatory properties. Alternative splicing is common in mammalian NCX genes (reviewed in Khananshvili, 2013); in rat (Lee et al., 1994) and rabbit (Kofuji et al., 1993), alternative splicing of NCX1 results in tissue-specific expression. As many as 32 possible splice variants were predicted for rabbit NCX1 (Kofuji et al., 1994); because some of the spliced exons contain a regulatory Ca^{2+} binding site (Matsuoka et al.,1993), the NCX1 variants could

demonstrate differential regulation by intracellular Ca^{2+} (Kofuji et al., 1994). Rat NCX3 also undergoes alternative splicing with an intron/exon pattern similar to NCX1 (Quednau et al., 1997).

In corals, the mechanisms behind calcification of the aragonite skeleton have not been determined. A widely accepted hypothesis involves the presence of a plasma membrane Ca^{2+}-ATPase (PMCA) in the apical membrane of cells which can deliver Ca^{2+} to the site of calcification. However, in vertebrates, it has been established that NCX and not PMCA is involved in calcification by osteoblast cells in chicken. NCX protein in Ca^{2+}-secreting osteoblast cells is located in the membrane facing the bone matrix, while PMCA is found in the membrane facing the marrow and is absent from the bone-secreting side (Akisaka et al.,1988; Stains & Gay, 1998). In addition, expression of NCX1 and NCX3 transcripts is constant during chicken osteoblast differentiation in culture, in comparison to the expression of PMCA, which declines, further supporting the hypothesis that NCX protein and not PMCA is responsible for transport of Ca^{2+} to bones (Stains et al., 2002). In cultured mouse osteoblast cells, NCX3 specifically is the isoform responsible for the majority of Ca^{2+} flux from the cell (Sosnoski & Gay, 2008). Due to some similarities between bone and aragonite calcification, these findings prompted my desire to investigate NCX as a potential source of Ca^{2+} delivery to the SCM in corals.

Objective

The goal of my PhD research has been to expand our limited knowledge about basic cell biology in corals, and in particular about acid/base sensing and calcification. It is only by first identifying and localizing enzymes and ion transporters within coral tissues that we are able to hypothesize about potential physiological roles and design the experiments necessary to

investigate them. The research in Chapters 1-3 of my dissertation lays the foundation for future work studying acid/base sensing and regulation and Ca^{2+} homeostasis and transport in corals.

Acknowledgements

The introduction, in part, is a reprint of material as it appears in the following citation: Tresguerres, M., Barott, K. L., Barron, M. E., Deheyn, D. D., Kline, D. I., & Linsmayer, L. B. (2017). Cell Biology of Reef-Building Corals: Ion Transport, Acid / Base Regulation, and Energy Metabolism. *Acid-Base Balance and Nitrogen Excretion in Invertebrates*, 193–218. https://doi.org/10.1007/978-3-319-39617-0. The dissertation author was a coauthor of this book chapter.

References

Akisaka, T., Yamamot, T., & Gay, C. V. (1988). Ultracytochemical Investigation of Calcium-Activated Adenosine Triphosphate (CA++-ATPase) in Chick Tibia, *3*(1), 19–25.

Al-Horani, F. A., Al-Moghrabi, S. M., & de Beer, D. (2003). The mechanism of calcification and its relation to photosynthesis and respiration in the scleractinian coral Galaxea fascicularis. *Marine Biology*, *142*, 419–426. https://doi.org/10.1007/s00227-002-0981-8

Allemand, D., Furla, P., & Bénazet-Tambutté, S. (1998). Mechanisms of carbon acquisition for endosymbiont photosynthesis in Anthozoa. *Canadian Journal of Botany*, *76*(6), 925–941. https://doi.org/10.1139/cjb-76-6-925

Allemand, D., Tambutté, É., Zoccola, D., & Tambutté, S. (2011). *Coral Calcification, Cells to Reefs*. *Coral Reefs: An Ecosystem in Transition*. https://doi.org/10.1007/978-94-007-0114-4

Awad, E. W., & Anctil, M. (1993). Positive coupling of beta-like adrenergic receptors with adenylate cyclase in the cnidarian Renilla koellikeri. *The Journal of Experimental Biology*, *182*, 131–46.

Barott, K. L., Helman, Y., Haramaty, L., Barron, M. E., Hess, K. C., Buck, J., Levin, L. R., Tresguerres, M. (2013). High adenylyl cylcase activity and in vivo cAMP fluctuations in corals suggest central physiological role. *Scientific Reports*, *3*(1379). https://doi.org/10.1038/srep01379

Beltran, C., Vacquier, V. D., Moy, G., Chen, Y., Buck, J., Levin, L. R., & Darszon, A. (2007). Particulate and soluble adenylyl cyclases participate in the sperm acrosome reaction. *Biochemical and Biophysical Research Communications*, *358*, 1128–1135. https://doi.org/10.1016/j.bbrc.2007.05.061

Bookbinder, L., Moy, G., & Vacquier, V. (1990). Identification of sea urchin sperm adenylate cyclase. *The Journal of Cell Biology*, *111*(November), 1859–1866.

Bracho, G. E., Fritch, J. J., & Tash, J. S. (1998). Identification of flagellar proteins that initiate the activation of sperm motility in vivo. *Biochemical and Biophysical Research Communications*, *242*(1), 231–7. https://doi.org/10.1006/bbrc.1997.7937

Braun, T., & Dods, R. F. (1975). Development of a Mn2 + -Sensitive , " Soluble " Adenylate Cyclase in Rat Testis, *72*(3), 1097–1101.

Buck, J., Sinclair, M. L., Schapal, L., Cann, M. J., & Levin, L. R. (1999). Cytosolic adenylyl cyclase defines a unique signaling molecule in mammals. *Proceedings of the National Academy of Sciences of the United States of America*, *96*(1), 79–84.

Cann, M. J., Hammer, A., Zhou, J., & Kanacher, T. (2003). A defined subset of adenylyl cyclases is regulated by bicarbonate ion. *The Journal of Biological Chemistry*, *278*(37), 35033–8. https://doi.org/10.1074/jbc.M303025200

Chen, Y., Cann, M. J., Litvin, T. N., Iourgenko, V., Sinclair, M. L., Levin, L. R., & Buck, J. (2000). Soluble adenylyl cyclase as an evolutionarily conserved bicarbonate sensor. *Science (New York, N.Y.)*, *289*(5479), 625–8.

Cooper, D. M. F. (2003). Regulation and organization of adenylyl cyclases and cAMP. *The*

Biochemical Journal, *375*(Pt 3), 517–29. https://doi.org/10.1042/BJ20031061

Esposito, G., Jaiswal, B. S., Xie, F., Krajnc-franken, M. A. M., Robben, T. J. A. A., Strik, A. M., Kuil, C., Philipsne, R. L. A., van Duin, M., Conti, M., Gossen, J. A. (2004). Mice deficient for soluble adenylyl cyclase are infertile because of a severe sperm-motility defect, *101*(9), 2993–2998.

Furla, P., Bénazet-Tambutté, S., Jaubert, J., & Allemand, D. (1998). Functional polarity of the tentacle of the sea anemone Anemonia viridis: role in inorganic carbon acquisition. *The American Journal of Physiology*, *274*(2 Pt 2), R303–R310.

Galliot, B., Welschof, M., Schuckert, O., Hoffmeister, S., & Schaller, H. C. (1995). The cAMP response element binding protein is involved in hydra regeneration. *Development (Cambridge, England)*, *121*(4), 1205–16.

Garbers, D., & Kopf, G. (1980). The regulation of spermatozoa by calcium and cyclic nucleotides. *in Cyclic Nucleotide Research. Volume 13.*, 251–307.

Gibbin, E. M., Putnam, H. M., Davy, S. K., & Gates, R. D. (2014). Intracellular pH and its response to CO2-driven seawater acidification in symbiotic versus non-symbiotic coral cells. *The Journal of Experimental Biology*, *217*(Pt 11), 1963–9. https://doi.org/10.1242/jeb.099549

Goreau, T. F., Goreau, N. I., & Yonge, C. M. (1971). Reef Corals: autotrophs or heterotrophs. *Biological Bulletin*, *141*, 247–260.

Hanoune, J., & Defer, N. (2001). Regulation and role of adenylyl cyclase isoforms. *Annual Review of Pharmacology and Toxicology*, *41*(1), 145-174.….

Hess, K. C., Jones, B. H., Marquez, B., Chen, Y., Ord, T. S., Kamenetsky, M., Miyamoto, C., Zippin, J. H., Kopf, G. S., Suarez, S. S., Levin, L. R., Williams, C. J., Buck, J., Moss, S. B. (2005). The "soluble" adenylyl cyclase in sperm mediates multiple signaling events required for fertilization. *Developmental Cell*, *9*(2), 249–59. https://doi.org/10.1016/j.devcel.2005.06.007

Johnston, I. S. (1980). The Ultrastructure of Skeletogenesis in Hermatypic Corals. *International Review of Cytology*, *67*, 171–214.

Khananshvili, D. (2013). The SLC8 gene family of sodium – calcium exchangers (NCX) – Structure, function, and regulation in health and disease. *Molecular Aspects of Medicine*, *34*(2–3), 220–235. https://doi.org/10.1016/j.mam.2012.07.003

Kleinboelting, S., Diaz, A., Moniot, S., van den Heuvel, J., Weyand, M., Levin, L. R., Buck, J., Steegborn, C. (2014). Crystal structures of human soluble adenylyl cyclase reveal mechanisms of catalysis and of its activation through bicarbonate. *Proceedings of the National Academy of Sciences of the United States of America*, *111*(10), 3727–32. https://doi.org/10.1073/pnas.1322778111

Knowlton, N., Brainard, R. E., Fisher, R., Moews, M., Plaisance, L., & Caley, M. J. (2006). Coral Reef Biodiversity. *Life in the World's Oceans: Diversity, Distribution, and Abundance*, 65–77.

Kofuji, P., Lederer, W. J., & Schulze, D. H. (1993). Na / Ca exchanger isoforms expressed in kidney. *The American Journal of Physiology*, *265*, F598–F603.

Kofuji, P., Lederer, W. J., & Schulze, D. H. (1994). Mutually Exclusive and Cassette Exons Underlie Alternatively Spliced Isoforms of the Na/Ca Exchanger. *The Journal of Biological Chemistry*, *269*(7), 5145–5149.

Laurent, J., Tambutté, S., Tambutté, É., Allemand, D., & Venn, A. (2013). The influence of photosynthesis on host intracellular pH in scleractinian corals. *The Journal of Experimental Biology*, *216*, 1398–404. https://doi.org/10.1242/jeb.082081

Lee, S.-L., Yu, A. S. L., & Lytton, J. (1994). Tissue-specific Expression of Na+-Ca2+ exchanger Isoforms. *The Journal of Biological Chemistry*, *269*(21), 14849–14852.

Li, Z., Matsuoka, S., Hryshko, L. V, Nicoll, D. A., Bersohn, M. M., Burke, E. P., Lifton, R. P., Philipson, K. D. (1994). Cloning of the NCX2 Isoform of the Plasma Membrane Na + -Ca2 + Exchanger, *269*(26), 17434–17439.

Linder, J. U. (2006). Class III adenylyl cyclases: molecular mechanisms of catalysis and regulation. *Cellular and Molecular Life Sciences : CMLS*, *63*(15), 1736–51. https://doi.org/10.1007/s00018-006-6072-0

Litvin, T. N., Kamenetsky, M., Zarifyan, A., Buck, J., & Levin, L. R. (2003). Kinetic properties of "soluble" adenylyl cyclase. Synergism between calcium and bicarbonate. *The Journal of Biological Chemistry*, *278*(18), 15922–6. https://doi.org/10.1074/jbc.M212475200

Marshall, A. T., Clode, P. L., Russell, R., Prince, K., & Stern, R. (2007). Electron and ion microprobe analysis of calcium distribution and transport in coral tissues. *The Journal of Experimental Biology*, *210*, 2453–2463. https://doi.org/10.1242/jeb.003343

Marshall, C. R., Fox, J. A., Butland, S. L., Ouellette, B. F. F., Brinkman, F. S. L., Tibbits, G. F. (2005). Phylogeny of Na+ / Ca 2+ exchanger (NCX) genes from genomic data identifies new gene duplications and a new family member in fish species, (28), 161–173. https://doi.org/10.1152/physiolgenomics.00286.2004.

Matsuoka, S., Nicoll, D. A., Reilly, R. F., Hilgemann, D. W., & Philipson, K. D. (1993). Initial localization of regulatory regions of the cardiac sarcolemmal Na+/Ca2+ exchanger. *Proceedings of National Academy of Science*, *90*, 3870–3874.

Moberg, F., & Folke, C. (1999). Ecological goods and services of coral reef ecosystems. *Ecological Economics*, *29*, 215–233.

Nicoll, D. A., Longoni, S., & Philipson, K. D. (1990). Molecular Cloning and Functional Expression of the Cardiac Sarcolemmal Na+-Ca2+ Exchanger. *Science*, *250*(4980), 562–565.

Nicoll, D. A., Quednau, B. D., Qui, Z., Xia, Y., Lusis, A. J., & Philipson, K. D. (1996). Cloning of a Third Mammalian Na + -Ca 2 + Exchanger , NCX3, *271*(40), 24914–24921.

Nomura, M., Beltrán, C., Darszon, A., & Vacquier, V. D. (2005). A soluble adenylyl cyclase from sea urchin spermatozoa. *Gene*, *353*(2), 231–8. https://doi.org/10.1016/j.gene.2005.04.034

Nomura, M., & Vacquier, V. D. (2006). Proteins associated with soluble adenylyl cyclase in sea urchin sperm flagella. *Cell Motility and the Cytoskeleton*, *63*(9), 582–90. https://doi.org/10.1002/cm.20147

On, C., Marshall, C. R., Chen, N., Moyes, C. D., & Tibbits, G. F. (2008). Gene Structure Evolution of the Na+-Ca2+ Exchanger (NCX) Family. *BMC Evolutionary Biology*, *8*(1), 127. https://doi.org/10.1186/1471-2148-8-127

Palty, R., Silverman, W. F., Hershfinkel, M., Caporale, T., Sensi, S. L., Parnis, J., Nolte, C., Fishman, D., Shoshan-Barmatz, V., Herrmann, S., Khananshvili, D., Sekler, I. (2010). NCLX is an essential component of mitochondrial Na+/Ca2+ exchange. *Proceedings of National Academy of Science*, *107*(1), 436–441. https://doi.org/10.1073/pnas.0908099107

Pastor-Soler, N., Beaulieu, V., Litvin, T. N., Da Silva, N., Chen, Y., Brown, D., Buck, J., Levin, L.R., Breton, S. (2003). Bicarbonate-regulated adenylyl cyclase (sAC) is a sensor that regulates pH-dependent V-ATPase recycling. *The Journal of Biological Chemistry*, *278*(49), 49523–9. https://doi.org/10.1074/jbc.M309543200

Philipson, K. D., & Nicoll, D. A. (2000). Sodium-Calcium Exchange: A Molecular Perspective. *Annual Reviews in Physiology*, *62*, 111–133.

Quednau, B. D., Nicoll, D. A., & Philipson, D. (1997). Tissue specificity and alternative splicing of the Na + / Ca2 + exchanger isoforms NCXl , NCX2 , and NCX3 in rat. *American Journal of Physiology*, *272*, C1250–C1261.

Ramos-Espiritu, L., Kleinboelting, S., Navarrete, F. A., Alvau, A., Visconti, P. E., Valsecchi, F., Starkov, A., Manfredi, G., Buck, H., Adura, C., Zippin, J. H., van de Heuvel, J., Glickman, J. F., Steegorn, C., Levin, L.R., Buck, J. (2016). Discovery of LRE1 as a specific and allosteric inhibitor os soluble adenylyl cyclase. HHS Public Access. *Nature Chemical Biology*, *12*(10), 838–844. https://doi.org/10.1038/nchembio.2151.Discovery

Roa, J. N., & Tresguerres, M. (2016). Soluble adenylyl cyclase is an acid-base sensor in epithelial base-secreting cells, (44), 340–349. https://doi.org/10.1152/ajpcell.00089.2016

Romano, S. L., & Cairns, S. D. (2000). Molecular phylogenetic hypotheses for the evolution of scleractinian corals. *Bulletin of Marine Science*, *67*(3), 1043–1068.

Romano, S. L., & Palumbi, S. R. (1996). Evolution of Scleractinian Corals Inferred from Molecular Systematics. *Science*, *271*(5249), 640–642.

Schuh, S. M., Carlson, A. E., McKnight, G. S., Conti, M., Hille, B., & Babcock, D. F. (2006). Signaling pathways for modulation of mouse sperm motility by adenosine and catecholamine agonists. *Biology of Reproduction*, *74*(3), 492–500. https://doi.org/10.1095/biolreprod.105.047837

Schuhmacher, H., & Zibrowius, H. (1985). Coral Reefs What is hermatypic? *Coral Reefs*, *4*, 1–9.

Seamon, K. B., Padgett, W., & Daly, J. W. (1981). Forskolin: unique diterpene activator of adenylate cyclase in membranes and in intact cells. *Proceedings of theNational Academy of Sciences*, *78*(6), 3363–3367.

Sosnoski, D. M., & Gay, C. V. (2008). NCX3 is a major functional isoform of the sodium-calcium exchanger in osteoblasts. *Journal of Cellular Biochemistry*, *103*(4), 1101–1110. https://doi.org/10.1002/jcb.21483

Spurgeon, J. P. G. (1992). The Economic Valuation of Coral Reefs. *Marine Polltution Bulletin*, *24*(11).

Stains, J. P., & Gay, C. V. (1998). Asymmetric Distribution of Functional Sodium-Calcium Exchanger in Primary Osteoblasts, *13*(12), 1862–1869.

Stains, J. P., Weber, J. A., & Gay, C. V. (2002). Expression of Na+/Ca2+ exchanger isoforms (NCX1 and NCX3) and plasma membrane Ca2+ ATPase during osteoblast differentiation. *Journal of Cellular Biochemistry*, *84*(3), 625–635. https://doi.org/10.1002/jcb.10050

Steegborn, C., Litvin, T. N., Hess, K. C., Capper, A. B., Taussig, R., Buck, J., Levin, L. R., Wu, H. (2005a). A novel mechanism for adenylyl cyclase inhibition from the crystal structure of its complex with catechol estrogen. *The Journal of Biological Chemistry*, *280*(36), 31754–9. https://doi.org/10.1074/jbc.M507144200

Steegborn, C., Litvin, T. N., Levin, L. R., Buck, J., & Wu, H. (2005b). Bicarbonate activation of adenylyl cyclase via promotion of catalytic active site closure and metal recruitment. *Nature Structural & Molecular Biology*, *12*(1), 32–7. https://doi.org/10.1038/nsmb880

Stolarski, J., Kitahara, M. V, Miller, D. J., Cairns, S. D., Mazur, M., & Meibom, A. (2011). The ancient evolutionary origins of Scleractinia revealed by azooxanthellate corals The ancient evolutionary origins of Scleractinia revealed by azooxanthellate corals. *BMC Evolutionary Biology*, *316*(October), 1–10.

Taussig, R., & Gilman, A. (1995). Mammalian membrane-bound adenylyl cyclases. *Journal of Biological Chemistry*.

Tresguerres, M. (2014). Biochimica et Biophysica Acta sAC from aquatic organisms as a model to study the evolution of acid / base sensing . *BBA - Molecular Basis of Disease*. https://doi.org/10.1016/j.bbadis.2014.06.021

Tresguerres, M., Barott, K. L., Barron, M. E., Deheyn, D. D., Kline, D. I., & Linsmayer, L. B. (2017). Cell Biology of Reef-Building Corals: Ion Transport, Acid/ Base Regulation, and Energy Metabolism, 193–218. https://doi.org/10.1007/978-3-319-39617-0

Tresguerres, M., Barott, K. L., Barron, M. E., & Roa, J. N. (2014). Established and potential physiological roles of bicarbonate-sensing soluble adenylyl cyclase (sAC) in aquatic animals. *The Journal of Experimental Biology*, *217*, 663–72. https://doi.org/10.1242/jeb.086157

Tresguerres, M., Buck, J., & Levin, L. R. (2010a). Physiological carbon dioxide, bicarbonate, and pH sensing. *Pflügers Archiv : European Journal of Physiology*, *460*(6), 953–64. https://doi.org/10.1007/s00424-010-0865-6

Tresguerres, M., Levin, L. R., & Buck, J. (2011). Intracellular cAMP signaling by soluble adenylyl cyclase. *Kidney International*, *79*(12), 1277–88. https://doi.org/10.1038/ki.2011.95

Tresguerres, M., Parks, S. K., Salazar, E., Levin, L. R., Goss, G. G., & Buck, J. (2010b). Bicarbonate-sensing soluble adenylyl cyclase is an essential sensor for acid/base homeostasis. *Proceedings of the National Academy of Sciences of the United States of America*, *107*(1), 442–7. https://doi.org/10.1073/pnas.0911790107

Venn, A. A., Tambutté, E., Lotto, S., Zoccola, D., Allemand, D., & Tambutté, S. (2009). Imaging intracellular pH in a reef coral and symbiotic anemone. *Proceedings of the National Academy of Science*, *106*(39), 16574–16579.

Venn, A., Tambutte, E., Holcomb, M., Allemand, D., & Tambutte, S. (2011). Live Tissue

Imaging Shows Reef Corals Elevate pH under Their Calcifying Tissue Relative to Seawater. *PloS One*, *6*(5). https://doi.org/10.1371/journal.pone.0020013

Wang, X., Wang, M., Jia, Z., Wang, H., Jiang, S., Chen, H., Wang, L., Song, L. (2016). Ocean acidification stimulates alkali signal pathway : A bicarbonate sensing soluble adenylyl cyclase from oyster Crassostrea gigas mediates physiological changes induced by CO 2 exposure. *Aquatic Toxicology*, *181*, 124–135. https://doi.org/10.1016/j.aquatox.2016.11.002

Wong, W., & Scott, J. D. (2004). AKAP signalling complexes: focal points in space and time. *Nature Reviews. Molecular Cell Biology*, *5*(12), 959–70. https://doi.org/10.1038/nrm1527

Xie, F., Garcia, M. A, Carlson, A. E., Schuh, S. M., Babcock, D. F., Jaiswal, B. S., Gossen, J. A., Esposito, G., van Duin, M., Conti, M. (2006). Soluble adenylyl cyclase (sAC) is indispensable for sperm function and fertilization. *Developmental Biology*, *296*(2), 353–62. https://doi.org/10.1016/j.ydbio.2006.05.038

Zaccolo, M., Di Benedetto, G., Lissandron, V., Mancuso, L., Terrin, A., & Zamparo, I. (2006). Restricted diffusion of a freely diffusible second messenger: mechanisms underlying compartmentalized cAMP signalling. *Biochemical Society Transactions*, *34*(Pt 4), 495–7. https://doi.org/10.1042/BST0340495

Zippin, J. H., Chen, Y., Nahirney, P., Kamenetsky, M., Wuttke, M. S., Fischman, D. A., Levin, L. R., Buck, J. (2003). Compartmentalization of bicarbonate-sensitive adenylyl cyclase in distinct signaling microdomains 1. *Journal of the Federation of American Societies for Experimental Biology*, *17*(1), 82–84. https://doi.org/10.1096/fj.02

Zippin, J. H., Farrell, J., Huron, D., Kamenetsky, M., Hess, K. C., Fischman, D. A., Levin, L. R., Buck, J. (2004). Bicarbonate-responsive "soluble" adenylyl cyclase defines a nuclear cAMP microdomain. *The Journal of Cell Biology*, *164*(4), 527–34. https://doi.org/10.1083/jcb.200311119

Zippin, J. H., Levin, L. R., & Buck, J. (2001). CO 2 / HCO 3 − -responsive soluble adenylyl cyclase as a putative metabolic sensor, *12*(8), 10–12.

CHAPTER 1: Soluble adenylyl cyclase in the coral, *Pocillopora damicornis*

Abstract

Corals, despite their thin tissues, are able to calcify large aragonite structures called coral reefs that form hotspots of diversity in the marine ecosystem. Corals experience daily fluctuations in the internal pH (pHi) of their tissues, which they must sense and regulate accordingly. Soluble adenylyl cyclase (sAC) is a bicarbonate-stimulated evolutionarily conserved pH sensor that regulates pHi in some marine organisms. Here, I present molecular evidence for the first sAC protein in a coral species, *Pocillopora damicornis*. sAC from *P. damicornis* (pdsAC) undergoes alternative splicing, with potential implications for tissue-specific gene expression and subcellular targeting. pdsAC is localized in all four coral tissue layers, where it may play a role in sensing changes in pH in response to multiple acid/base challenges, both internal and external in nature. Further experimentation is necessary to elucidate the specific mechanisms by which coral sAC regulates pHi in cells.

Introduction

As discussed in the introduction chapter, corals experience daily fluctuations in pHi primarily due to two cellular process that can counteract one another. Photosynthesis by symbiotic dinoflagellate algae, *Symbiodinium sp*., living within the gastrodermis tissue causes alkalosis in gastrodermal cells and in the coelenteron during day/light conditions; at the same time, cellular respiration, which produces CO_2 as a byproduct, is constantly acidifying pHi in all coral cells during the day and night (reviewed in Tresguerres et al., 2017). Corals also face a number of external acid/base disturbances in the form of temporal and spatial changes in seawater pH, some of which are anthropogenic in origin, e.g. ocean acidification. This raises the question-

how are corals able to sense changes in pHi, whether internal or external in origin, to regulate pHi?

A potential acid/base sensor in corals is soluble adenylyl cyclase (sAC), a bicarbonate-stimulate enzyme which produces the second messenger cAMP (Buck et al., 1999; Chen et al., 2000). sAC was first identified in mammals, where a number of splice variants have been identified. For example, a truncated ~50 kDa form of sAC, called sAC_t contains the two catalytic domains for enzymatic activity (Jaiswal & Conti, 2001), and shows up to 10x the catalytic activity compared to the 180 kDa full-length sAC protein (Buck et al., 1999). The difference in activity between these two sAC isoforms is attributed to the presence of a nine-amino acid autoinhibitory domain located immediately C-terminal to the C2 domain which is present in full length mammalian sAC but absent in truncated sAC (Chaloupka et al., 2006). In addition to differences in catalytic activity, alternative splicing also affects expression in tissue, with certain isoforms expressed preferentially in somatic vs germ cells, and subcellular localization, with certain isoforms targeted to the cilia in branchial cells (Chen et al., 2014; Farrell et al., 2008; Geng et al., 2005). Therefore, alternative splicing can provide additional regulation of sAC activity in diverse acid/base conditions throughout different types of cells.

Although sAC has been characterized best in mammals, it has more recently been described in a number of marine organisms, including sea urchin (Nomura et al, 2005), oyster (Wang et al., 2016), dogfish shark (Tresguerres et al., 2010) and ray (Roa & Tresguerres, 2016) (a review on the known and predicted physiological roles of sAC in marine organisms can be found in Tresguerres et al., 2014). In corals, it was recently discovered that cAMP production is stimulated by HCO_3^-, and that HCO_3^--stimulated cAMP production is inhibited by the known pharmacological inhibitor of sAC, KH7 (Barott et al., 2013; Hess et al., 2005). These findings

suggest that sAC is responsible for some portion of the high rates of cAMP production recorded in corals.

sAC generated cAMP can affect cell physiology in response to acid/base conditions through several mechanisms. First, cAMP can activate Protein Kinase A (PKA), which phosphorylates proteins and can cause them to translocate in cells. Second, cAMP can activate exchange protein activated by cAMP (EPAC), which in turn activates members of the Ras superfamily, with numerous potential downstream effects (Schmidt et al., 2013). And finally, cAMP can activate cyclic nucleotide gated channels, which modulate cell physiology through changes in membrane potential (reviewed in Cooper, 2003; Tresguerres et al., 2011; Zaccolo et al., 2006). In this chapter, I provide foundational evidence for sAC proteins in the Robust coral, *Pocillopora damicornis*.

Results

Phylogenetic analysis of coral sAC catalytic domains

Using a sAC transcript from the Robust coral *Stylophora pistillata* as reference, I designed primers for the amplification of the two conserved catalytic domains (C1 and C2) in *P. damicornis*. Phylogenetic analysis of this sequence with the sAC catalytic domains from other corals, invertebrates, and vertebrate species groups *P. damicornis* sAC closest with other coral sAC genes (Figure 1.1). As one would expect, *P. damicornis* sAC is most similar to *S. pistillata* sAC, the sequence used as reference in designing primers for its amplification because they are closely related species belonging to the same Family, *Pocilloporidae*. Similarly, coral sAC genes grouped along clade designation, with the Robust coral sAC genes showing the highest homology

to one another (*P. damicornis, S. pistillata, Orbicella faveolata*) rather than to corals from the Complex clade (*Porites lutea, Acropora yongei, Acropora digitifera*).

Identification of full-length sAC transcripts in P. damicornis

Because attempts to amplify the full-length sAC transcript in *P. damicornis* using primers designed against the *S. pistillata* transcript were unsuccessful, I used 5'and 3' RACE PCR to determine the sequence 5' and 3' to the C1 and C2 domains. 5'RACE PCR identified four distinct 5'UTR regions containing three different start codons (Accession numbers: 5'UTR1- KX218374.1, 5'UTR2- KY853039, 5'UTR3: KX218378.1, 5'UTR4: KY853041) (Figure 1.2). One 5'RACE product, containing 5'UTR4, contained an 88 bp deletion which resulted in early termination and was designated 5'UTR4s (KY853042) (Figure 1.2). 3'RACE amplified a single 3'RACE product (KY853036).

Using the newly identified 5' and 3' UTR regions, I cloned two complete sAC cDNA sequences. The first (KX910691), which contains 5'UTR1, has the longer open reading frame and encodes a 212.8 kDa protein. I refer to this sequence as *P. damicornis* sAC full length 1 ($pdsAC_{FL1}$). The second full length sequence (KY853034) has a different start codon as the result of containing 5'UTR3 and is named $pdsAC_{FL2}$. $pdsAC_{FL2}$ is six amino acids shorter than $pdsAC_{FL1}$ and differs in the first 17 amino acids, resulting in a slightly smaller 212.4 kDa protein. After their distinct N-terminal regions, the remaining 1868 amino acids are identical to one another. This region contains a number of conserved domains and features, including: the two catalytic domains (C1 and C2), two P-loop motifs, a histidine-rich region, a leucine zipper pattern, and four tetratricopeptide (TPR) -like helical domains (Figure 1.3). The histidine-rich region, leucine zipper, and TPR-like helical domains are all absent from the 3'RACE product, which lacks 3,181 bp encoding (amino acids 822-1882 in the full-length sequences). A sAC transcript containing the 3'RACE product as its C-terminal region would encode a predicted ~94

kDa protein ($pdsAC_{94}$) (Figure 1.3a). However, attempts at amplifying a full-length sequence of this shorter isoform by RT-PCR were unsuccessful. The PCR primers and cycles used in RT- and RACE-PCR are provided in Tables 1.1 and 1.2.

Validation of coral sAC antibody in P. damicornis

Custom polyclonal coral sAC antibodies were made against an epitope region in the second catalytic domain of *A. yongei* (Chapter 2). The epitope region is 86% conserved, with 12 out of 14 amino acids identical, in *P. damicornis*. Antibody specificity in *P. damicornis* was confirmed by Western blot analyzing GST-tagged recombinant protein (C1C2 domains). As expected, the custom coral sAC antibody recognized a ~84 kDa protein (the GST tag adds ~29 kDa to the 55 kDa C1C2 sequence) in *E. coli* when protein expression was induced with L-arabinose. This band was eliminated when the antibodies were first pre-adsorbed with antigen peptide overnight (Figure 1.4a). In homogenized *P. damicornis* tissue, the coral sAC antibodies recognized a ~90 kDa protein in tissues revealing that $pdsAC_{94}$ is the predominant sAC protein that is expressed in tissues. This band also disappeared when pre-adsorbed antibodies were used, confirming the coral sAC antibodies recognized a protein containing the sAC epitope region (Figure 1.4b).

P. damicornis sAC is abundantly expressed in tissues

The same custom coral sAC antibodies were used to immunolocalize sAC in decalcified *P. damicornis* tissue. Using immunofluorescence microscopy, sAC was found to be abundantly expressed in cells throughout all four tissue layers: the oral ectoderm, oral and aboral gastrodermis (in coral cells both with and without symbiotic algae) and in the calicoblastic epithelium (Figure 1.5, controls provided in Figure 1.6).

Discussion

This is the first full-length sAC sequence that has been confirmed by RT-PCR in a cnidarian (sAC from an additional coral species, *Acropora yongei*, is described in Chapter 2) and only the third in a marine invertebrate - sea urchin and oyster sAC have also been studied (Nomura et al., 2005; Wang et al., 2016). Even among the available transcriptomic and genomic databases that are available for coral species, most predicted sAC sequences (*A. digitifera*, *P. lutea*, and *O. faveolata*) contain unknown regions or are incomplete. These partial sequences still show high homology to sAC from *P. damicornis* (Figure 1.1). The lack of transcriptomic data available for sAC in corals may be due in part to the low abundance of sAC mRNA in tissues. To obtain sAC sequences from *P. damicornis*, the maximum recommended concentration of purified mRNA was used, sometimes with gene specific primers, to generate cDNA used in RT-PCR. Even then, two rounds of nested PCR were often required in order to obtain enough amplified transcript for cloning. Low abundance of sAC mRNA has been observed in the tissues of other organisms as well. For example, rat (Buck et al., 1999), human (Geng et al., 2005), shark (Tresguerres et al 2010) and rainbow trout (Tresguerres Lab, unpublished) have low sAC mRNA expression in all tissues except the testes. This low mRNA abundance also likely helps explain the failure to clone the predicted pdsAC$_{94}$ transcript in a single RT-PCR reaction. However, the cDNA used in the 3'RACE reaction, which allowed detection of the partial transcript, was also used as template in RT-PCR. Another possibility is that the four 5'UTR regions identified by 5'RACE PCR are not the only 5'UTR regions present in sAC transcripts, and that RT-PCR of pdsAC$_{94}$ was unsuccessful due to absence of a forward primer complementary to the true 5'UTR region of the mRNA.

P. damicornis sAC can undergo alternative splicing at multiple sites in the transcript, the first of which is within the 5'UTR region. Based on RT-PCR results, I have determined the

5'UTR, start codon, and N-terminal amino acid sequence found in pdsAC$_{FL1}$ are encoded in an exon that is spliced out of pdsAC$_{FL2}$. Therefore, the start codon for pdsAC$_{FL2}$ occurs earlier in the genome than the start codon for pdsAC$_{FL1}$. This reveals that *P. damicornis* relies on alternative promoters and alternative splicing to generate unique 5'UTR and N-terminal amino acid sequences in sAC transcripts. A similar alternatively spliced coral sAC variant is found in *A. yongei*, which is discussed at length in Chapter 2. Therefore, I predict that the two other 5'UTR regions (Figure 1.2) undergo similar splicing events as well; however, lack of homology between the *S. pistillata* genome and *P. damicornis* transcripts, have hindered attempts at aligning the sequences to determine intron/exon regions. Alternative promoters have been identified in sAC isoforms from cells in mice and human (Farrell et al., 2008; Geng et al., 2005) . The use of an alternative promoter has also been described in a splice variant of sAC found in normal human bronchial epithelial (NHBE) cells; transcripts containing the alternative start codon and N-terminal amino acid sequence are targeted to the cilia, where this sAC variant regulates ciliary beat frequency (Chen et al., 2014). In coral, differences in the 5'UTR regions and N-terminal peptide sequence could also determine localization and subcellular targeting. sAC protein was immunolocalized to all four tissue layers, where pH conditions vary greatly both spatially and temporally; alternative promoters and signaling peptides could potentially target sAC splice variants to tissue-specific or subcellular localizations where they are catalytically most effective.

The second example of alternative splicing occurs within the first catalytic domain. 5'RACE product 5'UTR4s contains an 88 bp deletion which results in early termination of the protein. The protein encoded by this splice variant is one predicted to be only 12.81 kDa in size, and does not contain the complete C1 domain. Therefore, this splice variant cannot produce cAMP but it might play regulatory roles.

A third example of alternative splicing is predicted based on the 3'RACE product, which has 3,181bp missing compared to $pdsAC_{FL1}$ and $pdsAC_{FL2}$. The predicted sAC protein encoded ($pdsAC_{94}$) contains both catalytic domains and the P-loop motif that are common in sAC proteins (Buck et al., 1999; Tresguerres et al., 2010) but lacks the other conserved C-terminus domains that are present in $pdsAC_{FL1\&2}$ (Figure 1.3a). What is the significance of these conserved domains? Absent from $pdsAC_{94}$, but present in both $pdsAC_{FL}$ sequences, are a histidine-rich region, a leucine zipper pattern, and four TPR like helical domains. The leucine zipper pattern and TPR domains are typical in sAC proteins (reviewed in Steegborn, 2014; Tresguerres et al., 2011) and are most likely involved in binding DNA for transcriptional regulation purposes and protein-protein interactions, respectively (Alber, 1992; Blatch & Lassle, 1999). However, their exact roles are unknown. Interestingly, the histidine region has not been reported in sAC proteins from other animals and so its function in coral sAC is difficult to predict. In some other mammalian proteins, histidine-rich sequences, regardless of position (N-terminal, C-terminal, middle), target proteins to the nuclear speckles compartment in the nucleus, where alternative splicing occurs (Ledda et al., 2009), so the histidine region in coral sAC could have a similar function.

The additional domains present in $pdsAC_{FL1\&2}$ may confer some regulatory function to sAC proteins; however, their physiological significance is unknown. Furthermore, the predominant sAC isoform in *P. damicornis*, as indicated by Western blot (Figure 1.3), is the smaller 94 kDa protein. As mentioned previously, full-length mammalian sAC has about one tenth of the catalytic activity of truncated sAC due to the presence of a nine-amino acid autoinhibitory region directly C-terminal to the second catalytic domain (Chaloupka et al., 2006). However, the autoinhibitory region is absent in coral sAC proteins, suggesting the *P. damicornis* sAC splice variants have similar catalytic activities. This is an interesting finding considering that

the rate of cAMP production in corals are the highest recorded in the literature (Barott et al., 2013).

Immunofluorescence microscopy indicates that sAC protein is abundantly expressed throughout all coral tissues. Of particular interest are the physiological roles of sAC in gastrodermal cells containing the symbiotic, photosynthetic algae, and in the calicoblastic cells, which calcify the coral skeleton. Further research found, through inhibiting sAC with the pharmacological drug KH7, that sAC was responsible for regulating pHi in symbiont-containing and symbiont-free cells in the dark, indicating that sAC senses pHi acidification caused by metabolic activity (Barott et al., 2017). Furthermore, sAC was also implicated in pHi regulation in symbiont-containing cells in the light, which suggests it senses pHi disturbances induced by photosynthetic activity of the symbionts (Barott et al., 2017). Finally, sAC activity was also essential for maintaining pHi in gastrodermal cells exposed to external acidification, indicating sAC senses and help regulate responses to changes in pHe (Barott et al., 2017). The mechanisms linking sAC-generated cAMP to downstream pHi regulation have not yet been determined, though they likely involve PKA-phosphorylation of ion transporting proteins. In dogfish, sAC produced cAMP causes the vacuolar H^+-ATPase to translocate to the basolateral membrane, where it can exude H^+ ions into the blood in response to post-feeding blood alkalosis (Tresguerres et al 2010; Roa & Tresguerres, 2016). VHA, which is expressed in the coral-derived symbiosome membrane surrounding the symbiotic algae (Barott et al, 2015b) , could potentially undergo a similar regulation by sAC in order to increase or decrease the rate of photosynthesis and thus reduce acidosis in the host cell. However, a major limitation for follow up studies on coral is the lack of knowledge about their basic cellular physiology. Simply put, it is impossible to design experiments to elucidate the downstream targets of sAC without first knowing what proteins are present in which cells.

Coral sAC could also potentially regulate pHi in the calicoblastic epithelium via PKA-phosphorylation of proteins responsible for regulating the ionic composition of the subcalicoblastic media (SCM) where calcification occurs. A number of ion transporters, which either directly or indirectly help transport Ca^{2+} or HCO_3^-, two ions required for calcification, have been identified in coral calicoblastic epithelium. These include the Na^+/K^+-ATPase (NKA), Na^+/HCO_3^- Cotransporter (NBC), Plasma membrane Ca^{2+}-ATPase (PMCA), and Na^+/Ca^{2+}-Exchanger (NCX) (Barott et al., 2015a; Chapter 3). In *A. yongei*, NBC was observed primarily in the basolateral membrane, but sometimes in the apical membrane (Barott et al., 2015a), suggesting that it may play a role in HCO_3^- secretion to the SCM, which would increase the pH of the SCM while simultaneously providing an additional source of dissolved inorganic carbon for the skeleton. *S. pistillata* also has NBC localized in the calicoblastic epithelium (Zoccola et al., 2014). Another way sAC could regulate pHi is through the activation of PMCA, which is localized in the calicoblastic epithelium(Barott et al., 2015a; Zoccola et al., 2004). The calcification reaction produces H^+ ions as byproduct, which must first be removed from the SCM in order for calcification to continue, and then from the calicoblastic epithelium in order to avoid acidosis. PMCA in either intracellular vesicles or basolateral membrane could sequester or remove these H^+ from the cell. Although there is no evidence directly linking sAC activity to the activation or translocation of NBC or PMCA in calicoblastic epithelium, sAC is implicated indirectly- inhibition of sAC by KH7 causes pH in the SCM to decrease, creating a less favorable environment for calcification (Tresguerres lab, unpublished results). Thus, in a mechanism that has yet to be determined, sAC is involved with pH regulation of the SCM and with calcification.

An exciting possibility is that sAC helps explain light enhanced calcification, which is the ~3x increase in calcification rates that occurs in corals during light conditions both in the field and in the laboratory (reviewed in Allemand et al., 2011). During the day, the concentration of HCO_3^- in coral tissues can be ~50x higher compared to the night (Furla et al., 2000).

Furthermore, cAMP levels in *P. damicornis* are also highest during the day (Barott et al., 2013). This concurrent increase in [HCO_3^-] and cAMP during the day may be the result of sAC activity, which in turn might stimulate Ca^{2+} and HCO_3^- transporting proteins with the end result of light enhanced calcification. However, testing this hypothesis is complicated by the ubiquitous presence of sAC throughout coral tissues (which preclude exposing whole corals to sAC inhibitors and measuring calcification rate), by the lack of cellular models for studying coral physiology, and by the abovementioned lack of information about basic coral physiology.

In summary, this research presents molecular evidence for the first sAC protein in corals. pdsAC is alternatively spliced to produce a number of transcripts, with potential implications for tissue-specific expression and subcellular targeting in coral cells. sAC protein is abundantly expressed in all four coral tissue layers, where it helps regulate pHi in response to multiple acid/base disturbances of both internal and external origin. sAC was recently discovered to regulate pHi in gastrodermal cells and sAC is implicated in regulating pHi in the calicoblastic epithelium and in the SCM. Thus, sAC is an important pH sensor in coral cells and further experimentation is necessary to elucidate the specific pathways in which it regulates pHi in cells.

Methods

Coral

Colonies of *P. damicornis* were provided by the Birch Aquarium at Scripps Institution of Oceanography (SIO) and corals were maintained at Hubbs Hall (SIO) in warmed (25 °C) flow-through seawater under a modified 12:12 hour light:dark cycle. Modifications included a 4-hour simulated “moonlight” period at the start of each 12-hour dark period and 15 minute simulated “sunrise” and “sunset” periods programmed by a preset protocol (M3) with an Orbit Marine LED Fixture, model 14103-B.

RT-PCR

To prepare cDNA for RT-PCR, a ~2 cm coral fragment was flash frozen in liquid nitrogen and crush into a fine powder using a chilled mortar and pestle. The powder was homogenized in TRIzol Reagent (Invitrogen, Carlsbad, CA, USA). Total RNA was extracted following the recommended protocol with some modifications, including an overnight precipitation of the RNA at -80 °C and a second wash step performed using 75% ethanol. Total RNA was incubated at 37 °C for two hours and then run on an agarose gel to check for degradation. Total RNA was cleaned and concentrated using an RNEasy Plus Mini kit (Qiagen, Hilden, Germany). cDNA was synthesized using SuperScript III Reverse Transcriptase (Invitrogen). cDNA was made using random hexamers or Oligo(dT) primers included with the kit, following the recommended protocol. The cDNA was used as template for RT-PCR, and both full-length sAC sequences were obtained following two rounds of PCR using Phusion High Fidelity Taq polymerase (New England Biolabs, Ipswich, MA, USA) and NucleoSpin gel purification kits (Macherey-Nagel, Duren, Germany). In the second round, "nested" PCR primers included oligonucleotide overhands for In-Fusion Cloning (Clontech, Mountain View, CA, USA) into a PCR2.1 vector (Invitrogen).

5' and 3'RACE PCR

mRNA was purified from total RNA using a Poly(A)Purist MAG kit (Applied Biosystems, Foster City, CA, USA) and then used to synthesize cDNA for 5' and 3' Rapid Amplification of cDNA Ends (RACE) PCR (Invitrogen). Following two rounds of PCR using Platinum Taq polymerase (Invitrogen), RACE products were cloned into a PCR2.1 vector by TOPO-TA cloning (Invitrogen). The primer combinations and cycle conditions used in the first and second (nested) rounds or RT-PCR and RACE PCR are provided in Tables 1.1 and 1.2. All cloned PCR products were sequenced by Retrogen (San Diego, CA, USA) using a combination of custom, internal primers and commercially available vector primers: M13F(-20) and M13R

(Invitrogen). The phylogenetic analysis was performed using the software Phylogent.fr with 500 bootstraps (http://phylogeny.fr/) (Dereeper et al., 2008). Protein domain analyses were performed using PROSITE (http://prosite.expasy.org/) (Sigrist et al., 2012) and InterPro http://www.ebi.ac.uk/interpro/) (Finn et al., 2017).

Recombinant protein expression

The first 499 amino acids of pdsAC$_{FL1}$, which include the two catalytic domains, were cloned into a PCR2.1 vector and "shuffled" into the GST-coding plasmid, pDEST15 (Invitrogen) via an LR Recombination reaction (Invitrogen). The plasmid was transformed into BL21-AI *E. coli* (Invitrogen) and the recombinant, GST-tagged protein was expressed in *E. coli* following induction by L-arabinose.

Western blot

The recombinant protein, along with homogenized *P. damicornis* tissue (coral tissues were homogenized in S22 Buffer [450 mM NaCl, 10 mM KCl, 58 mM $MgCl_2$, 10 mM $CaCl_2$, 100 mM Hepes, final pH 7.8] supplemented with Protease Inhibitor Cocktail (Sigma) and PhosStop (Roche)), were used in Western blot with custom polyclonal antibodies (epitope: LPGDKHEDDPARAL) designed against the second catalytic domain in a predicted *A. digitifera* sAC sequence. The antibodies were used at a concentration of 5.5 ng ml^{-1}. Controls using pre-immune serum and antibodies pre-adsorbed with excess antigen peptide shows no signal, indicating that the coral sAC antibodies specifically recognize both native and recombinant pdsAC.

Immunofluorescence microscopy

Coral fragments were fixed overnight in S22 buffer with 3% paraformaldehyde at 4 °C. Corals were then decalcified in Ca^{2+}-free S22 buffer containing 0.5 M EDTA. The buffer was replaced daily until the skeleton was completely dissolved (~7-10 days later). The tissue was then dehydrated, embedded in paraffin wax, and sectioned (7-10 μm thick) on slides at stored at 4 °C.

Staining of slides followed the protocol previously described (Barott & Tresguerres, 2015). The coral sAC antibodies were diluted 1:500, or approximately 0.11 μg ml^{-1}.

Acknowledgements

Chapter 1, in part, is a reprint of material as it may appear in the following citation: Barott, K. L., Barron, M. E., & Tresguerres, M. (2017). Identification of a molecular pH sensor in coral. *Proceedings of the Royal Society B,* 284, 1–8.201 The dissertation author was a coauthor of this paper.

Figures

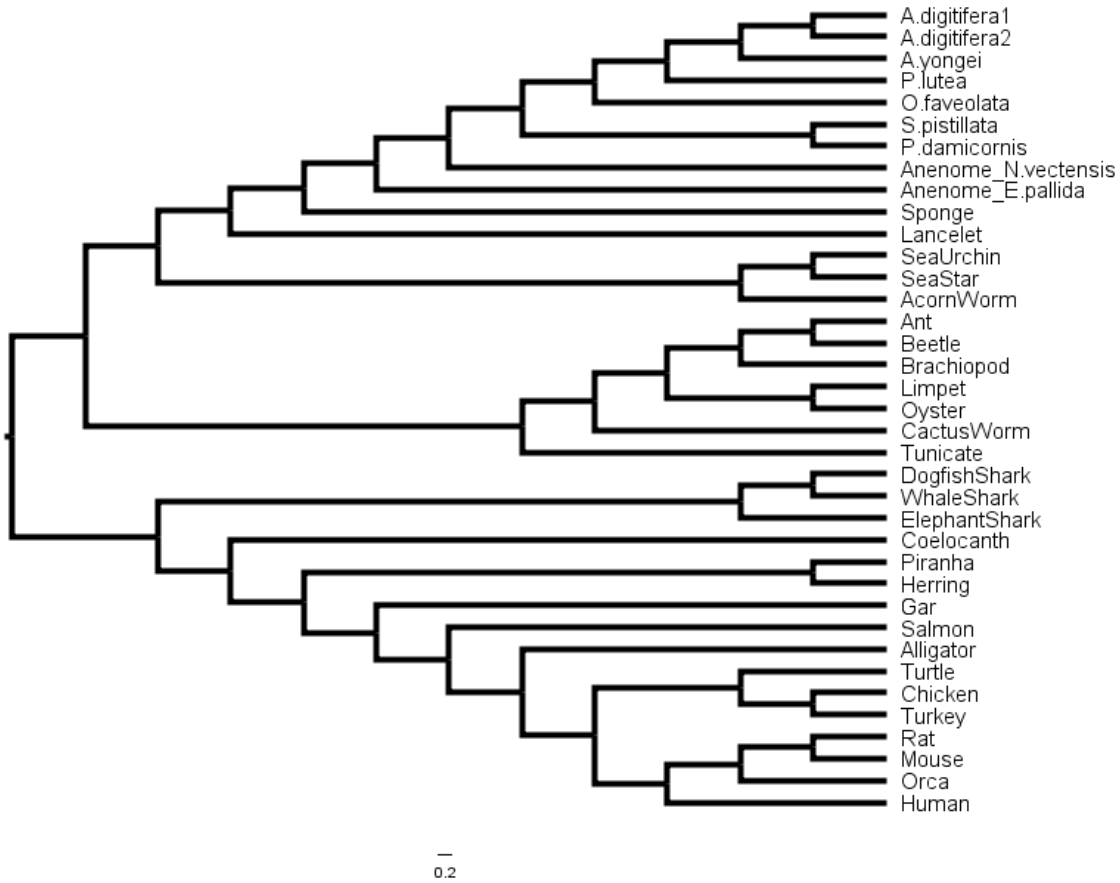

Figure 1.1: Phylogenetic tree of sAC proteins. The following accession numbers were used: Sponge (*Amphimedon queenslandica*) XP_019849124.1, Anenome_E.pallida (*Exaiptasia pallida*) KXJ11039.1, Anenome_N.vectensis (*Nematostella vectensis*) XP_001623318.1, A.digitifera1 (*Acropora digitifera*) aug_v2a.21187.t, A.digitifera2* (*Acropora digitifera*) aug_v2a.10515.t1, A.yongei (*Acropora yongei*) (#), Coral_PdFL1 (*Pocillopora damicornis*) KX910691.1, Coral_PdFL2 (*Pocillopora damicornis*) KY853034, S.pistillata (*Stylophora pistillata*) Spis23569, P.lutea* (*Porites lutea*) plut2.m8.9427.m1, O.faveolata* (*Orbicella faveolta*) XP_020628213.1, Brachiopod (*Lingula anatina*) XP_013401312.1, CactusWorm (*Priapulus caudatus*) XP_014673338.1, AcornWorm* (*Saccoglossus kowalevskii*) XP_006812110.1, Ant (*Solenopsis invicta*) XP_011171092.1, Beetle (*Tribolium castaneum*) XP_015836168.1, Oyster (*Crassostrea gigas*) EKC32844.1, Limpet (*Lottia gigantea*) XP_009062519.1, SeaStar (*Acanthaster planci*) XP_022103708.1, SeaUrchin (*Strongylocentrotus purpuratus*) NP_001020380.1, Lancelet (*Branchiostoma belcheri*) XP_019625790.1, Tunicate (*Ciona intestinalis*) XP_002121896.2, Coelocanth (*Latimeria chalumnae*) XP_014348984.1, ElephantShark (*Callorhinchus milii*) XP_007888388.1, DogfishShark (*Squalus acanthias*) ACA52542.1, WhaleShark (*Rhincodon typus*) XP_020369480.1, Gar (*Lepisosteus oculatus*) XP_015214518.1, Herring (*Clupea harengus*) XP_012693776.1, Salmon (*Salmo salar*) XP_014007204.1, Piranha (*Pygocentrus nattereri*) XP_017540731.1, Turtle (*Chrysemys picta bellii*) XP_008172009.1, Alligator (*Alligator sinensis*) XP_006017814.1, Chicken (*Gallus gallus*) XP_015136281.1, Turkey (*Meleagris gallopavo*) XP_019466264.1, Orca (*Orcinus orca*) XP_004269766.1, Rat (*Rattus norvegicus*) NP_067716.1, Mouse (*Mus musculus*) EDL39226.1, Human (*Homo sapiens*) AAF65931.1. *used to denote that the sequence is incomplete and missing part of the C2 domain.

Figure 1.2: Alignment of 5'RACE PCR products. Five 5'RACE PCR sequences with four different 5'UTR regions are shown: 5UTR1 (KX910691), 5UTR2 (KY853039), 5UTR3 (KY853034), 5UTR4 (KY853041) and 5UTR4s (KY853042). The first methionine in each sequence, indicating the start of the coding region, is highlighted (green). An early start codon in 5UTR4s, which is created by a deletion, is shown highlighted (red). The unique region of each sequence is indicated by color: 5UTR1 (blue), 5UTR2 (orange), 5UTR3 (purple), and 5UTR4 (teal). 5UTR2 and 5UTR3 have the same start codon despite having slight sequence differences in their 5'UTRs.

A.

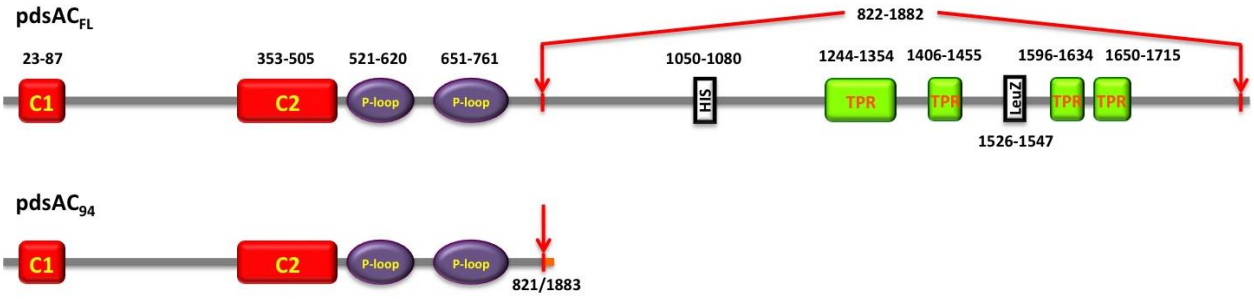

B.

```
pdsACFL1        MKHLVFKKDLSDLKNSPLSSLFIGFTSLCETYSLKASEAESCGTDKLTFTLNTYLGKIIE
pdsACFL2        ------MPRVKHMVGVCMFADISGFTSLCETYSLKASEAESCGTDKLTFTLNTYLGKIIE
                      :..: .  : : : ************************************

pdsACFL1        DILKHGGDVLKFAGDALLALWKAEYGGNLDDLTLLINKAIICSIAIQEECDNYMTDVGVL
pdsACFL2        DILKHGGDVLKFAGDALLALWKAEYGGNLDDLTLLINKAIICSIAIQEECDNYMTDVGVL
                ************************************************************

pdsACFL1        LRVKIALSVGKMQITHVGVTESKHFDLSGSAVSDVNAAEKWAEPGSIILSLLAFSNCDQS
pdsACFL2        LRVKIALSVGKMQITHVGVTESKHFDLSGSAVSDVNAAEKWAEPGSIILSLLAFSNCDQS
                ************************************************************

pdsACFL1        LFLFETIDNGMYYRVAGARVEEESATVSTVHPTGVQLALMSGVLSTGAVLTSTPSVAKRI
pdsACFL2        LFLFETIDNGMYYRVAGARVEEESATVSTVHPTGVQLALMSGVLSTGAVLTSTPSVAKRI
                ************************************************************

pdsACFL1        FAPHVGTLLSRYYPQMKLPRIYRKKGQSEQKEQICKTTGNLLKSDSCHDPGHRTYIYSKL
pdsACFL2        FAPHVGTLLSRYYPQMKLPRIYRKKGQSEQKEQICKTTGNLLKSDSCHDPGHRTYIYSKL
                ************************************************************

pdsACFL1        NDQDIEDLRAYVPKTVLSRIDHGQDLEWLSEMRQVSVLFINMELPIKGNSHSWALQRAFE
pdsACFL2        NDQDIEDLRAYVPKTVLSRIDHGQDLEWLSEMRQVSVLFINMELPIKGNSHSWALQRAFE
                ************************************************************

pdsACFL1        VIHECARRLRGNLNKVFSFDKGCTFIVIFGLPGDKHDDDPTRALKAGHRIMDSLHQIMDI
pdsACFL2        VIHECARRLRGNLNKVFSFDKGCTFIVIFGLPGDKHDDDPTRALKAGHRIMDSLHQIMDI
                ************************************************************
```

Figure 1.3: Conserved domains in *P. damicornis* sAC. A) A schematic indicated conserved domains (C1C2: the two catalytic domains, P-loop: P-loop motifs, HIS: Histidine-rich region, TPR: Tetratricopeptide-like helical domains, leuZ: Leucine zipper pattern) in pdsAC$_{FL}$ and in the predicted pdsAC$_{94}$ protein. pdsAC$_{94}$ is missing the histidine-rich region, TPR, and leucine zipper domains due to a predicted alternative splicing event that removes amino acids 822-1882. Although the nucleotide sequences align again, the ORF in the spliced transcript is different, resulting a unique C-terminal amino acid sequence before the stop codon (indicated in orange). B) Alignment of the full-length sAC sequences from *P. damicornis*, pdsACFL1(KX910691.1) and pdsACFL2 (KY853034). The domains are color coded to match the schematic in 3A. Each sequence contains: C1C2 (red), two P-loop motifs (purple), a histidine-rich region (light grey), a leucine zipper pattern (dark grey), and four TPR (green). The 1061 amino acids that are spliced out of pdsAC94 are shown underlined. The alignment was made online using Clustal Omega Multiple Sequence Alignment (http://www.ebi.ac.uk/Tools/msa/clustalo/).

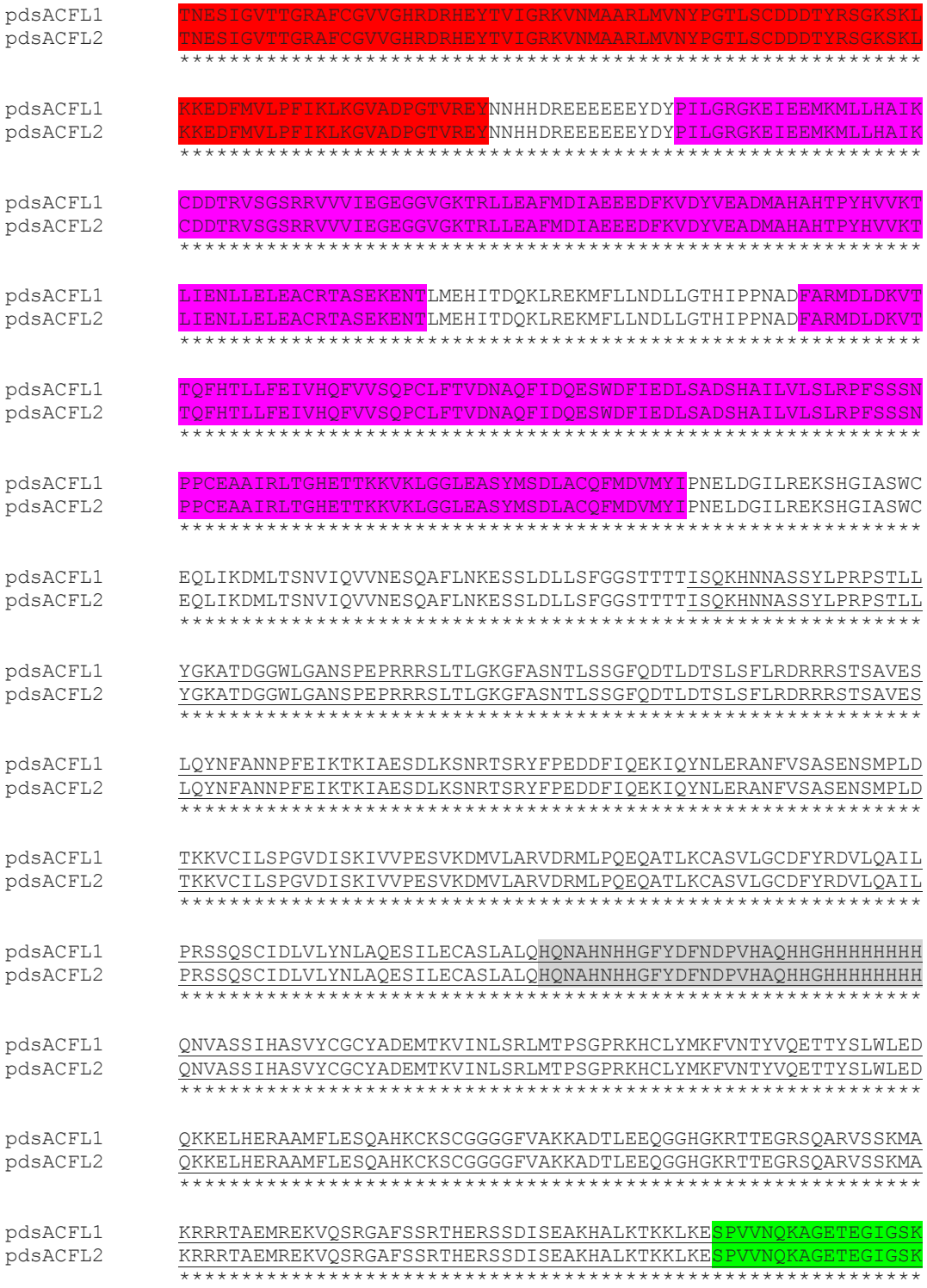

Figure 1.3: Conserved domains in *P. damicornis* sAC *continued.*

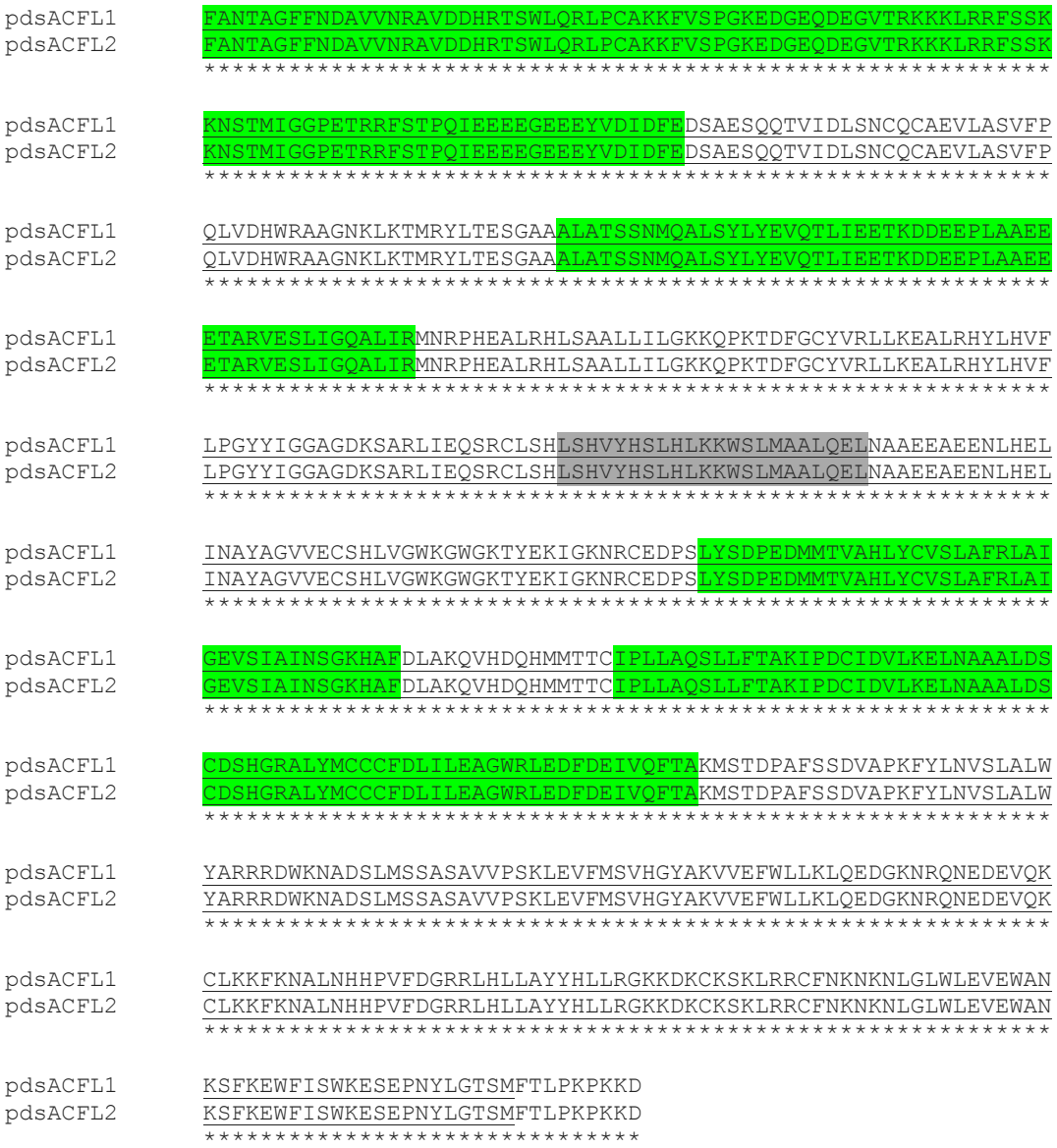

Figure 1.3: Conserved domains in *P. damicornis* sAC *continued.*

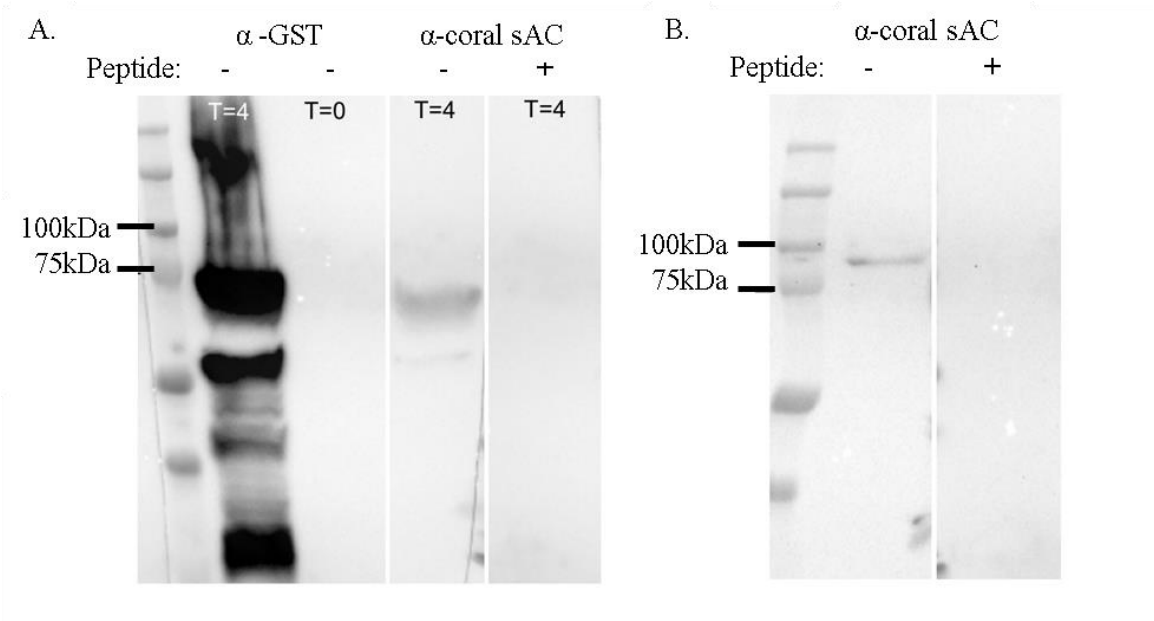

Figure 1.4: Specificity of anti-coral sAC antibodies. A) Lysed *E. coli* cells express recombinant GST-tagged pdsAC within four hours of induction with L-arabinose (T=4). The recombinant protein is visible as a ~84 kDa band recognized by antibody against the GST tag (α-GST) and antibodies against coral sAC (α-coral sAC). The band disappears when α-coral sAC is incubated is pre-adsorbed with antigen peptide (+). B) Homogenized coral tissues have an abundant ~90 kDa band that also disappears with the pre-adsorbed control (+).

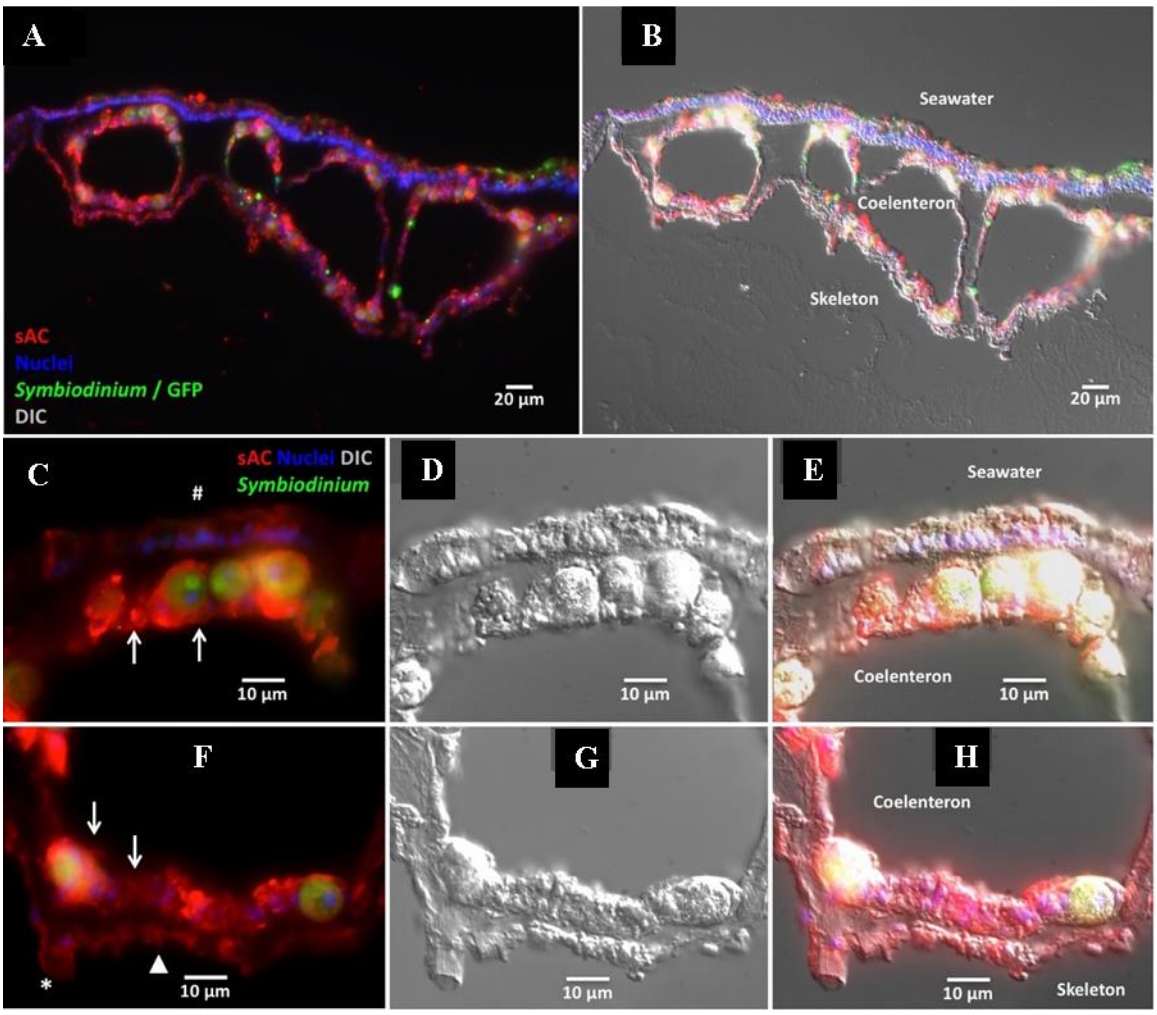

Figure 1.5: Immunolocalization of sAC in *P. damicornis* tissue. sAC is indicated by red fluorescence, nuclei by blue, and Symbiodinium by green (autofluorescence). A) General view of a coenosarc region in the coral showing widespread sAC localization throughout all four coral tissues. B) is the same image overlaid with a differential interference contrast (DIC image). C) sAC is abundantly expressed in gastrodermal cells (white arrows) and in ectodermal cells (white hash sign) in the oral tissue; D) shows the corresponding DIC image and E) is a merge of the two. F) sAC is abundant in aboral gastrodermal tissue (white arrows) and in calicoblastic cells (white arrowhead) and a desmocyte (white asterisk); G) shows the corresponding DIC image and H) is a merge of the two.

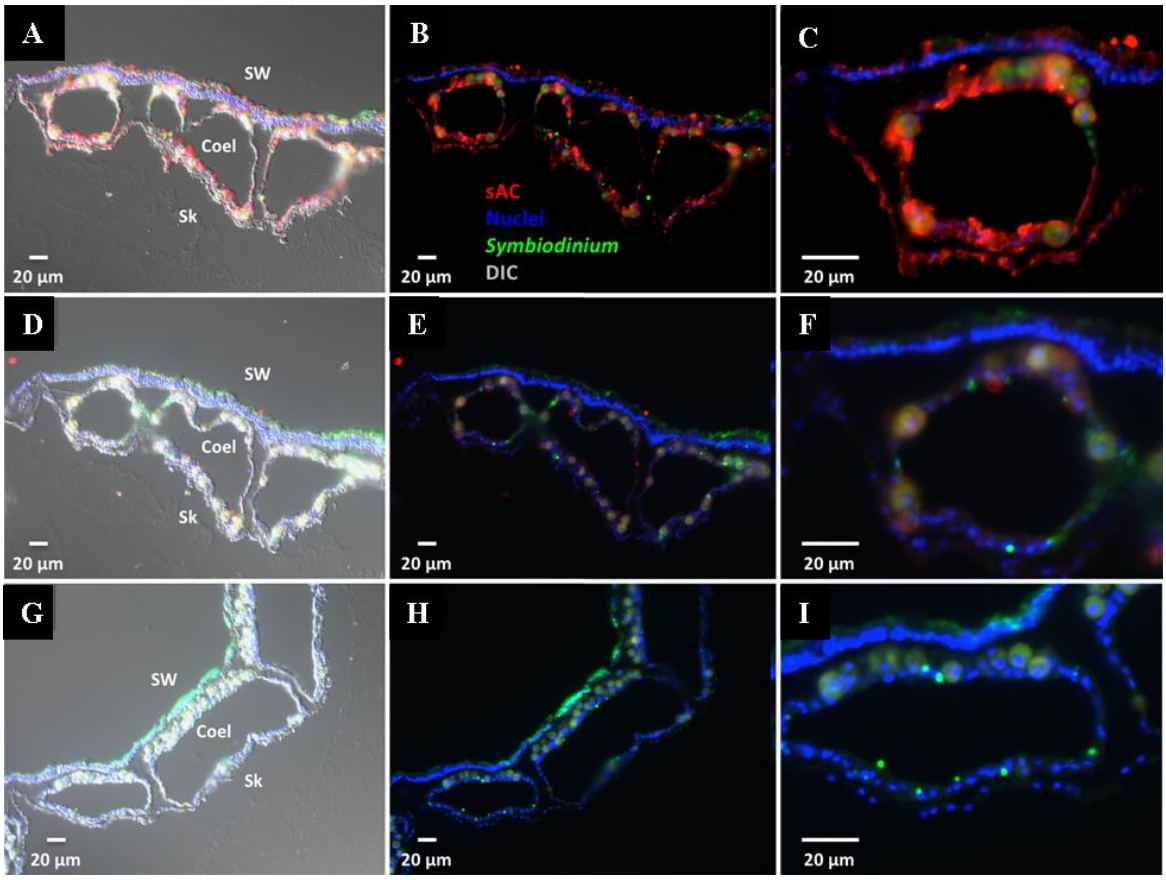

Figure 1.6: Validation of anti-coral sAC antibodies in *P. damicornis* tissues. A-C) anti-sAC antibodies A) contains a DIC image merged with B) a general view of the coenosarc; C) shows the same region at higher magnification. D-E) anti-coral sAC antibodies pre-adsorbed with antigen peptide D) contains a DIC image merged with E) a general view of the coenosarc; F) shows the same region at higher magnification. G-I) no primary antibody G) contains a DIC image merged with H) a general view of the coenosarc; I) shows the same region at higher magnification. In all controls, signal is significantly reduced compared to tissue stained with the anti-coral sAC primary antibody, validating our antibody for use in microscopy.

Table 1.1: PCR primers

Primers used in RT-PCR, 5'RACE PCR, and 3'RACE PCR. Primer AUAP is the Abridged Universal Adapter Primer included with the Invitrogen 5'RACE kit. Primers containing "GIB" at the end of their names were used for In-Fusion cloning- the oligonucleotide overhangs complementary to the cloning vector (PCR2.1) are in bold.

Primer Name	Sequence (5' → 3')
5UTR1b	CTAACTTTCCCACTCTCTTGAGTC
5UTR1cGIB	AGTAACGGCCGCCAGTGTGCTGGAGGTCTTCACTCCTTCCCAAACAGCA
5UTR3a	TCAGGTGCAATCCGTCAAA
5UTR3bGIB	AACGGCCGCCAGTGTGCTGGCCTGGTGCCCAAAGAAATTG
3UTR1b	AGAGGTCCAGATCTACAGGTAA
3UTR1bGIB	AGCGGCCGCCAGTGTGATGGATAGAGGTCCAGATCTACAGGTAAAAGTTGT
Pdam5RACEGSP2L	CCCACTTCTCCGCCGCATTTAC
Pdam5RACENEST	GACGCCAACATCTGTCATGTA
Pdam3RACEGSP3	ATGCGGCAGGTCTCAGTGCTATT
Pdam3RACEGSP4	CCCTCAAAGCTGGACACAGAATA
AUAP Invitrogen)	GGCCACGCGTCGACTAGTAC

Table 1.2: PCR protocols

Primer combinations and PCR cycle conditions. All PCR reactions were performed using 35 cycles. The temperature and length of the denaturation and annealing steps were done according to the manufacturer's protocol for either Phusion HF Taq polymerase or Platinum Taq polymerase.

Sequence	Accession #	PCR Round	Primers (FWD / REV)	Polym.	Anneal Temp, Extension Length
$pdsAC_{FL1}$	KX910691	First Round (cDNA)	5UTR1b / 3UTR1b	Phusion	61 °C, 90 sec (per cycle), 10 min final
		Nested PCR	5UTR1cGIB / 3UTR1bGIB	Phusion	69 °C, 90 sec (per cycle), 10 min final
$pdsAC_{FL2}$	KY853034	First Round (cDNA)	5UTR3a / 3UTR1b	Phusion	64 °C, 90 sec (per cycle), 10 min final
		Nested PCR	5UTR3bGIB / 3UTR1bGIB	Phusion	58 °C, 90 sec (per cycle), 10 min final
5'UTR (partial)	KY853039 KY853041	First Round (cDNA)	AUAP / Pdam5RACEGSP2L	Platinum	55 °C, 60 sec (per cycle), 5 min final
		Nested PCR	AUAP / Pdam5RACENEST	Platinum	57.6 °C, 60 sec (per cycle), 5 min final
3'UTR (partial)	KY853037	First Round (cDNA)	Pdam3RACEGSP3 / AUAP	Platinum	58.5 °C, 120 sec (per cycle), 5 min final
		Nested PCR	Pdam3RACEGSP4 / AUAP	Platinum	58.5 °C, 120 sec (per cycle), 5 min final

References

Alber, T. (1992). Structure of the leucine zipper. *Current Opinion in Genetics & Development*, *2*(2), 205–210.

Allemand, D., Tambutté, É., Zoccola, D., & Tambutté, S. (2011). *Coral Calcification, Cells to Reefs*. *Coral Reefs: An Ecosystem in Transition*. https://doi.org/10.1007/978-94-007-0114-4

Barott, K. L., Barron, M. E., Tresguerres, M. (2017). Identification of a molecular pH sensor in coral. *Proceedings of the Royal Society B*, 284, 1-8.

Barott, K. L., Helman, Y., Haramaty, L., Barron, M. E., Hess, K. C., Buck, J., Levin, L.R. Tresguerres, M. (2013). High adenylyl cylcase activity and in vivo cAMP fluctuations in corals suggest central physiological role. *Scientific Reports*, *3*(1379). https://doi.org/10.1038/srep01379

Barott, K. L., Perez, S. O., Linsmayer, L. B., & Tresguerres, M. (2015a). Differential localization of ion transporters suggests distinct cellular mechanisms for calcification and photosynthesis between two coral species. *American Journal of Physiology - Regulatory, Integrative and Comparative Physiology*, *309*(3), R235–R246. https://doi.org/10.1152/ajpregu.00052.2015

Barott, K. L., & Tresguerres, M. (2015). Immunolocalization of Proteins in Corals: the V-type H+-ATPase Proton Pump. *Bio-Protocol*, *5*(17), 1–10.

Barott, K. L., Venn, A. A., Perez, S. O., Tambutté, S., & Tresguerres, M. (2015b). Coral host cells acidify symbiotic algal microenvironment to promote photosynthesis, *112*(2). https://doi.org/10.1073/pnas.1413483112

Blatch, G. L., & Lassle, M. (1999). The tetratricopeptide repeat: a structural motif mediating protein-protein interactions. *BioEssays*, *21*, 932–939.

Buck, J., Sinclair, M. L., Schapal, L., Cann, M. J., & Levin, L. R. (1999). Cytosolic adenylyl cyclase defines a unique signaling molecule in mammals. *Proceedings of the National Academy of Sciences of the United States of America*, *96*(1), 79–84.

Chaloupka, J. A., Bullock, S. A., Iourgenko, V., & Levin, L. R. (2006). Autoinhibitory Regulation of Soluble Adenylyl Cyclase. *Molecular Reproduction and Development*, *368*(September 2005), 361–368. https://doi.org/10.1002/mrd.20409

Chen, X., Baumlin, N., Buck, J., Levin, L. R., Fregien, N., & Salathe, M. (2014). A soluble adenylyl cyclase form targets to axonemes and rescues beat regulation in soluble adenylyl cyclase knockout mice. *American Journal of Respiratory Cell and Molecular Biology*, *51*(6), 750–760. https://doi.org/10.1165/rcmb.2013-0542OC

Chen, Y., Cann, M. J., Litvin, T. N., Iourgenko, V., Sinclair, M. L., Levin, L. R., & Buck, J. (2000). Soluble adenylyl cyclase as an evolutionarily conserved bicarbonate sensor. *Science (New York, N.Y.)*, *289*(5479), 625–8.

Cooper, D. M. F. (2003). Regulation and organization of adenylyl cyclases and cAMP. *The Biochemical Journal*, *375*(Pt 3), 517–29. https://doi.org/10.1042/BJ20031061

Dereeper, A., Guignon, V., Blanc, G., Audic, S., Buffet, S., Chevenet, F., Dufayard, J.F., Guindon, S., Lefort, V., Lescot, M., Claverie, J. M., Gascuel, O. (2008). Phylogeny .fr: robust phylogenetic analysis for the non-specialist. *Nucleic Acids Research*, *36*(Web Server Issue), 465–469. https://doi.org/10.1093/nar/gkn180

Farrell, J., Ramos, L., Tresguerres, M., Kamenetsky, M., Levin, L. R., & Buck, J. (2008). Somatic " Soluble " Adenylyl Cyclase Isoforms Are Unaffected in Sacytm1Lex / Sacytm1Lex " Knockout " Mice. *PLoS ONE*, *3*(9), 1–9. https://doi.org/10.1371/journal.pone.0003251

Finn, R. D., Attwood, T. K., Babbitt, P. C., Bateman, A., Bork, P., Bridge, J., Chang, H. Y., Dosztanyi, Z., El-Gebali, S., Fraser, M., Gough, J., Haft, D., Holliday, G. L., Huang, H., Huang, X., Letunic, I., Lopez, R., Lu, S., Marchler-Bauer, A., Mi, H., Mistry, J., Natale, D. A., Necci, M., Nuka, G., Orengo, C. A., Park, Y., Pesseat, S., Piovesan, D., Potter, S. C., Rawlings, N. D., Redaschi, N., Richardson, L., Rivoire, C., Sangrador-Vegas, A., Sigrist, C.m Sillitoe, I., Smithers, B., Squizzato, S., Sutton, G., hanki, N., Thomas, P. D., Tosatto, S. C. E., Wu, C. H., Xenarios, I., Yeh, L., Young, S., Mitchell, A. L. (2017). InterPro in 2017 – – beyond protein family and domain annotations. *Nucleic Acids Researcg*, *45*(September), 190–199. https://doi.org/10.1093/nar/gkw1107

Furla, P., Galgani, I., Durand, I., & Allemand, D. (2000). Sources and mechanisms of inorganic carbon transport for coral calcification and photosynthesis. *The Journal of Experimental Biology*, *203*, 3445–3457.

Geng, W., Wang, Z., Zhang, J., Reed, B. Y., Pak, C. Y. C., & Moe, O. W. (2005). Cloning and characterization of the human soluble adenylyl cyclase. *American Journal of Physiology Cell Physiology*, *288*, 1305–1316. https://doi.org/10.1152/ajpcell.00584.2004.

Hess, K. C., Jones, B. H., Marquez, B., Chen, Y., Ord, T. S., Kamenetsky, M., Miyamoto, C., Zippin, J. H., Kopf, G. S., Suarez, S. S., Levin, L. R., Williams, C. J., Buck, J., Moss, S. B. (2005). The "soluble" adenylyl cyclase in sperm mediates multiple signaling events required for fertilization. *Developmental Cell*, *9*(2), 249–59. https://doi.org/10.1016/j.devcel.2005.06.007

Jaiswal, B. S., & Conti, M. (2001). Identification and Functional Analysis of Splice Variants of the Germ Cell Soluble Adenylyl Cyclase. *Journal of B*, *276*(34), 31698–31708.

Ledda, A., Mularoni, L., Alba, M. M., & Luna, S. D. la. (2009). Genome-Wide Analysis of Histidine Repeats Reveals Their Role in the Localization of Human Proteins to the Nuclear Speckles Compartment. *PloS Genetics*, *5*(3). https://doi.org/10.1371/journal.pgen.1000397

Nomura, M., Beltrán, C., Darszon, A., & Vacquier, V. D. (2005). A soluble adenylyl cyclase from sea urchin spermatozoa. *Gene*, *353*(2), 231–8. https://doi.org/10.1016/j.gene.2005.04.034

Roa, J. N., & Tresguerres, M. (2016). Soluble adenylyl cyclase is an acid-base sensor in epithelial base-secreting cells, (44), 340–349. https://doi.org/10.1152/ajpcell.00089.2016

Schmidt, M., Dekker, F. J., & Maarsingh, H. (2013). Exchange Protein Directly Activated by cAMP (epac): A Multidomain cAMP Mediator in the Regulation of Diverse Biological Functions. *Pharmacological Reviews*, *65*, 670–709.

Sigrist, C. J. A., Castro, E. De, Cerutti, L., Cuche, B. A., Hulo, N., Bridge, A., Bougueleret, L., Xenarios, I. (2012). New and continuing developments at PROSITE. *Nucleic Acids Research*, *41*(November 2012), 344–347. https://doi.org/10.1093/nar/gks1067

Steegborn, C. (2014). Structure , mechanism , and regulation of soluble adenylyl cyclases — similarities and differences to transmembrane adenylyl cyclases. *BBA - Molecular Basis of Disease*, *1842*(12), 2535–2547. https://doi.org/10.1016/j.bbadis.2014.08.012

Tresguerres, M., Barott, K. L., Barron, M. E., Deheyn, D. D., Kline, D. I., & Linsmayer, L. B.

(2017). Cell Biology of Reef-Building Corals : Ion Cell Biology of Reef-Building Corals : Ion Transport , Acid / Base Regulation , and Energy Metabolism. *Acid-Base Balance and Nitrogen Ecretion in Invertebrates*, (January), 193–218. https://doi.org/10.1007/978-3-319-39617-0

Tresguerres, M., Barott, K. L., Barron, M. E., & Roa, J. N. (2014). Established and potential physiological roles of bicarbonate-sensing soluble adenylyl cyclase (sAC) in aquatic animals. *The Journal of Experimental Biology*, *217*, 663–72. https://doi.org/10.1242/jeb.086157

Tresguerres, M., Levin, L. R., & Buck, J. (2011). Intracellular cAMP signaling by soluble adenylyl cyclase. *Kidney International*, *79*(12), 1277–88. https://doi.org/10.1038/ki.2011.95

Tresguerres, M., Parks, S. K., Salazar, E., Levin, L. R., Goss, G. G., & Buck, J. (2010). Bicarbonate-sensing soluble adenylyl cyclase is an essential sensor for acid/base homeostasis. *Proceedings of the National Academy of Sciences of the United States of America*, *107*(1), 442–7. https://doi.org/10.1073/pnas.0911790107

Wang, X., Wang, M., Jia, Z., Wang, H., Jiang, S., Chen, H.,Wang, L., Song, L. (2016). Ocean acidification stimulates alkali signal pathway : A bicarbonate sensing soluble adenylyl cyclase from oyster Crassostrea gigas mediates physiological changes induced by CO 2 exposure. *Aquatic Toxicology*, *181*, 124–135. https://doi.org/10.1016/j.aquatox.2016.11.002

Zaccolo, M., Di Benedetto, G., Lissandron, V., Mancuso, L., Terrin, A., & Zamparo, I. (2006). Restricted diffusion of a freely diffusible second messenger: mechanisms underlying compartmentalized cAMP signalling. *Biochemical Society Transactions*, *34*(Pt 4), 495–7. https://doi.org/10.1042/BST0340495

Zoccola, D., Ganot, P., Bertucci, A., Caminiti-segonds, N., Techer, N., Voolstra, C. R., Aranda, M., Tambutte, E., Allemand, D., Casey, J. R., Tambutté, S. (2014). Bicarbonate transporters in corals point towards a key step in the evolution of cnidarian calcification. *Nature Publishing Group*, 1–11. https://doi.org/10.1038/srep09983

Zoccola, D., Tambutté, E., Kulhanek, E., Puverel, S., Scimeca, J. C., Allemand, D., & Tambutté, S. (2004). Molecular cloning and localization of a PMCA P-type calcium ATPase from the coral Stylophora pistillata. *Biochimica et Biophysica Acta - Biomembranes*, *1663*(1–2), 117–126. https://doi.org/10.1016/j.bbamem.2004.02.010

CHAPTER 2: Identification, characterization, and localization of soluble adenylyl cyclase in *Acropora yongei*

Abstract

Soluble adenylyl cyclase (sAC) is a bicarbonate-stimulated source of the second messenger, cyclic adenosine monophosphate (cAMP). sAC genes and transcripts have been identified in diverse phyla, suggesting that sAC is an evolutionarily conserved CO_2/pH/HCO_3^- sensor. Here, I identified a full-length sAC transcript encoding a 68 kDa protein, as well as evidence for additional splice variants and sAC proteins, in a member of the Complex clade of corals, *Acropora yongei*. I cloned and expressed the catalytic domains of *A. yongei* sAC in *E. coli*, and used the recombinant protein to generate dose-response curves to known pharmacological inhibitors of sAC from mammals and fish. Antibodies designed against coral sAC recognized an abundant ~90 kDa protein in homogenized *A. yongei* tissue. Immunofluorescence microscopy localized sAC protein to all four tissue layers in coral, with some differential abundance and localization between cell types. Finally, I found evidence for sAC localization in nuclei, where it could potentially play a role in gene expression. Determining the properties and localization of coral sAC contributes to a greater understanding of coral biology, and on acid/base regulation in marine organisms in general.

Introduction

Corals are the vital component of coral reef ecosystems, which provide a number of ecological and economical services (Moberg & Folke, 1999). Globally, coral health is threatened by climate change increasing the temperature of seawater and ocean acidification lowering its pH (Hoegh-Guldberg et al., 2008). Because corals lack organs with specialized functions, such as pH regulation, their ability to cope with changes in external/environmental pH (pHe) depends on

mechanisms that regulate the pH of internal fluids (pHi) at the cellular level (a review of acid/base regulation in corals can be found in Tresguerres et al., 2017). In any case, in order to regulate pH, corals must first be able to sense acid/base status either directly (H^+), or by proxy (CO_2 / HCO_3^-).

As discussed in the previous chapter of this dissertation, a potential acid/base sensor in coral cells is soluble adenylyl cyclase (sAC). sAC is an evolutionarily conserved, HCO_3^- -stimulated enzyme that produces the second messenger cyclic adenosine monophosphate (cAMP) (Buck et al., 1999; Chen et al., 2000). sAC- generated cAMP is involved in wide range of physiological processes in mammals, from sperm activation to promoting axonal growth in neurons, potentially linking changes in pH to a variety of downstream processes (reviewed in Tresguerres et al., 2011). The ability of cAMP to simultaneously effect control over multiple, sometimes contradictory physiological processes is likely due to the localization and anchoring of cAMP-targeted proteins such as Protein Kinase A (PKA) and Phosphodiesterases (PDEs), which break down cAMP and help regulate the scope/extent and duration of cAMP signals, by A-Kinase Anchoring Proteins (AKAPs) into microdomains throughout the cell (reviewed in Cooper, 2003; reviewed in Tresguerres et al., 2011; Wong & Scott, 2004; Zaccolo et al., 2006; Zippin et al., 2003). sAC is localized in the nuclei of some mammalian cells, and it has recently been demonstrated that sAC-generated cAMP can activate PKA in the nucleus to phosphorylate the cAMP response element binding protein (CREB) (Zippin et al., 2003; Zippin et al., 2004). Indirect activation of CREB, a transcription factor, by sAC-generated cAMP in the nucleus provides a mechanism whereby changes in pHi can potentially regulate gene expression (Zippin et al., 2004).

In addition, animal cells (including coral) (Barott et al 2013) have another source of cAMP, the more traditional transmembrane adenylyl cyclases (tmACs) that are regulated by

hormones and other external signals *via* G protein coupled receptors and G protein (Taussig & Gilman, 1995). One way of distinguishing between regulatory functions by sAC and tmAC is by using specific agonist and antagonist pharmacological drugs, especially for animals such as corals for which genetic manipulations are not established. For example, production of cAMP by mammalian sAC is inhibited by the small molecule KH7 (Hess et al., 2005), which later was confirmed to also inhibit sAC from sea urchin and dogfish shark (Beltran et al., 2007; Tresguerres et al., 2010). Other pharmacological drugs include sAC-selective inhibitors that are derivatives of catechol estrogen (e.g. 2CE, 4CE) (Steegborn et al., 2005a), and a tmAC-specific inhibitor 2',5'-dideoxyadenosine (or 'P-sites' named after the site it blocks) (reviewed in Tresguerres et al., 2011). However, drugs against proteins from vertebrates cannot be assumed to have the same specificity against coral proteins. For example, the widely used Na^+/K^+-ATPase inhibitor, Ouabain, has been recently shown to not be effective against coral Na^+/K^+-ATPase activity (Barott et al 2015). Thus, before using KH7, 4CE and P-sites in coral experiments, it is essential to validate their specificity.

In my previous chapter, I discussed soluble adenylyl cyclase as a physiological pH sensor in the coral *Pocillopora damicornis*. In this chapter, I discuss the identification, characterization, and localization of sAC in a second coral species, *Acropora yongei*. I amplified sAC transcripts from *A. yongei* based on sequences identified in *Acropora digitifera* genome and transcriptome databases. I characterized the sensitivity of recombinant *A. yongei* sAC to known pharmacological inhibitors of adenylyl cyclases- characterization which will be useful for future research investigating the physiological significance of coral sAC. Furthermore, I investigated sAC expression and localization in *A. yongei* tissue, with the potential implications of its intracellular localization in nuclei, with respect to pH regulation via gene expression, discussed below.

Results

Identification of Acropora digitifera sAC transcripts

Using NCBI BLAST, I identified two potential sAC transcripts from the *A. digitifera* transcriptome (Shinzato et al., 2011). One transcript (aug_v2a.21187.t1) encodes a predicted ~173.3 kDa protein, although this sequence has regions with unidentified nucleotides and amino acids (indicated by X's) and lacks a stop codon. I called this sequence adsACtrans1. The second transcript (aug_v2a.10515.t1) encodes a much smaller, predicted 28 kDa protein and is also incomplete. I called this sequence adsACtrans2. Both adsACtrans1 and adsACtrans2 transcripts align with the same genomic region (Genbank: BACK02013590.1) and if correct, would be the result of alternative promoters and alternative splicing within a single sAC gene. The two *A. digitifera* sequences, while useful as a good "starting point", contained incorrect and/or unknown regions, reflecting the complexity of bioinformatic data and the difficulty of creating accurate gene models and predictions *in silico*. Thus, the transcriptomic data available for sAC in *A. digitifera* required confirmation via RT-PCR and sequencing.

Acropora yongei sAC transcripts are alternatively spliced

Using primers designed around the *A. digitifera* sequences (Table 2.1) and based on the sAC sequences from mammals (Buck et al 1999; Chen et al., 2000; Steegborn et al., 2005b), I was able to amplify the C1 and C2 catalytic domains in *A. yongei*. The two catalytic domains were highly conserved between *A. yongei* and the two *A. digitifera* transcripts (Figure 2.2). The sequence, from the start codon through the end of the second catalytic domain (539 amino acids encoding 60 kDa protein) is called $aysAC_{60}$ in this chapter.

While trying to amplify the full-length sAC sequence, I also amplified a transcript with an early stop codon resulting in a transcript encoding for a 68.3 kDa sAC protein ($aysAC_{68}$).

Alignment of this transcript with the *A. digitifera* genome indicates its stop codon is the result of either an alternative 5' splice donor site or intron retention. Interestingly, there is a region of ~44 nucleotides, between the end of the second catalytic domain and the stop codon, which does not align with the *A. digitifera* sAC gene. A second region of ~24 nucleotides also diverges from the genome, although this part of the sequence occurs 153 bases after the stop codon and does not affect the protein sequence.

5'RACE PCR was performed in order to confirm whether the two 5'UTR/start codons identified in *A. digitifera* were present in *A. yongei*. I identified three distinct 5'UTR regions: aysAC5UTR1, aysAC5UTR2, and aysAC5UTR3, each with its own start codon. These three sAC isoforms are most likely the result of alternative promoters located within alternatively spliced exons (a helpful review on alternative promoters can be found in Ayoubi & Van De Ven, 1996). When aligned with the *A. digitifera* sAC gene, aysAC5UTR2 contains the "earliest" (most 5') start codon. The promoter, 5'UTR, and start codon for aysAC5UTR2 are located within an exon that is spliced out of aysAC5UTR1. Similarly, the promoter, 5'UTR, and start codon for aysAC5UTR3 are located within an exon that is spliced out of both aysAC5UTR1 and aysAC5UTR2. Therefore, even though the exon containing the promoter and 5'UTR of aysAC5UTR1 aligns to the *A. digitifera* gene in the most 5' location, the start codon for aysAC5UTR1 is found in a later exon (the exon 3' to aysAC5UTR2's unique exon containing its start codon)- this is why the start codon for aysAC5UTR2 occurs "earlier" than the start codon for aysAC5UT1. A simplified model of this alternative splicing is provided in Figure 2.1.

aysAC5UTR1 does not correspond to either transcript from *A. digitifera*. aysAC5UTR2 contains the same 5'UTR and start codon as $aysAC_{60}$, $aysAC_{68}$, and adTrans1. This confirms that the catalytic domains first amplified by RT-PCR ($aysAC_{60}$) are most likely from the same transcript as $aysAC_{68}$, although there are some single nucleotide polymorphisms (SNPs) between

the two nucleotide sequences, resulting in five differences at the protein level. These SNPs could be the result of sequencing errors or they could originate from different alleles of the same gene. aysAC5UTR3 contains the 5'UTR and start codon found in adsACTrans2. An alignment of the ay sAC transcripts and 5'RACE products with the *A. digitifera* sAC transcripts is provided in Figure 2.2.

Validation of coral sAC antibody in A. yongei

Custom polyclonal antibodies were made in rabbit against an epitope region in the second catalytic domain of sAC, for use in Western blot and immunofluorescence microscopy. Antibody specificity was validated on recombinant HIS-tagged aysAC$_{60}$ protein. As expected, the antibodies recognized a ~63 kDA protein (the tag increases size by 3 kDa) in homogenates of *E. coli* in which HIS-aysAC$_{60}$ production has been induced by L-arabinose, but not in uninduced cells (Figure 2.4b). The 63 kDa band in induced *E. coli* was eliminated when the membrane was incubated with the pre-adsorbed antibody (Figure 2.4b). The antibodies recognized two major proteins in homogenized coral tissue: a ~90 kDa protein and a ~50 kDa protein (Figure 2.4a). Both bands disappeared when the membrane was incubated with antibodies that had been pre-adsorbed overnight with antigen peptide, or with the pre-immune serum. Western blot using homogenized *A. yongei* tissue, when imaged using a longer, 600 second exposure, revealed numerous, less abundant immunoreactive bands between ~40 and 60 kDa in size, and a faint but clean band indicating a larger >200 kDa protein (Figure 2.4c). Those bands likely correspond to different aysAC splice variants, although non-specific antibody cross reactivity with other proteins cannot be ruled out.

Characterization of aysAC activity

Adenylyl cyclase assays using homogenized coral tissue found a dose-response increase in cAMP production with bicarbonate, with half-maximum stimulation (EC_{50}) of ~10 mM HCO_3^-, and maximum stimulation (Vmax) at ~20 mM HCO_3^- (Figure 2.3a).

I also characterized the enzymatic activity of recombinant, purified $aysAC_{60}$. The kinetic characteristics of sAC, such as the EC_{50} of bicarbonate stimulation and the sensitivity to drugs, are typically determined by the C1-C2 domains (Chaloupka et al., 2006; Chen et al., 2000; Kobayashi et al., 2004; Litvin et al., 2003; Steegborn et al., 2005b; Tresguerres, et al., 2010). Smaller proteins are also more easily expressed by *E. coli*, so this truncated form of the sAC protein was chosen over $aysAC_{68}$. Recombinant $aysAC_{60}$ was maximally stimulated by 5 mM Mn^{2+}, which is a hallmark of sAC activity (Braun & Dods, 1975). This maximum activity was inhibited by KH7 and 4CE with a half minimal inhibitory concentration (IC_{50}) of ~6 µM; however, KH7 demonstrated a greater inhibitory effect (Figure 2.3b). On the other hand, the IC_{50} for the tmAC inhibitor, 2',5'-dideoxyadenosine, was ~300 µM. Therefore, 2'5'-dideoxyadenosine does not inhibit sAC activity in corals. Similar results have been found in mammal (Bitterman et al., 2013) and in shark (Roa & Tresguerres, 2016).

I also investigated HCO_3^- -stimulation of recombinant $aysAC_{60}$ testing a variety of combinations of potential cofactors (Table 2.2). An example of one successful assay is shown in Figure 2.3c. Unfortunately, results were not always reproducible possibly due to a combination of low protein abundance and sub-optimal assay conditions. Another possibility is that $aysAC_{60}$ is not completely functional; in this case, assays should be performed using recombinant $aysAC_{68}$.

aysAC is abundantly expressed throughout coral tissue and in nuclei

The coral sAC antibody was used to immunostain 10 µm thick slices of decalcified coral tissues. Red fluorescence indicative of sAC staining clearly labeled all four coral tissue layers (Figure 2.5ab), and it was most abundant in the calicoblastic epithelium (Figure 2.5cde). In the

oral ectodermis, sAC was most abundant near the apical membrane of ciliated support cells, where the cilia are located (Figure 2.5fgh). However, sAC was not present in every cell type of the oral ectodermis, for example, it was completely absent in nematocysts, a type of specialized cell used for predation and defense (Figure 2.5g). In oral gastrodermis (Figure 2.5fgh), aboral gastrodermis (Figure 2.5ijk), and in the calicoblastic epithelium (Figure 2.5ijk), sAC staining is cytosolic. In oral and aboral gastrodermis, sAC is present in the cytoplasm of coral cells both with and without endosymbiotic algae (*Symbiodinium*).

In some cells, sAC appeared to be present in the nucleus (Figure 2.7a). In coral nuclei isolated by centrifugation, there also appeared to be localization of sAC in some, but not all, nuclei (Figure 2.7b). To explore this observation in detail, we prepared and stained thinner (400 nm) slices of coral tissues. In these thinner sections, sAC antibody fluorescence colocalized with blue Hoechst fluorescence, confirming that sAC is found in the nuclei of some cells (Figure 2.7c).

Discussion

Similar to my results in *P. damicornis*, I have identified multiple sAC mRNA transcripts that result from alternative splicing of a single sAC gene. Alternative promoters and splicing of the sAC gene also occurs in mammals (Farrell et al., 2008; Geng et al., 2005; Jaiswal & Conti, 2001) and in fish (Tresguerres Lab, unpublished). Like *P. damicornis* sAC, *A. yongei* sAC contains alternative promoters that are found in alternatively spliced exons, resulting in multiple 5'UTR and N-terminal amino acid sequences. Although the function of these sequence differences has yet to be determined for coral sAC, alternative promoters can have different tissue specificity and can react differently to signals, allowing for differential expression of a single gene (reviewed in Ayoubi & Van De Ven, 1996). Furthermore, UTR regions can affect mRNA nuclear transport, cytoplasmic localization, translational efficiency and stability, and can also

contain binding sites for regulatory proteins, allowing for additional regulation at the mRNA level (reviewed in Hughes, 2006). Finally, the translated regions, the N-terminal amino acids (including the start codons), can contain signaling peptides involved in intracellular trafficking of protein. However, I have not identified any known domains or tags for specific intracellular domains in these coral sAC isoforms other than potential targeting of aysAC5UTR1 to the mitochondria; however, probability was only 0.49, which is very weak (Claros & Vincens, 1996). Although the purpose of the different alternative promoters, 5'UTR and N-terminal protein sequences are unknown, the presence of them in both *P. damicornis* and *A. yongei* sAC isoforms suggests they are significant.

I identified one complete full-length (start codon through stop codon) sAC transcript in *A. yongei* encoding a 68 kDa protein. A band around this size is observed in Western blot with our custom sAC antibody, but only after long exposure (Figure 2.4c). The most abundant sAC protein observed in *A. yongei* as indicated by Western blot is a larger 90 kDa isoform (Figure 2.4a). This 90 kDa protein is the same size as the most abundant sAC protein observed in *P. damicornis* Western blots (Chapter 1), which I identified based on 3'RACE PCR. Like *P. damicornis*, the second most abundant sAC protein in homogenized *A. yongei* tissue, after the 90 kDa protein, is a 55 kDa isoform. While I lack sequencing data providing evidence for a sAC protein this size, I predict it is a truncated form of sAC which ends immediately after the second catalytic domain, which I have confirmed is approximately this size through our C1C1 clone, $aysAC_{60}$. A highly catalytically active truncated form of sAC this size, the product of alternative splicing, has been well characterized in mammals (Buck et al., 1999; Jaiswal & Conti, 2001) and is also present in fish (Tresguerres laboratory, unpublished). Additionally, I identified a ~200 kDa band in homogenized *A. yongei* tissue when imaged with an extended/high exposure (Figure 2.4c). It is significant that both *P. damicornis* and *A. yongei* are very similar in the relative abundance and sizes of their sAC proteins. These two coral species diverged from one another

between 300 and 400 million years ago (Romano & Palumbi, 1996; Stolarski et al., 2011), so this high degree of conservation at the nucleotide and protein level highlights the importance of sAC-dependent processes in coral cell biology. The lack of sequencing data corresponding a 90 kDa, 55 kDa protein, or even 200kDa band is most likely due to the low abundance of sAC mRNA in coral cells- all amplifications of sAC required at least two rounds of PCR, each with 35 cycles. Often, multiple PCR reactions were required to obtain enough yield for gel purification and cloning. The difficulties in working with corals are discussed further in the Discussion Chapter.

HCO_3^- -stimulated cAMP production in homogenized *A. yongei* tissue provided evidence for active sAC protein in coral tissues. Subsequent experiments showed that HCO_3^- -stimulated cAMP production in homogenized tissues was inhibited by the drug KH7 (Barott et al., 2013). The EC_{50} for HCO_3^-- stimulated cAMP production in homogenized coral tissue is ~10 mM, which differs from the EC_{50} determined for purified recombinant sAC in mammals: ~20 mM (Chaloupka et al., 2006; Chen et al., 2000; Litvin et al., 2003) and in sharks: ~5 mM (Tresguerres et al., 2010). Changes in $[HCO_3^-]$ around the EC_{50} induce the most pronounced changes in cAMP production rate because the EC_{50} is in the steepest part of the dose-response curve. This has important physiological implications: for example, in mammals and shark, sAC HCO_3^- EC_{50} values match normal intracellular $[HCO_3^-]$ and therefore sAC is posed to be a good HCO_3^- sensor within the physiologically relevant range (EC_{50} values for sAC in marine organisms are reviewed Tresguerres et al., 2014). Thus, I hypothesize coral sAC regulates physiological processes that involve variations in $[HCO_3^-]$ revolving around 10 mM; for example, in the transition between dark and light (night and day). $[HCO_3^-]$ within *Stylophora pistillata* tissues dramatically increases from 3.7 mM in the dark to 147 mM in the light (Furla et al., 2000). In *P. damicornis*, cAMP peaks during light conditions as well (Barott et al., 2013). Coral tissues alkalinize during the day due to photosynthesis removing CO_2; perhaps the increase in HCO_3^- , from below to well above the EC_{50} concentration, triggers sAC to generate cAMP and regulate pHi in response to this

alkalization. However, it is worth noticing this is an *apparent* EC_{50} because it was estimated from coral homogenates instead of purified coral sAC protein.

The use of purified, recombinant sAC ($aysAC_{60}$) in cAMP assays investigating coral sAC sensitivity to pharmacological inhibitors of ACs eliminated the potential effects/contributions of other proteins, such as tmACs, that could occur when using tissue homogenates. The dose-response curves generated by this study will prove essential in future experiments when selecting which drugs and concentrations will most efficiently inhibit sAC vs. tmAC activity. Additionally, though KH7 and 4CE both inhibit coral sAC more strongly than 2',5'-dideoxyadenosine does, KH7 demonstrates a more complete inhibition than that produced by 4CE. Similar results have been found using truncated, recombinant dogfish sAC (Tresguerres et al., 2010).

Recombinant $aysAC_{60}$ was also used in cAMP assays to investigate HCO_3^--stimulated production of cAMP; however, while such stimulation was sometimes observed (Figure 2.3b), it was inconsistent. cAMP production sometime was stimulated at low concentrations of HCO_3^-, but not every time. This could be because the wrong combinations of cofactors were tested with HCO_3^-; as previously stated, the concentrations of Ca^{2+}, Mg^{2+}, and Mn^{2+} stimulating sAC varies by organism (Table 2.3), presumably reflecting differences in the physiologically relevant intracellular concentrations of these ions. Although many combinations of these cofactors were assayed with HCO_3^- (Table 2.2), they may have been incorrect / nonrelevant combinations. The inconsistent findings may also have been because of the protein misfolding during expression in *E. coli*. It was observed that cultures incubated at lower temperature during recombinant protein expression (16 °C) produced higher cAMP activity in cAMP assay compared to those grown at a higher temperature (30 °C) (unpublished data). Another explanation could be autoinhibition as a result of inserting the stop codon too early in the sequence, creating a truncated protein with the wrong termination sequence. Mammalian sAC has an autoinhibitory domain only nine amino

acids after the second catalytic domain (Chaloupka et al., 2006)- perhaps some or all of this domain was included in aysAC$_{60}$. However, considering that all sAC proteins investigated to date show a degree of HCO_3^--stimulation, it is unlikely coral sAC is the exception. The most likely explanation is an issue with the recombinant protein or assay conditions.

Immunofluorescence microscopy indicates that sAC is present in all four tissue layers of coral. In the oral ectoderm, sAC appears to be concentrated near the apical membrane, where cilia are present. In human airway epithelia, sAC-generated cAMP regulates the cilia beat frequency (Schmid et al., 2007). In corals, cAMP produced by sAC near the membrane could potentially regulate the movement of cilia in order to aid nutrition and/or to remove waste products from the diffuse boundary layer. Furthermore, both the Na^+/K^+-ATPase (NKA) and Na^+/HCO_3^- Cotransporter (NBC) are found in the apical membrane in *A. yongei*; the colocalization of these two proteins suggests that NBC uses the Na^+ gradient created by NKA to take up HCO_3^- from seawater (Barott et al., 2015). This HCO_3^- could potentially stimulate the subset of sAC near the apical plasma membrane, which in turn could coordinate downstream mechanisms. In the other three tissue layers: the oral gastrodermis, aboral gastrodermis, and calicoblastic epithelium, sAC appears to be evenly distributed throughout the cytoplasm, although it is more abundantly expressed in the calicoblastic cells. In *A. yongei*, sAC in these tissue layers could be involved in similar physiological roles as hypothesized in the previous chapter for *P. damicornis*. Such roles include regulation of pHi in gastrodermal cells, where sAC prevents acidification caused by metabolic CO_2/H^+ production (Barott et al., 2017), and regulation of pHi in the calicoblastic epithelium, the tissue that modulates the pH and ionic composition of the subcalicoblastic media (SCM), where calcification occurs. NKA and NBC, as well as the Plasma Membrane Ca^{2+}-ATPase (PMCA) and Na^+/Ca^{2+}-Exchanger (NCX) are also localized in the membrane or cytoplasm of the calicoblastic epithelium, and could assist in ion transport affecting pHi of calcifying cells and pHe of the SCM (Barott et al., 2015; Chapter 3)

Nuclear sAC staining was reported in a subset of mammalian cells together with Protein Kinase A (PKA) and phosphorylated CREB, which constitute a sAC-cAMP nuclear signaling microdomain (Zippin et al., 2004). I have observed a similar expression pattern in corals, with sAC localized to some but not all coral cells so I propose corals, like mammals, have a nuclear signaling microdomain. Once phosphorylated, CREB, a transcription factor, recruits a co-activator, CREB-binding protein (CBP), to a cAMP-responsive element (CRE) found upstream in genes. CBP is associated with RNA polymerase III and has intrinsic acetyltransferase activity that promotes gene transcription (reviewed in Mayr & Montminy, 2001). By identifying CREB pathways in corals, we can predict which transcripts may have expression capable of regulation by nuclear sAC.

In hydra, which belong to the same phylum, Cnidaria, as corals, the sequence of the CREB is highly evolutionarily conserved in the DNA-binding domain and in a distinct phosphorylation domain, with a serine residue (Ser67) as the likely target for post-transcriptional regulation by phosphorylation (Galliot et al., 1995). In hydra, the CREB pathway appears to be involved in multiple developmental processes, such as the self-renewal of stem cells, the proliferation of progenitors, and neurogenesis (Chera et al., 2007). CREB proteins could be responsible for similar physiological processes in corals. In fact, a transcriptomic analysis of heat stress in *Acropora palmata* found a 2.32-fold increase in the cAMP-responsive element-binding protein CREB-like 2 transcript after one day (Desalvo et al., 2010). A second transcriptomic study in *A. palmata* investigating the effect of darkness stress on gene expression also found up-regulation of CREB-like 2, as well as two other genes involved in CREB pathways: cAMP-responsive element modulator (CEM), and cAMP-dependent transcription factor ATF-4 (DeSalvo et al., 2012). These studies suggest CREB plays an important role in corals in responding to external stressors, though whether such stressors activate CREB through cAMP generated by tmACs or sAC, and which genes are then targeted by CREB in response to these stressors, needs

to be determined. However, sAC is a good candidate for the adenylyl cyclase responsible for cAMP as pHi oscillates within coral tissues between light/dark conditions (due to photosynthesis and respiration) (Al-Horani et al., 2003; Venn et al., 2009; Venn et al., 2011). Such changes in pHi could stimulate sAC and thus cAMP could cascade down the CREB pathway. Furthermore, in *P. damicornis,* a full-length sAC transcript contains a histidine-rich region with 10 histidine residues, which I predict may play a role in localization of sAC protein into the nucleus (Chapter 1).

In conclusion, sAC is abundantly expressed in *A. yongei* tissues, where it most likely plays a role in intracellular pH regulation, and potentially in gene expression. Future experiments in *A. yongei* will focus on linking HCO_3^-- stimulated cAMP production by sAC to specific physiological roles in corals. A better understanding of coral cell biology will be valuable in predicting and mitigating the effects of climate change and ocean acidification.

Methods

Coral

A. yongei colonies were obtained from the Birch Aquarium at Scripps Institution of Oceanography (SIO). The corals were maintained at Hubbs Hall (SIO) in warmed (25 °C) flow through seawater under a 12:12 hour light:dark cycle. Some corals decalcified for immunofluorescence microscopy were grown with a simulated 4 hours "moonlight" period at the beginning of the 12-hour dark period. 15 minute long "sunrise" and "sunset" conditions were simulated as well, using the preset M3 protocol programmed with Orbit Marine LED Fixture model 4103-B.

RT-PCR

Two potential coral sAC transcripts were identified by BLAST search of the *Acropora digitifera* genome: aug_v2a.10515 and aug_v2a.21187 (http://marinegenomics.oist.jp/acropora_digitifera). Primers used in RT-PCR were designed based on these two *A. digitifera* sequences. Total RNA from *A. yongei* was obtained from a branch of *A. yongei* (less than 5 cm in length) vortexed in 1 ml TRIzol Reagent (Thermo Fisher) in an RNase-free environment. The recommended TRIzol RNA extraction protocol was followed with some slight modifications to the volumes of reagents used: 250 µl of Chloroform, 670 µl isopropanol, 200 µl of 75% ethanol, and 30 µl water (elution). Furthermore, the suggested final 20 minute water bath was excluded. cDNA was synthesized from 5 µg total RNA utilizing an EcoDry premix (Clontech) following the recommended protocol. PCR was performed using one of two commercially available polymerases: Sapphire (Clontech) and Platinum Taq (Invitrogen); the number and length of cycles were optimized for each pair of primers used. PCR products were run through a 1%-1.5% agarose gel and imaged before excision and purification using commercially available DNA clean-up columns (Zymo). Purified PCR products were TOPO-TA cloned into a PCR2.1 sequencing vector (Invitrogen) before sequencing by Retrogen (San Diego). Sequences were edited by removing ambiguous bases at the 3' and 5' ends and aligned to create consensus sequences using the computer software Sequencher, licensed to the Marine Biology Department at SIO. Protein sequences were aligned (Figure 2.2) using Clustal Omega (http://www.ebi.ac.uk/Tools/msa/clustalo/)(Sievers et al., 2011).

5' RACE PCR

The sequences obtained by RT-PCR were used to design new, *A. yongei*- specific primers for use in RACE-PCR. These new primers (Table 2.1) were modified to include oligonucleotide overhangs compatible with In-Fusion Cloning (Clontech). RNA extractions were modified from previous protocols to minimize degradation and obtain a high yield of total RNA. In the new

protocol, a coral branch was flash-frozen in liquid N_2, crushed to powder (by pestle/mortar), and immediately homogenized in TRIzol reagent using an autoclaved glass homogenizer. An additional 10 minute centrifugation step at 12,000 g was performed to remove polysaccharides. The TRIzol protocol was otherwise followed normally, yielding 500 µl of ~324 ng μl^{-1} total RNA. Total RNA was incubated at 37ºC for 2 hours and separated by agarose gel to confirm no degradation had occurred. 5 µg of mRNA was purified from total RNA using a MicroPurist Poly(A) kit (Ambion). RACE-ready cDNA synthesis was performed using a SMARTer 5'/3' RACE kit (Clontech). 5' RACE products were obtained using the protocol's recommended Touchdown (TD) PCR protocol, and amplified further using the products as template in a second round of TD PCR. Bands were gel-extracted and purified using NucleoSpin columns (Macherey-Nagel) and cloned into the pRACE vector by In-Fusion cloning (Clontech). Plasmids were sequenced by Retrogen using M13 sequencing primers and custom primers. Sequencer was used to analyze sequences. Seven colonies were aligned to create the consensus of aysAC5UTR1, five colonies were used for aysAC5UTR2, and two colonies were used for aysAC5UTR3.

cAMP assay with homogenized coral tissue

Each reaction contained 27.5 µl coral tissue sample (2.48 µg protein), 57.5 µl of a Master Mix (final concentrations: 100 mM TRIS pH7.2, 0.5 mM IBMx, 1 mM DTT, 20 mM CP, 1.58xCP CPK, and 5 mM $MgCl_2$), 10 µl of $NaHCO_3^-$/NaCl stock solutions (final $[HCO_3^-]$: 0, 5, 10, 20, 40 mM, with NaCl used to control for Na^+ ions), and 5 µl 100 mM ATP. Assays were performed in triplicate for each condition. After a 90 minute incubation shaking at 300 rpm, the reactions were stopped using 100 µl 0.2 N HCl. The solutions were then assayed using a cAMP EIA kit (Enzo Life Sciences), following the standard protocol.

Recombinant protein expression and cAMP assay

Based on the nucleotides sequences obtained by RT-PCR, primers were designed around the C1C2 catalytic domains and modified for use with the Gateway Cloning Technology system (Invitrogen). Modifications included the addition of a four nucleotide-long overhang to the forward primer which allowed for the insertion of the catalytic domains into a pENTR/D-TOPO entry vector (Invitrogen) and a stop codon to the reverse primer. The truncated sAC gene was then "shuffled" into pDEST17, a destination vector that adds an N-terminal 6xHis tag to the inserted sequence via a LR Recombination reaction (Invitrogen). PCR amplification and sequencing of both plasmids confirmed the sequence was unaltered and remained in the correct reading frame through each step. The pDEST17 vector containing the truncated sAC gene was then used to transform BL21-(AI) *E. coli* cells, which allow induction of gene expression through the addition of L-arabinose. The protocol used for expressing and purifying recombinant aysAC$_{60}$ was modified from the Gateway protocol. As suggested, transformed BL21-(AI) *E. coli* cells were cultured in LB broth containing ampicillin (100 μg ml^{-1}) overnight and diluted to an OD_{600} of 0.05-0.1 the follow morning. For maximum yield, the final volume of cell cultures was scaled up from the manual's suggested 250 μl to 1 L. These cultures were incubated until a new OD_{600} of ~0.4 was reached (~3 hours later). Expression was then induced with 20% L-arabinose. The cultures were incubated at 18 °C, shaking, for six hours. The *E. coli* were then pelleted and stored at -80 °C. Cultures used for determining sAC stimulation by bicarbonate were grown at ~30 °C instead of 18 °C. Pellets were thawed and lysed, and the recombinant protein was purified using Ni-NTA Superflow columns (Qiagen). Western blot using an anti-HIS tag antibody (Qiagen) was performed on fractions from each step of the purification, to confirm the expression and elution of the recombinant protein. The elution containing coral aysAC$_{60}$ was immediately used in cAMP assays [100 mM Tris (pH 7.5), 1 mM DTT, varying $MgCl_2$, $MnCl_2$, $CaCl_2$, and NaCl (see Table 2.2) 5 mM ATP] and stopped with 0.1 N HCl to minimize the potential loss of enzymatic activity and stored at -20 °C. Assays using recombinant aysAC$_{60}$ were performed to

measure HCO_3^--stimulated cAMP production and measure dose-responses (0 μM-1 mM; concentrations prepared by serial dilution) to the drugs KH7, 4CE, and 2',5'-dideoxyadenosine (dissolved in DMSO). cAMP was measured using either cAMP EIA kits (Enzo Life Sciences) or cAMP ELISA kit (Arbor Assays).

Western blot

Custom, polyclonal antibodies were created against an epitope predicted by the *A. yongei* sAC transcript. The peptide (LPGDKHEDDPARAL) lies in a highly conserved region of the enzyme's second catalytic domain. Coral tissue was removed from the calcium carbonate skeleton using pressurized air and collected into filtered seawater supplemented with 2 mM PMSF. The tissue was spun down for 10 minutes at 3,000 g to remove any symbiotic zooxanthellae. Coral tissues were also homogenized in S22 Buffer (450 mM NaCl, 10 mM KCl, 58 mM $MgCl_2$, 10 mM $CaCl_2$, 100 mM Hepes, final pH 7.8) with Protease Inhibitor Cocktail (Sigma) and PhosStop (Roche) added. A Bradford protein assay was used to determine the protein concentrations of samples. Tissue samples were combined with 2x Laemmli buffer (5% β-mercaptoethanol) in a 1:1 ratio, and denatured at 96 ºC for 5 minutes (or 70 º for 15 minutes; no differences were observed by changing the denaturation step) before loading into a polyacrylamide gel (Bio-Rad Mini-Protean TGX gel). Protein concentrations ensured that equal amounts of sample protein were loaded, then gels were run at 60 V for 30 minutes and then 200-300 V until finished. Blotting was performed using 0.2 μm PVDF membranes and the Standard Molecular Weight protocol (TransBlot Turbo, BioRad). Membranes were incubated overnight at 4 ºC in primary antibodies (coral sAC, 1:10,000 or 1:20,000) prepared in milk/TBST. The following day, membranes underwent three 10 minute washing steps with TBS-T before incubation for 1 hour in secondary antibodies (Goat Anti Rabbit-HRP 1:10,000), also prepared in milk/TBS-T. Membranes were imaged following three additional TBS-T washes. To validate

the coral sAC antibody, pre-immune and pre-adsorption controls were performed using both homogenized tissue and recombinant protein from transformed *E. coli* (+/- induction by L-arabinose).

Immunofluorescence Microscopy

Coral fragments were fixed overnight in S22 buffer with 3% paraformaldehyde at 4 ºC. The corals were then decalcified using Ca-free S22 Buffer with 0.5 M EDTA; the buffer was replaced daily until the skeleton had completely dissolved (~7-10 days later). The tissue was then dehydrated, embedded in paraffin, and sectioned (7 or 10 μm thick) on slides and stored at 4 ºC until later use. Before staining, tissue sections were rehydrated and permeabilized with 0.2% triton-x in PBS for 60 minutes, and then blocked with 2% normal goat serum in PBS for 60 minutes. Samples were then incubated with the coral sAC antibody (1:100) overnight at 4 ºC, stained with the secondary antibody GAR (Alexa555 1:500), and stained with Hoescht (1:1000) to visualize DNA/nuclei. Wash steps were performed using PBS-Tx and controls with pre-adsorbed peptide (6x), pre-immune serum, or without primary antibody (secondary antibody only) added were performed as well. Slides were imaged using an epifluorescence microscope (Zeiss AxioObserver Z1).

To prepare thin sections for microscopy, *A. yongei* fragments were fixed overnight at 4 °C in 4% paraformaldehyde in S22 buffer. Corals were then decalcified as described above. Fixed tissue was then washed with 0.15 M glycine/phosphate buffer, embedded in 10% gelatin/phosphate buffer and infused with 2.3 M sucrose/phosphate buffer overnight at 4 °C. One cubic millimeter cell blocks were mounted onto specimen holders and snap frozen in liquid nitrogen. Ultracryomicrotomy was carried out at 100 °C on a Leica Ultracut UCT with EM FCS cryoattachment (Leica, Bannockburn, IL) using a Diatome diamond knife (Diatome US, Hatfield, PA). Frozen sections (90 nm for TEM or 400 nm for immunofluorescence) were picked up with a

1:1 mixture of 2.3 M sucrose and 2% methyl cellulose (15cp), as described by Liou et al. (Liou et al., 1996). Slides were blocked for 1 hour and incubated overnight with sAC antibody was at a dilution of 1:100.

Isolated coral nuclei were prepared from ~3-5 cm coral nubbins homogenized with glass beads (425-600 μm) in homogenization buffer ([final] = 2x Phosphate Buffer Solution, 200 mM EDTA, 0.5% sucrose) supplemented with protease inhibitors ([final] = DTT 2 mM, PMSF 1 mM, BHH 10 mM, and IBMX 0.5 mM). The coral was vortexed with the beads in buffer for 2 minutes, in pulses, and the slurry was pulled through a 21g syringe to shear the mucus. The crude homogenate was layered over an equal volume of chilled 20% sucrose and centrifuged at 2000 g for 2 minutes at 4 °C. The top layer was removed and centrifuged at 1000 g for 5 minutes at 4 °C. The pellet was resuspended in homogenization buffer with protease inhibitors. An equal volume of 1 M sucrose and 2x volume of Optiprep ([final] = 30%) were added to the sample. The tubes were inverted to mix and then centrifuged at 10,000 g for 20 minutes at 4 °C. The pellet was resuspended in a minimal volume of homogenization buffer and protease inhibitors and then stained with sAC antibody (diluted 1:100) overnight.

Nuclear isolation Western blot

A fragment of *A. yongei* was flash frozen in liquid nitrogen and tissue was removed from the skeleton using 5 ml of S22 Buffer supplemented with Protease Inhibitor Cocktail (Sigma) and PhosStop (Promega)(S22+). Homogenized tissue was passed through a 19g then 21g needle to break up the slime. 1 ml of homogenized tissue was set aside and stored on ice as "Crude Homogenate". The remaining homogenized tissue was divided into four 750 μl aliquots. Each aliquot was carefully layered over 750 μl of a 20% sucrose solution. These tubes were centrifuged at 2000 g for 2 minutes to pellet the zooxanthellae. The supernatant was removed and then centrifuged a second time at 1000 g for 5 minutes. This new supernatant (S1) was set aside

on ice for a future step. Each pellet was resuspended in 50 µl 1 M sucrose, 50 µl of S22+, and 100 µl of 60% Optiprep (total volume for each pellet was 200 µl, the [final] of Optiprep = 30%) and centrifuged at 10,000 g for 20 minutes. The supernatant was discarded and each pellet was resuspended in 50 µl S22+ Buffer. The four aliquots were recombined for a total volume of 200 µl and centrifuged again at 10,000 g for 20 minutes and the pellets were resuspended in 100 µl S22+ Buffer and stored on ice labeled as the "nuclear" fraction. (S1) was then centrifuged at maximum speed (21,000 g) for 30 minutes. The supernatant was saved as the "Cytosol" fraction and the pellet was resuspended in S22+ Buffer and labeled as the "membrane-enriched fraction". The protein concentration of the Crude Homogenate (CH), Nuclear (N), Cytosol/Soluble (C), and Membrane-enriched (M) fractions was determined by Bradford Assay. Samples were combined with 2x Laemmli Buffer (BioRad) and incubated at 70 °C for 15 minutes if they were to be used with the coral sAC antibody, or at room temperature for 15 minutes if they were going to be used with an antibody against the Na+/K+-ATPase (NKA) as was optimized previously (Barott et al., 2015). Each lane of the polyacrylamide gel was loaded with 4.45 µg of protein. The gel was run and the membrane was blotted and blocked in milk TBS-T as described above. The left half of the membrane was incubated in sAC antibody (1:10,000) and the right half was incubated in NKA antibody (1:5,000) overnight.

Acknowledgements

Chapter 2, in part, is a reprint of material as it may appear in the following citation: Barott, K. L., Helman, Y., Haramaty, L., Barron, M. E., Hess, K. C., Buck, J., Levin, L. R., Tresguerres, M. (2013). High adenylyl cyclase activity and in vivo cAMP fluctuations in corals suggest central physiological role. *Scientific Reports*, *3* (1379). https://doi.org/10.1038/srep01379. The dissertation author was a coauthor on this paper. Chapter 2, in part, also contains material as

it may appear in the following citation Tresguerres, M., Barott, K. L., Barron, M. E., & Roa, J. N. (2014). Established and potential physiological roles of bicarbonate-sensing soluble adenylyl cyclase (sAC) in aquatic animals. *The Journal of Experimental Biology, 217,* 663–72. https://doi.org/10.1242/jeb.086157. The dissertation author was a coauthor on this publication.

Figures

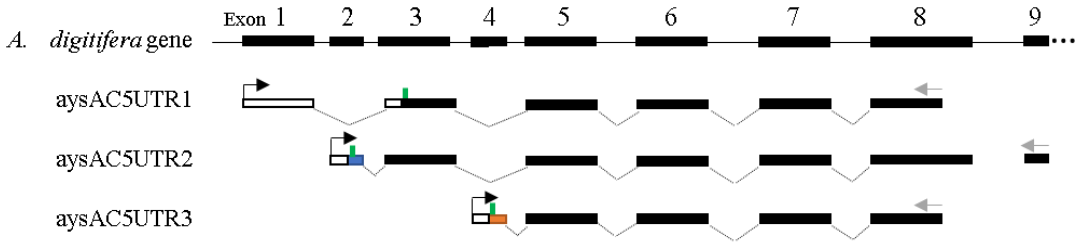

Figure 2.1: 5'RACE products aligned with the *A. digitifera* sAC gene. For simplicity, the introns (thin black lines, shown in *A. digitifera* gene sequence only) and exons (thick boxes, numbered 1-9 above the gene) are not shown to scale. White boxes represent untranslated exon sequence (regions occurring after the promoter, indicated by right facing arrows, but before the start codon, indicated by vertical green lines). Black boxes are translated regions of exons. The blue and orange boxes indicate regions in translated exons that are unique to the splice variants. Thin, dotted lines in V shapes indicate splicing between exons. aysAC5UTR1 has the longest 5'UTR, which is derived from two exons (Exon 1 and Exon3). The promoter, 5'UTR, and start codon for aysAC5UTR2 are located on an exon (Exon 2) that is spliced out of aysAC5UTR1. Similarly, the promoter, 5'UTR, and start codon for aysAC5UTR3 are located on an exon (Exon 4) that is spliced out of both aysAC5UTR1 and aysAC5UTR2. Gray, left-facing arrows indicate the reverse primer binding sites. Each transcript likely extends further than is indicated by the RACE PCR product.

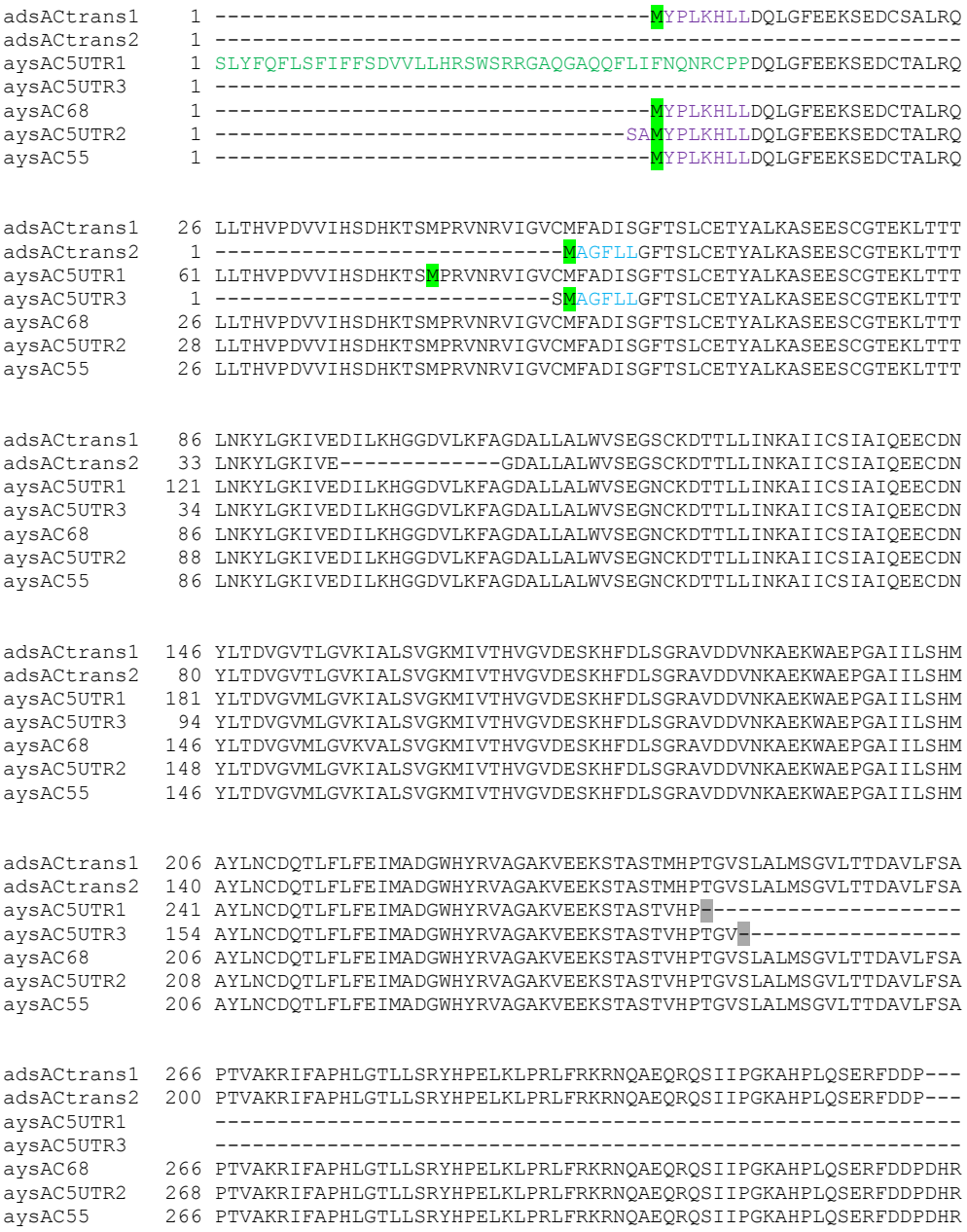

Figure 2.2: Alignment of *A. yongei* and *A. digitifera* sAC sequences. The accession numbers for *A. yongei* PCR products are: aysAC5UTR1 (MG269969), aysAC5UTR2 (MG269970), aysAC5UTR3 (MG269971), and aysAC$_{68}$ (MG269972). The accession numbers for *A. digitifera* transcripts are: adsACtrans1 (aug_v2a.21187), adsACtrans2 (aug_v2a.10515). Only aysAC$_{68}$ encodes for a full-length sAC protein, the others are partial sequences. There are three 5'UTR regions (their unique regions are shown in green, purple, and blue text respectively) with three different start codons (the first methionine of each sequence is highlighted green). The region of aysAC$_{68}$ transcript that does not match the genome is indicated by red text. The location of the stop codon is shown highlighted red. The end of PCR sequences (determined by PCR- not a stop codon) are highlighted gray.

```
adsACtrans1  323 ------------------------------------------------------------
adsACtrans2      ------------------------------------------------------------
aysAC5UTR1       ------------------------------------------------------------
aysAC5UTR3       ------------------------------------------------------------
aysAC68      326 TDVFTKLSEQDIADLRAYVSKPVLSKIDHGQDLDWLSEMRQVSVLFINMVLPTKGNSNSL
aysAC5UTR2   328 TDVFTKLSEQDIADLRAYVSKPVLSKIDHGQ-----------------------------
aysAC55      326 TDVFTKLSEQDIADLRAYVSKPVLSKIDHGQNLDWLSEMRQVSVLFINMVLPTKGNSNSL


adsACtrans1  323 -----------------GNLNKVFSFDKGCTFVVIFGLPGDKHEDDPARALKAAHRILDS
adsACtrans2      ------------------------------------------------------------
aysAC5UTR1       ------------------------------------------------------------
aysAC5UTR3       ------------------------------------------------------------
aysAC68      386 ALQKAFEVIYECSKRLRGNLNKVFSFDKGCTFVVIFGPPGDKHEDDPARALKAAHRIVDT
aysAC5UTR2       ------------------------------------------------------------
aysAC55      386 ALQKAFEVIYECSKRHRGNLNKVFSFDKGCTFVVIFGLPGGKHEDDPARALKAAHRIVDT


adsACtrans1  366 LHQIMDITNESIGVTTGRAFCGVVGHRDRHEYTVIGRKVNMAARLMMNYPRVLSCDDDTY
adsACtrans2      ------------------------------------------------------------
aysAC5UTR1       ------------------------------------------------------------
aysAC5UTR3       ------------------------------------------------------------
aysAC68      446 LHQIMDITNESIGVTTGRAFCGVVGHRDRHEYTVIGRKVNMAARLMMNYPGVLSCDDDTY
aysAC5UTR2       ------------------------------------------------------------
aysAC55      446 LHQIMDITNESIGVTTGRAFCGVVGHRDRHEYTVIGRKVNMAARLMMNYPGVLSCDDDTY


adsACtrans1  426 RLAKSKLKKEDFVTLPFVELKGIAEPGIVREYNKHHEITKKFESWCTLQFSHFEIRCHPG
adsACtrans2      ------------------------------------------------------------
aysAC5UTR1       ------------------------------------------------------------
aysAC5UTR3       ------------------------------------------------------------
aysAC68      506 RLAKSKLKKEDFVTLPFVELKGIAEPGIVREYNKHHDREVEEEEFE---------YPIIG
aysAC5UTR2       ------------------------------------------------------------
aysAC55      506 RLAKSKLKKEDFVTLPFVELKGIAEPGIVREYNK-------------------------


adsACtrans1  486 RSDEVNEIKQLLQTIKSNDALGTSNTRFVSIEGEGGIGKTRILEEIMDVAEDEDYKVDFV
adsACtrans2      ------------------------------------------------------------
aysAC5UTR1       ------------------------------------------------------------
aysAC5UTR3       ------------------------------------------------------------
aysAC68      557 RSDEVNEIKQLLQTIKSNDALGTSNTRFVSIEGEGGIGKTRILEEIMDVAEDEDYK----
aysAC5UTR2       ------------------------------------------------------------
aysAC55            ----------------------------------------------------------


adsACtrans1  546 EADLGHAHTPYYVVQNLVTNLLELDTCRTAPEREHALMQHITDLKLRERMFLLNYLLGTH
adsACtrans2      ------------------------------------------------------------
aysAC5UTR1       ------------------------------------------------------------
aysAC5UTR3       ------------------------------------------------------------
aysAC68          ------------------------------------------------------------
aysAC5UTR2       ------------------------------------------------------------
aysAC55          ------------------------------------------------------------


adsACtrans1  606 IPPNPDFAYLDSDEIIAHFHTLLFEIVHQFAVSQPCLFAVDNAQFIDPESWDFLEDLSKD
adsACtrans2      ------------------------------------------------------------
aysAC5UTR1       ------------------------------------------------------------
aysAC5UTR3       ------------------------------------------------------------
aysAC68          ------------------------------------------------------------
aysAC5UTR2       ------------------------------------------------------------
aysAC55          ------------------------------------------------------------
```

Figure 2.2: Alignment of *A. yongei* and *A. digitifera* sAC sequences *continued*.

```
adsACtrans1  666 SHAILVLALRPFSSSNPPCETAERLIGHNTTKRIKLGGLPAEVMSDLACQLMDVMYIPSE
adsACtrans2      ------------------------------------------------------------
aysAC5UTR1       ------------------------------------------------------------
aysAC5UTR3       ------------------------------------------------------------
aysAC68          ------------------------------------------------------------
aysAC5UTR2       ------------------------------------------------------------
aysAC55          ------------------------------------------------------------

adsACtrans1  726 LDEIIRRKSQGVASWCEQLIKDMLTSDIIKIVDSNQAFSDPDDHTESSATSTSIFASQNH
adsACtrans2      ------------------------------------------------------------
aysAC5UTR1       ------------------------------------------------------------
aysAC5UTR3       ------------------------------------------------------------
aysAC68          ------------------------------------------------------------
aysAC5UTR2       ------------------------------------------------------------
aysAC55          ------------------------------------------------------------

adsACtrans1  786 KDRPEVSRPLTPFYSEDDHLKAGREDLQRKSFLKPQSLFEGRRVSQGATENLLSPAGRWS
adsACtrans2      ------------------------------------------------------------
aysAC5UTR1       ------------------------------------------------------------
aysAC5UTR3       ------------------------------------------------------------
aysAC68          ------------------------------------------------------------
aysAC5UTR2       ------------------------------------------------------------
aysAC55          ------------------------------------------------------------

adsACtrans1  846 KLDAPISNSFFSFRRVSELPEQELLEEVQSFHLDPKDFVRASRNSMPFDTNNVCIVTPGV
adsACtrans2      ------------------------------------------------------------
aysAC5UTR1       ------------------------------------------------------------
aysAC5UTR3       ------------------------------------------------------------
aysAC68          ------------------------------------------------------------
aysAC5UTR2       ------------------------------------------------------------
aysAC55          ------------------------------------------------------------

adsACtrans1  906 DLAKVVVPDSVKDMVLARVDRMLPLEQLTLKCSSILGAEFHRNLLQAILPKSIQKRLDLV
adsACtrans2      ------------------------------------------------------------
aysAC5UTR1       ------------------------------------------------------------
aysAC5UTR3       ------------------------------------------------------------
aysAC68          ------------------------------------------------------------
aysAC5UTR2       ------------------------------------------------------------
aysAC55          ------------------------------------------------------------

adsACtrans1  966 VYNLAKESILECASLAAQHQIAHNHHGFYDFNDPTHSQQHXXXXXXXXXXNVASSIHASV
adsACtrans2      ------------------------------------------------------------
aysAC5UTR1       ------------------------------------------------------------
aysAC5UTR3       ------------------------------------------------------------
aysAC68          ------------------------------------------------------------
aysAC5UTR2       ------------------------------------------------------------
aysAC55          ------------------------------------------------------------

adsACtrans1 1026 YCGCHADEVTKVLNLSRLMTPNGPKKHCLYLKFVNTYVQETLYSLWLEDQRKEIHEKAAM
adsACtrans2      ------------------------------------------------------------
aysAC5UTR1       ------------------------------------------------------------
aysAC5UTR3       ------------------------------------------------------------
aysAC68          ------------------------------------------------------------
aysAC5UTR2       ------------------------------------------------------------
aysAC55          ------------------------------------------------------------
```

Figure 2.2: Alignment of *A. yongei* and *A. digitifera* sAC sequences *continued*.

```
adsACtrans1 1086 FLESQAHKCKSCGGGGFVISIDLSQQASHNKDVKRVTGMTGRTRAEVSSKMAKKRKSSEM
adsACtrans2      ------------------------------------------------------------
aysAC5UTR1       ------------------------------------------------------------
aysAC5UTR3       ------------------------------------------------------------
aysAC68          ------------------------------------------------------------
aysAC5UTR2       ------------------------------------------------------------
aysAC55          ------------------------------------------------------------

adsACtrans1 1146 RQKVQSQGAFSARAHERSEVRSKIRTSQTGDKESQEHTSDRRRADRKLPETSEAIKNAVI
adsACtrans2      ------------------------------------------------------------
aysAC5UTR1       ------------------------------------------------------------
aysAC5UTR3       ------------------------------------------------------------
aysAC68          ------------------------------------------------------------
aysAC5UTR2       ------------------------------------------------------------
aysAC55          ------------------------------------------------------------

adsACtrans1 1206 EQTEGGKKRSCLCRFFCGKSVNPTKEESSETQNQLLLKISHKDKSAVNGKGIVSDESASR
adsACtrans2      ------------------------------------------------------------
aysAC5UTR1       ------------------------------------------------------------
aysAC5UTR3       ------------------------------------------------------------
aysAC68          ------------------------------------------------------------
aysAC5UTR2       ------------------------------------------------------------
aysAC55          ------------------------------------------------------------

adsACtrans1 1266 SSCSSSDGASNSRKKTTYIRSRVLHQNSQRSSETLFARVFTRLLHWRGRMINAYAGVIEC
adsACtrans2      ------------------------------------------------------------
aysAC5UTR1       ------------------------------------------------------------
aysAC5UTR3       ------------------------------------------------------------
aysAC68          ------------------------------------------------------------
aysAC5UTR2       ------------------------------------------------------------
aysAC55          ------------------------------------------------------------

adsACtrans1 1326 AHLVGWNGWGKTYEEIGKNRCQDSSLYLDAVDMLTVAHLYCVSLAFRLAIGGVTTAISSG
adsACtrans2      ------------------------------------------------------------
aysAC5UTR1       ------------------------------------------------------------
aysAC5UTR3       ------------------------------------------------------------
aysAC68          ------------------------------------------------------------
aysAC5UTR2       ------------------------------------------------------------
aysAC55          ------------------------------------------------------------

adsACtrans1 1386 EHALAIAKQVQDSHLKTACIPLLAQGFLMAAKISSCLEVLKELNSSAQESNDLHGQALYM
adsACtrans2      ------------------------------------------------------------
aysAC5UTR1       ------------------------------------------------------------
aysAC5UTR3       ------------------------------------------------------------
aysAC68          ------------------------------------------------------------
aysAC5UTR2       ------------------------------------------------------------
aysAC55          ------------------------------------------------------------

adsACtrans1 1446 CCCFDVILEAGWKLEDISNVMQFTITMSSDPAFSADVLPKFYLNASLALWYARKRDWENA
adsACtrans2      ------------------------------------------------------------
aysAC5UTR1       ------------------------------------------------------------
aysAC5UTR3       ------------------------------------------------------------
aysAC68          ------------------------------------------------------------
aysAC5UTR2       ------------------------------------------------------------
aysAC55          ------------------------------------------------------------
```

Figure 2.2: Alignment of *A. yongei* and *A. digitifera* sAC sequences *continued*.

```
adsACtrans1 1506 ESFFSTASALEPPTLEVYMSVHGFVKMIEFWLLKFQENGKIKQQQQEIQRV-
adsACtrans2      ----------------------------------------------------
aysAC5UTR1       ----------------------------------------------------
aysAC5UTR3       ----------------------------------------------------
aysAC68          ----------------------------------------------------
aysAC5UTR2       ----------------------------------------------------
aysAC55          ----------------------------------------------------
```

Figure 2.2: Alignment of *A. yongei* and *A. digitifera* sAC sequences *continued*.

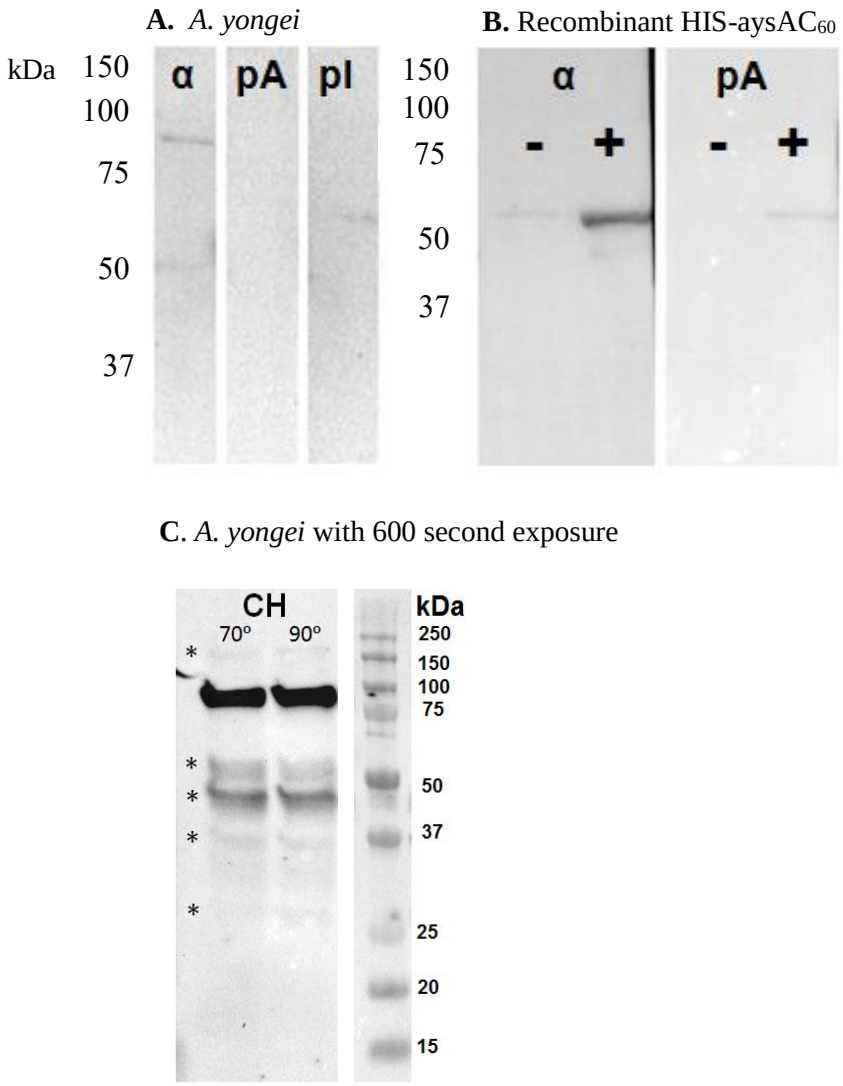

Figure 2.3: Western blot validation of the sAC antibody. Western blot of A) homogenized *A. yongei* tissue incubated with coral sAC antibody (α) indicates a 90 kDa protein and a 50 kDa protein. Both bands disappear when the membrane is incubated with antibody pre-adsorbed overnight with peptide (pA) or incubated with pre-immune serum (pI), as expected. When B) recombinant aysAC$_{60}$ protein from *E. coli* is used, the antibody (α) recognizes a ~63 kDa (the size is slightly increased by the 6x HIS tag) protein in induced cells (+) and faint basal expression in uninduced cells (-). The 63 kDa band is greatly reduced when the membrane is incubated with antibody pre-adsorbed with peptide (pA). These westerns show the sAC antibody recognizes sAC with high specificity. When membranes containing protein from C) homogenized *A. yongei* tissue are viewed with a longer, 600 second exposure, additional bands visible (~40-60 kDa, >200 kDa), as indicated by asterisks (*). Samples denatured at 70 °C vs 90 °C showed no difference in band pattern.

A. Homogenized *A. yongei* tissue

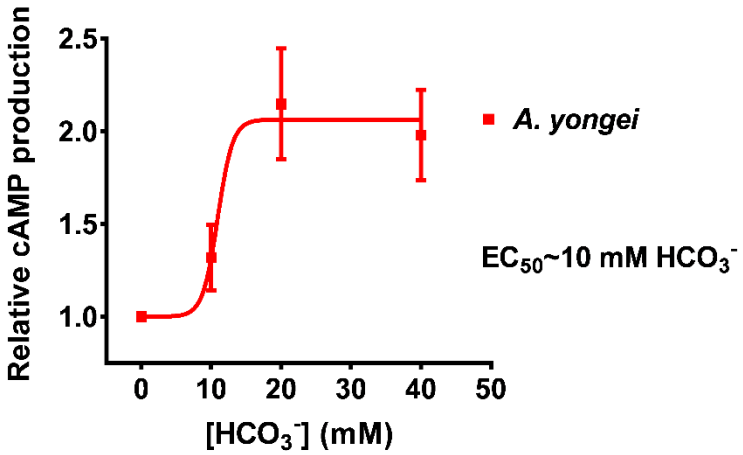

B. Recombinant aysAC$_{60}$ with drugs

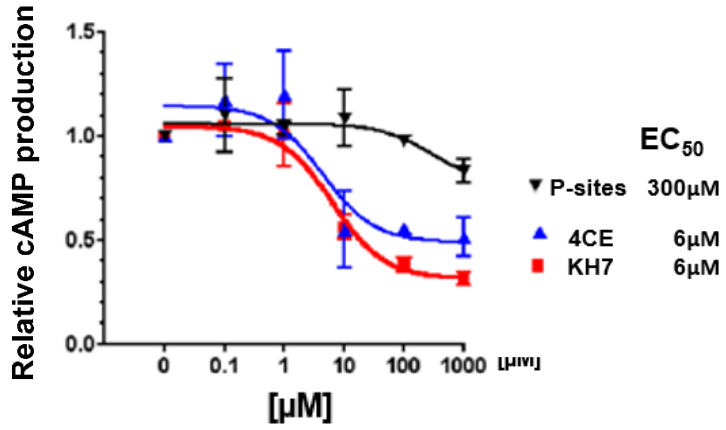

C. Recombinant aysAC$_{60}$ with HCO_3^-

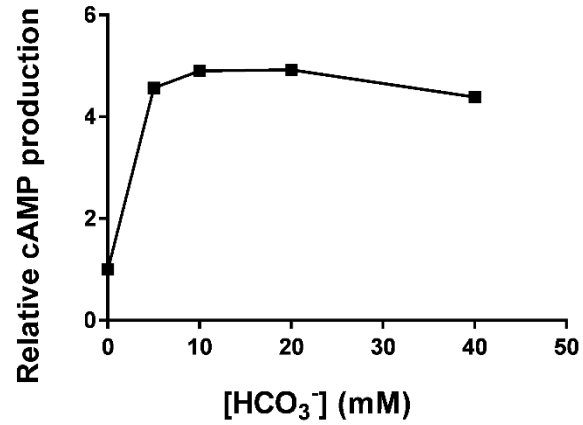

Figure 2.4: cAMP production by coral tissue and aysAC$_{60}$. A) Homogenized *A. yongei* tissue is stimulated by increasing concentrations of HCO_3^-. The EC$_{50}$ is ~10 mM HCO_3^-. B) Recombinant aysAC$_{60}$ was sensitive to the sAC inhibitors, 4CE and KH7; each had an EC$_{50}$ of ~6 µM drug. aysAC$_{60}$ was not inhibited by the tmAC inhibitor P-sites (2,5-dideoxyadenosine). C) Recombinant aysAC$_{60}$ was sometimes stimulated by bicarbonate, but results varied. Only one example of a bicarbonate stimulation curve is shown here.

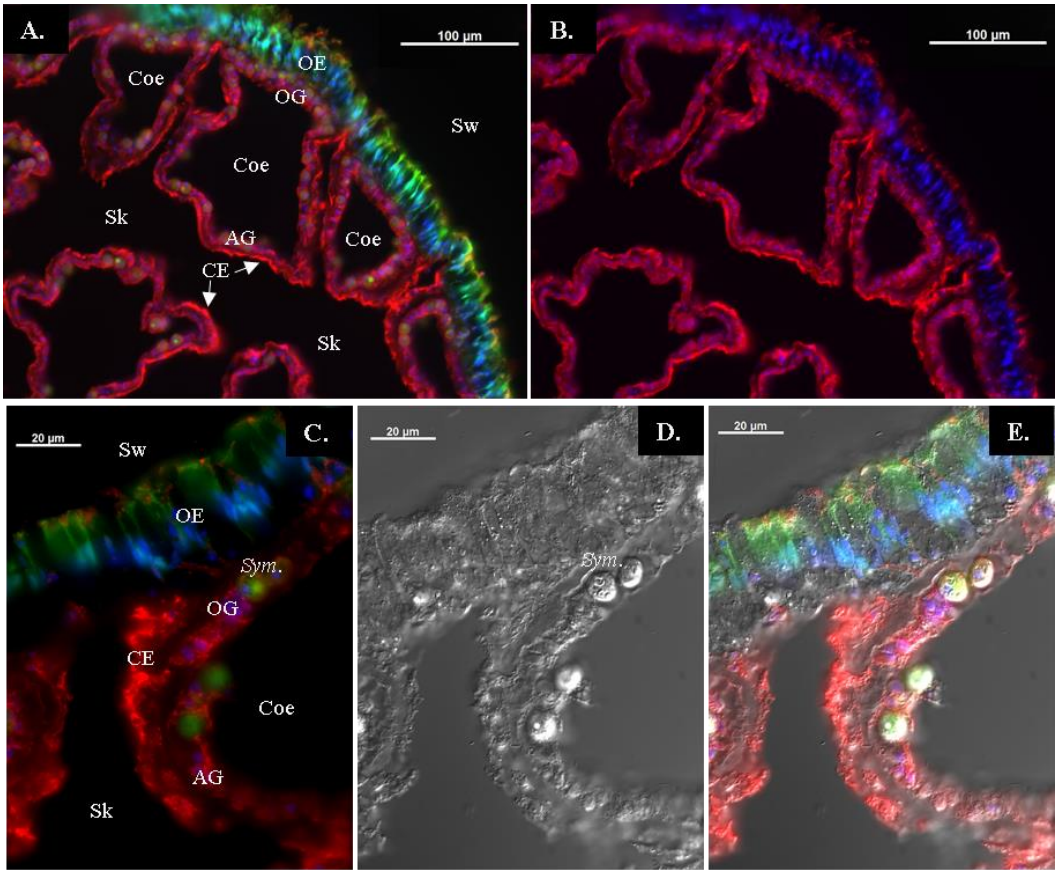

Figure 2.5: Immunofluorescence microscopy. sAC (red fluorescence) is located in all four tissue layers of coral as seen A) with endogenous Green Fluorescent Protein (GFP) (green fluorescence) and B) without. In all images, nuclei are stained by Hoechst (blue fluorescence). A) sAC is most abundantly expressed in the calicoblastic epithelium, indicated by white arrows. C) At higher magnification, it is confirmed that sAC is most abundantly expressed in the calicoblastic epithelium. D) Differential Interference Contrast (DIC) and E) merged images are also shown. F) At higher magnification, staining in the oral ectodermis shows sAC near the apical membrane (white arrows) and absent from nematocyst cells (white asterisks). Furthermore, sAC staining occurs in gastrodermis cells both with and without *Symbiodinium* G) DIC and H) merged images also shown. I) Higher magnification of the aboral tissues shows that staining in the calicoblastic epithelium is robust and cytosolic. J) DIC and K) merged imaged are also shown. Nuclei (blue fluorescence) are also stained.

Abbreviations: Sw- Seawater, Coe- Coelenteron, Sk- Skeleton, *Sym*.- *Symbiodinium* (algae), OE- Oral Ectodermis, OG- Oral Gastrodermis, AG- Aboral Gastrodermis, CE- Calicoblastic Epithelium

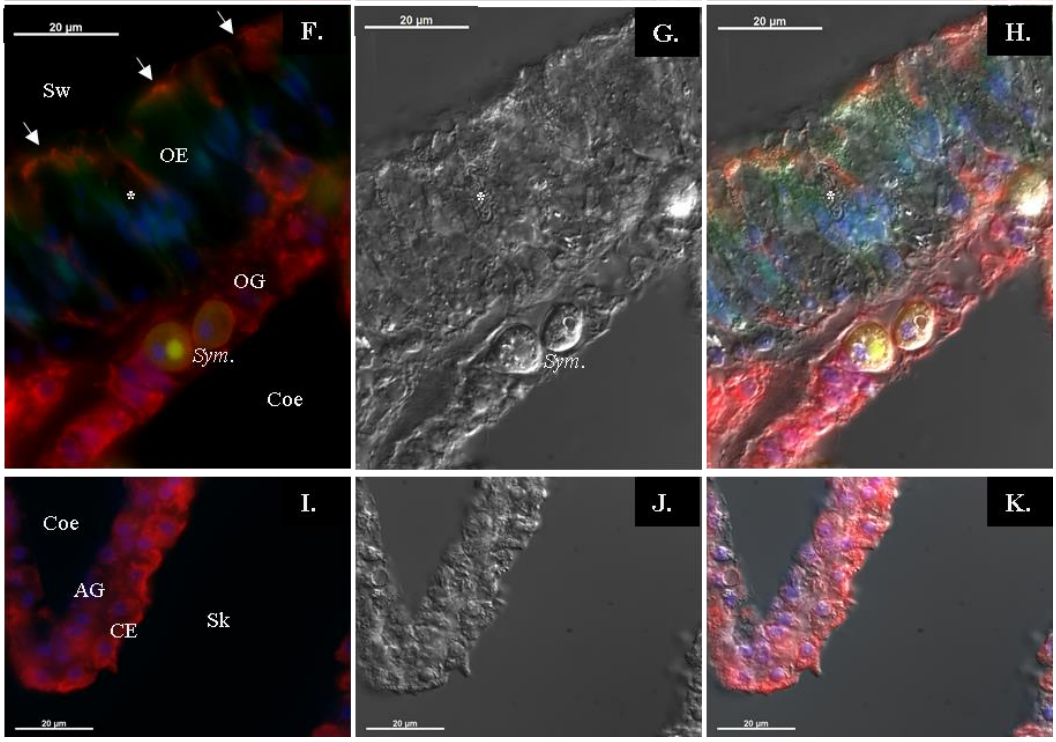

Figure 2.5: Immunofluorescence microscopy *continued.*

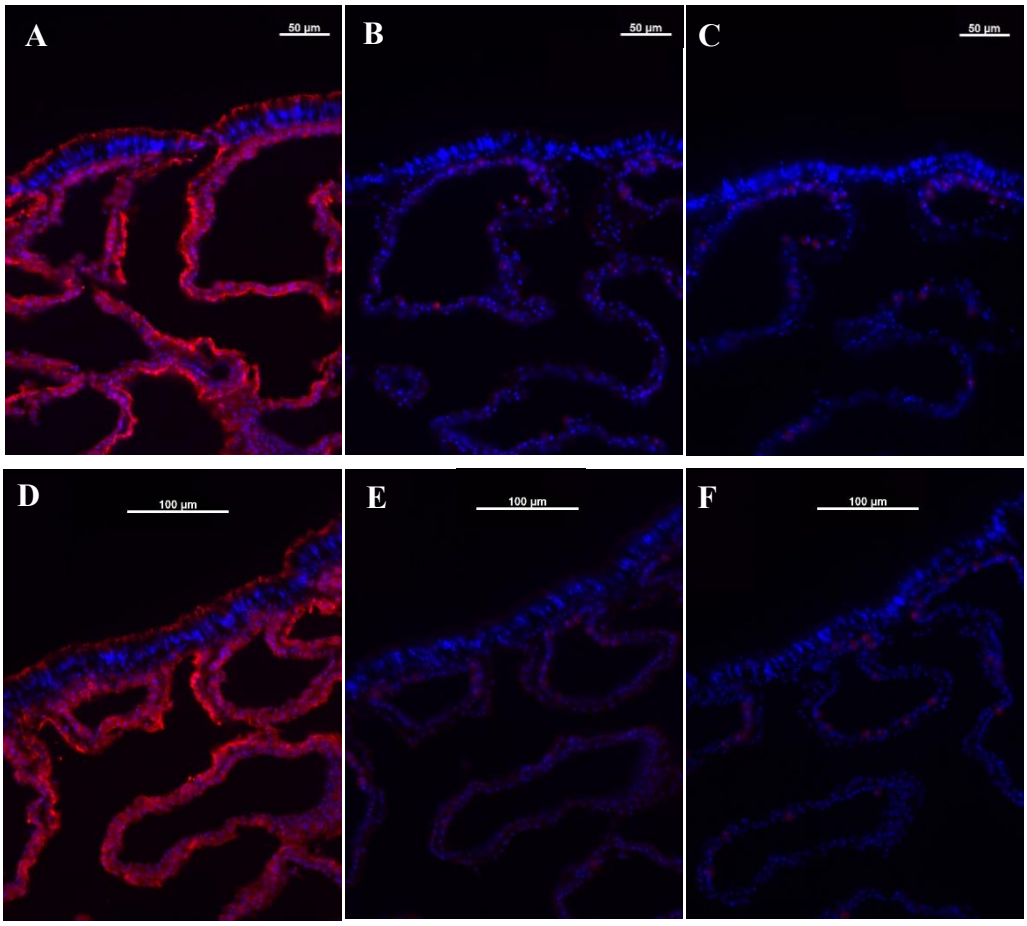

Figure 2.6: Immunofluorescence microscopy controls indicate the sAC antibody (red fluorescence) is specific. *A. yongei* tissue stained with A) sAC antibody B) sAC antibody pre-adsorbed overnight with peptide and C) no primary antibody (secondary antibody only) imaged at the same exposure time. *A. yongei* tissue stained with D) sAC antibody E) pre-immune serum and F) no primary antibody (secondary antibody only) imaged at the same exposure time. Nuclei were stained with Hoechst (blue fluorescence).

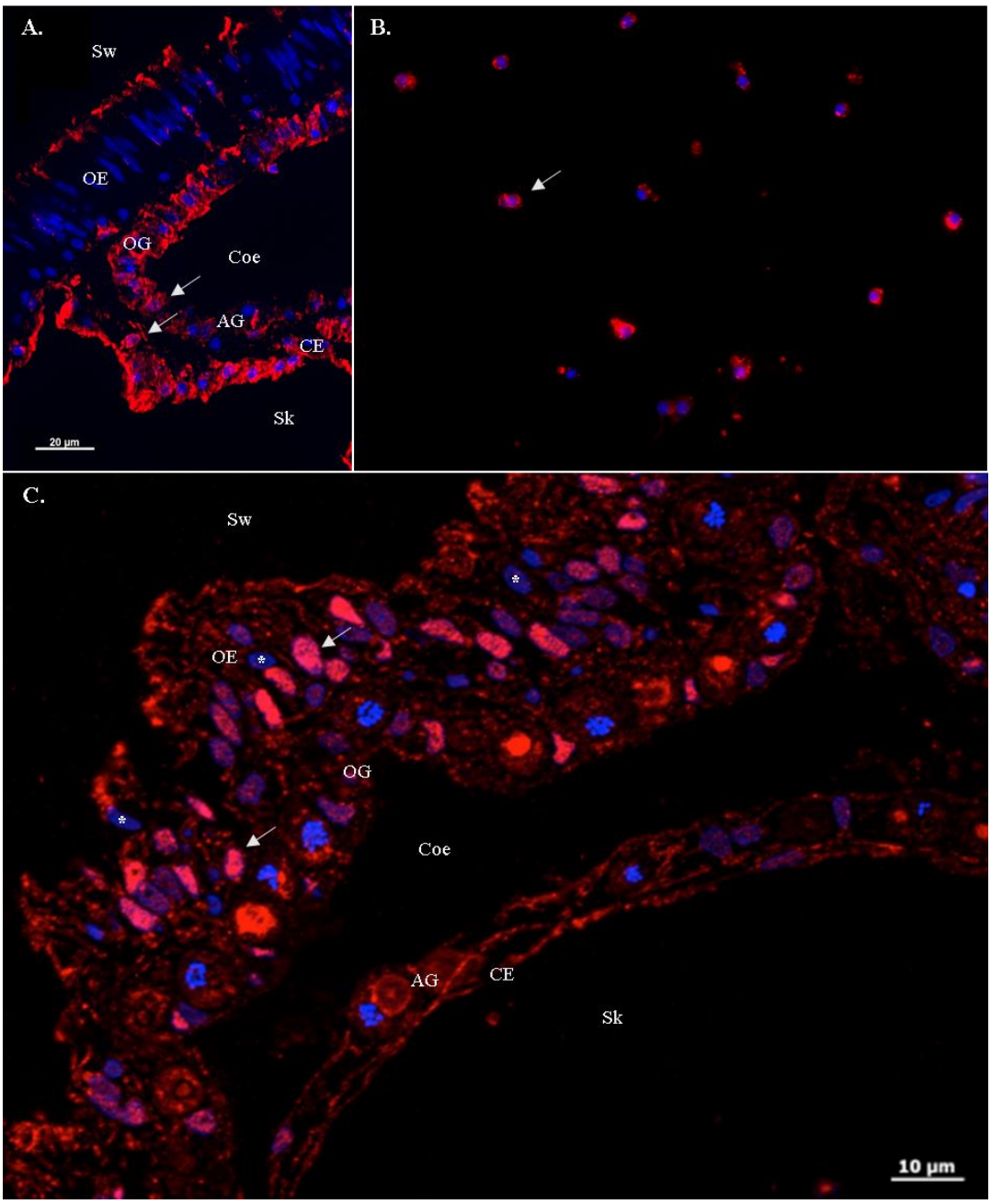

Figure 2.7: Immunofluorescence microscopy shows sAC staining (red fluorescence) in the nuclei (Hoechst- blue fluorescence) of *A. yongei* cells. sAC was observed in A) nuclei of a small number of coral cells (indicated by white arrows) in10µm-thick tissue sections, B) nuclei isolated by centrifugation (white arrows), and C) many nuclei (white arrows), but not all (sAC-free nuclei indicated by white asterisks) in coral cells from 400 nm- thin tissue sections (unpublished results, Dr. Katie Barott).

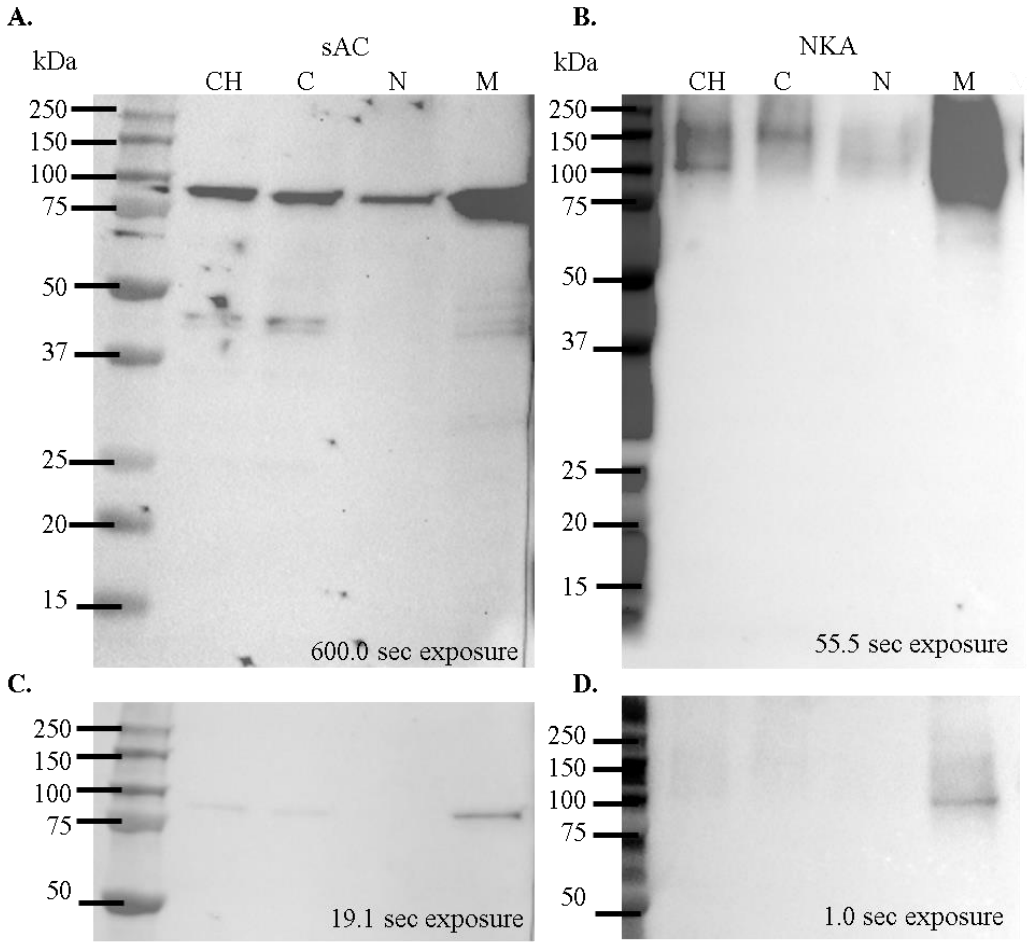

Figure 2.8: Western blot confirmation of fractionation protocol. A) Long exposure of fractionated cellular components (4.45 µg / lane) from homogenized *A. yongei* tissue using the coral sAC antibody. sAC is present in the nuclear fraction (N), but also in the crude homogenate (CH), cytosol (C) and associated with the membrane (M). B) The same samples (4.45 µg / lane) were incubated with primary antibody against the Na^+/K^+-ATPase (NKA). At a long exposure (the exposure times for the two antibodies are not comparable, as they have differing concentrations and affinities) there is not a clear band (100 kDa expected size) in the nuclear fraction; the low signal present is significant less than what is observed for the membrane-enriched fraction (M). This indicates the nuclear fraction was not contaminated with membrane samples during the nuclear isolation protocol. C) and D) show the same membranes at much shorter exposure times, before any oversaturation occurred.

Table 2.1: Primers used in RT-PCR, 5'RACE PCR, and sequencing of *A. yongei* sAC

Primer Name	Primer Sequence 5'--> 3'	Purpose
Set 1 FWD	GTGGAACGGAGAAACTAACGA	confirm/identify coral sAC
Set 1 REV	CTTCTACTTTAGCTCCAGCGACTC	transcripts using RT-PCR
Dup Set 1 FWD	CACGTGTTAATCGCGTGATAGG	
Dup Set 1 REV	CAACTTCCCTCAGATACCCACAAG	
0001F_MB	ATGTATCCATTGAAACATCTTTTAGATCAACT	clone sAC C1C2 cat. domains into
0002R_MB	CTTGTTGTATTCCCTCACTATTCCCGG	sequencing vector (TOPO cloning)
0003F_MB	CACCATGTATCCATTGAAACATCTTTTAGA	clone sAC C1C2 cat. domains into
0004F_MB	CACCATGTATCCATTGAAACATCTT	entry vector (pENTR/SD-TOPO)
0005R_MB	TCACTTGTTGTATTCCCTCACTATT	
0006F_MB	CCGTTATCACCCTGAACTCAA	obtain full-length sAC sequence
0007R_MB	ATCTGCCTCCACGAAATCAA	by PCR and RACE PCR (Clontech)
0008F_MB	GAAGTTCGAGAGTTGGTGTACTT	
0009R_MB	GGCCACCTAGTTTGATTCTCTT	
0010F_MB	GCAGCATATCACTGACCTCAA	
0011R_MB	GAATCTGGGACCACCACTTTAG	
0012F_MB	TGCAACTGAGAACCTTCTATCC	
0013R_MB	TAACCCGTTTCACGTCCTTATT	
0014F_MB	TACAGGAGACGTTATATTCCCTTTG	
0015R_MB	ATCCATTCCAACCAACCAGAT	
0016F_MB	GCGCTTCAAATTCTCGGAAA	
0017R_MB	TTGAAACTTCAACAGCCAGAAC	
0018F_MB	CGCGTGATAGGCGTGTGCATGTTTG	obtain full-length sAC sequence
0019F_MB	CAGGCCGAGCAGTTGATGACGTGAAT	by RACE PCR (Clontech)
0020F_MB	CCACAGTGCACCCAACTGGCGTTAG	
0021F_MB	GCTTGGCTCTCATGTCCGGCGTCCTTAC	
0022F_MB	GGAGATGCGCCAGGTCTCAGTGCTGTTC	
0007F_MB	TTGATTTCGTGGAGGCAGAT	look for splice variants in
0008*f_MB	GTCGAAGAAGAAGAATTCGAATATCC	unknown section between
0010R_MB	TTGAGGTCAGTGATATGCTGC	0008F and 0009R
0009aR_MB	TGGGAATCCTTGGACAGAT	
0009bR_MB	CAAACAGAAGAGTGTGGAAATG	
0068R_MB	TTACTTGTAGTCTTCATCTTCT	Gateway Clone aysAC$_{68}$
0069R_MB	TTACTTGTAGTCTTCATCTTCTGCCA	splice variant from 3F/7R
0070R_MB	TTACTTGTAGTCTTCATCTTCTGCCACG	

Table 2.2: Combinations of cofactors tested for HCO_3^- stimulation of recombinant aysAC$_{60}$

Mg^{2+}	**Mn^{2+}**	**Ca^{2+}**	**+ NaCl***	**[HCO_3^-] assayed**
-	-	-	-	0 mM, 10 mM, 20 mM
5 mM	-	-	-	0 mM, 10 mM, 20 mM
5 mM	-	-	300 mM	0 mM, 10 mM, 20 mM
10 mM	-	-	-	0 mM, 10 mM, 20 mM
10 mM	-	-	300 mM	0 mM, 2.5 mM, 5 mM, 10 mM, 20 mM, 40 mM
15 mM	-	-	-	0 mM, 10 mM, 20 mM
20 mM	-	-	-	0 mM, 10 mM
-	5 mM	-	-	0 mM
-	-	5 mM	-	0 mM, 20 mM
5 mM	0.1 mM	-	-	0 mM, 5 mM, 10 mM, 20 mM
5 mM	0.5 mM	-	-	0 mM, 10 mM
7 mM	0.1 mM	-	-	0 mM, 5 mM, 10 mM, 20 mM
10 mM	0.1 mM	-	-	0 mM, 5 mM, 10 mM, 20 mM, 40 mM
10 mM	0.3 mM	-	-	0 mM, 5 mM, 10 mM, 20 mM
10 mM	0.5 mM	-	-	0 mM, 10 mM
10 mM	-	0.5 mM	-	0 mM, 10 mM
20 mM	0.1 mM	-	-	0 mM, 5 mM, 10 mM, 20 mM
20 mM	0.3 mM	-	-	0 mM, 5 mM, 10 mM, 20 mM
20 mM	0.5 mM	-	-	0 mM, 20 mM

*NaCl includes [NaCl] included with HCO_3^- assay (~40 mM Na^+, 0-40 mM Cl^-)

Table 2.3: Summary of currently described properties of sAC in marine organisms

Organism (protein accession number)	Co-factors	HCO_3^- EC_{50} (mM)	pH sensit-ivity	Tissue distribution	Notes
Mammals *Homo sapiens* (NP_060887.2); *Rattus sp.* (NP_067716.1)	Mn^{2+} ‡,A Mg^{2+} + Ca^{2+} ∗,B	~11-25[B-D]	No[D]	Testes, eye, airways, pancreas, colon, brain, nervous system, immune cells, bone, embryos, muscle, kidney, epididymis (reviewed in[E])	-K_m for ATP = ~1-3 mmol l^{-1} [B-D] -Multiple splice variants[F] -Present in most (all?) mammals, including *Orcinus orca* (XP_004269766.1), *Tursiups truncatus* (XP_004329889), *Trichechus manatus* (XP_004384133), *Odobenus rosmarus* (XP_004408373.1).
Bony fishes *Opsanus beta*, *Sparus aurata* (based on heterologous antibodies and pharmacology)	*ND*	*ND*	*ND*	Intestine[J,K]	Present in *Oncorhynchus mykiss* (TSA EZ789694.1, EZ814745.1), *Salmo salar* (5 WGS contigs), *Lepisosteus oculata* (WGS AHAT01020068.1), *Latimeria* chalumnae (17 WGS contigs), *Latimeria menadoensis* (TSA GAPS01010686.1)
Cartilaginous fishes *Squalus acanthias* (ACA52542.1)	Mn^{2+} ‡ Mg^{2+} + Mn^{2+} ∗,G	~5[G]	No[G]	Gill[G], rectal gland, red blood cells[H]	Present in *Leucoraja erinacea* (15 WGS contigs*); Triakis semifasciata* and *Urbatis hallerii* gill, rectal gland, testes, muscle, eye, intestine (heterologous antibodies)[I]; *Callorhinchus milii* (WGS AAVX02006506.1)
Sea urchin *Strongylocentrotus purpuratus* (NP_001020380.1)	Mn^{2+} ‡,L Mg^{2+} ∗,M	20[K]	Yes[L]	Sperm[L-N], embryonic primary mesenchymal cells[O]	-Kinetics determined from semi-purified native protein. Present in *Patiria miniata* (WGS AKZP01091244.1)
Mollusks Oyster *Crassostrea gigas* (EKC32844.1)	*ND*	*ND*	*ND*	Mantle, gill, hemocytes[P]	Present in *Ruditapes philippinarium* (TSA JO105222.1) and *Lottia gigantea* (EST FC684349.1, WGS AMQO01004501.1)
Cnidarians *Acropora spp.*, *Pocillopora damicornis* (Based on pharmacology on tissue homogenates)	Mg^{2+} P	~10[P]	*ND*	Not in symbiotic *Symbiodinium* or mucus[Q]	Present in *Acropora* (aug_v2a.21187.t1, aug_v2a.10515.t1)[R]; *Nematostella vectensis* (XP_001623318.1)

ND, not determined; TSA, transcriptomic shotgun assembly; WGS, whole genome shotgun Database; EST, expressed sequence tag. Accession numbers are from NCBI unless otherwise noticed. * =supports HCO_3^--stimulation. ‡ = maximum activity. Identification of sAC orthologs is based on BLAST searches using the two catalytic domains of dogfish sAC (amino acids 1-485) as the query.

Also present in **Poriferans (***Amphimedon queenslandica* XP_003384443.1); **Placozoans** (*Trichoplax adherens* XP_002117857.1); **Hemichordates** (*Saccoglossus kowalevskii* XP_002731233); **Amphioxus** (*Branchiostoma floridae* XP_002610143.1; XP_002610144.1)[S] **Tunicates** (*Oikopleura dioica* 7 WGS contigs; *Ciona intestinalis* XP_002121952.1); **Reptiles** (*Chrysemys picta bellii* XP_005308389.1; XP_005314924.1; *Chelonia mydas* EMP34522.1; *Alligator mississippiensis* XP_006273015.1; *Python morulus* 6 WGS contigs).

[A]Buck et al., 1999; [B]Litvin et al., 2003; [C]Chaloupka et al., 2006; [D]Chen et al., 2000; [E]Tresguerres et al., 2011; [F]See "Discovery of mammalian sAC" for details; [G]Tresguerres *et al.*, 2010c; [H]This paper. [I]Roa *et al.* (2012); [J]Carvalho et al., 2012; [K]Tresguerres et al., 2010b; [L]Nomura *et al.*, 2005; [M]Beltran et al., 2007; [N]Bookbinder et al., 1990; [O]Zhu et al., 2001; [P]Barron *et al.* (2012); [Q]Barott et al., 2013; [R]http://marinegenomics.oist.jp/; [S]most likely a single protein

Table is taken directly from (Tresguerres et al., 2014)

References

Al-Horani, F. A., Al-Moghrabi, S. M., & Beer, D. De. (2003). Microsensor study of photosynthesis and calcification in the scleractinian coral , Galaxea fascicularis : active internal carbon cycle. *Journal of Experimental Marine Biology and Ecology*, *288*, 1–15. https://doi.org/10.1016/S0022-0981(02)00578-6

Ayoubi, T. A. Y., & Van De Ven, W. J. M. (1996). Regulation of gene expression by alternative promoters. *The FASEB Journal*, *10*(4), 453–460.

Barott, K. L., Barron, M. E., Tresguerres, M. (2017). Identification of a molecular pH sensor in coral. *Proceedings of the Royal Society B*, 284, 1-8.

Barott, K. L., Helman, Y., Haramaty, L., Barron, M. E., Hess, K. C., Buck, J., Levin, L. R., Tresguerres, M. (2013). High adenylyl cylcase activity and in vivo cAMP fluctuations in corals suggest central physiological role. *Scientific Reports*, *3*(1379). https://doi.org/10.1038/srep01379

Barott, K. L., Perez, S. O., Linsmayer, L. B., & Tresguerres, M. (2015). Differential localization of ion transporters suggests distinct cellular mechanisms for calcification and photosynthesis between two coral species. *American Journal of Physiology - Regulatory, Integrative and Comparative Physiology*, *309*(3), R235–R246. https://doi.org/10.1152/ajpregu.00052.2015

Beltran, C., Vacquier, V. D., Moy, G., Chen, Y., Buck, J., Levin, L. R., & Darszon, A. (2007). Particulate and soluble adenylyl cyclases participate in the sperm acrosome reaction. *Biochemical and Biophysical Research Communications*, *358*, 1128–1135. https://doi.org/10.1016/j.bbrc.2007.05.061

Bitterman, J. L., Ramos-espiritu, L., Diaz, A., Levin, L. R., & Buck, J. (2013). Pharmacological Distinction between Soluble and Transmembrane Adenylyl Cyclases. *The Journal of Pharmacology and Experimental Therapeutics*, *5*(December), 589–598.

Braun, T., & Dods, R. F. (1975). Development of a Mn2 + -Sensitive , " Soluble " Adenylate Cyclase in Rat Testis, *72*(3), 1097–1101.

Buck, J., Sinclair, M. L., Schapal, L., Cann, M. J., & Levin, L. R. (1999). Cytosolic adenylyl cyclase defines a unique signaling molecule in mammals. *Proceedings of the National Academy of Sciences of the United States of America*, *96*(1), 79–84.

Chaloupka, J. A., Bullock, S. A., Iourgenko, V., & Levin, L. R. (2006). Autoinhibitory Regulation of Soluble Adenylyl Cyclase. *Molecular Reproduction and Development*, *368*(September 2005), 361–368. https://doi.org/10.1002/mrd.20409

Chen, Y., Cann, M. J., Litvin, T. N., Iourgenko, V., Sinclair, M. L., Levin, L. R., & Buck, J. (2000). Soluble adenylyl cyclase as an evolutionarily conserved bicarbonate sensor. *Science (New York, N.Y.)*, *289*(5479), 625–8.

Chera, S., Kaloulis, K., & Galliot, B. (2007). The cAMP response element binding protein (CREB) as an integrative HUB selector in metazoans: Clues from the Hydra ... *BioSystems*, *87*, 191–203. https://doi.org/10.1016/j.biosystems.2006.09.014

Claros, M. G., & Vincens, P. (1996). Computational method to predict mitochondrially imported proteins and their targeting sequences. *European Journal of Biochemistry*, *786*, 779–786.

Cooper, D. M. F. (2003). Regulation and organization of adenylyl cyclases and cAMP. *The Biochemical Journal*, *375*(Pt 3), 517–29. https://doi.org/10.1042/BJ20031061

DeSalvo, M. K., Estrada, A., Sunagawa, S., & Medina, M. (2012). Transcriptomic responses to darkness stress point to common coral bleaching mechanisms. *Coral Reefs*, *31*, 215–228. https://doi.org/10.1007/s00338-011-0833-4

Desalvo, M. K., Sunagawa, S., Voolstra, C. R., & Medina, M. (2010). Transcriptomic responses to heat stress and bleaching in the elkhorn coral Acropora palmata. *Marine Ecology Progress Series*, *402*, 97–113. https://doi.org/10.3354/meps08372

Farrell, J., Ramos, L., Tresguerres, M., Kamenetsky, M., Levin, L. R., & Buck, J. (2008). Somatic " Soluble " Adenylyl Cyclase Isoforms Are Unaffected in Sacytm1Lex / Sacytm1Lex " Knockout " Mice. *PLoS ONE*, *3*(9), 1–9. https://doi.org/10.1371/journal.pone.0003251

Furla, P., Galgani, I., Durand, I., & Allemand, D. (2000). Sources and mechanisms of inorganic carbon transport for coral calcification and photosynthesis. *The Journal of Experimental Biology*, *203*, 3445–3457.

Galliot, B., Welschof, M., Schuckert, O., Hoffmeister, S., & Schaller, H. C. (1995). The cAMP response element binding protein is involved in hydra regeneration. *Development (Cambridge, England)*, *121*(4), 1205–16.

Geng, W., Wang, Z., Zhang, J., Reed, B. Y., Pak, C. Y. C., & Moe, O. W. (2005). Cloning and characterization of the human soluble adenylyl cyclase. *American Journal of Physiology Cell Physiology*, *288*, 1305–1316. https://doi.org/10.1152/ajpcell.00584.2004.

Hess, K. C., Jones, B. H., Marquez, B., Chen, Y., Ord, T. S., Kamenetsky, M., Miyamoto, C., Zippin, J. H., Kopf, G. S., Suarez, S. S., Levin, L. R., Williams, C. J., Buck, J., Moss, S. B. (2005). The "soluble" adenylyl cyclase in sperm mediates multiple signaling events required for fertilization. *Developmental Cell*, *9*(2), 249–59. https://doi.org/10.1016/j.devcel.2005.06.007

Hoegh-Guldberg, O., Mumby, P. J., Hooten, A. J., Stenech, R. S., Greenfield, P., Gomez, E., Harvell, C. D., Sale, P. F., Edwards, A. J., Caldeira, K., Knowlton, N., Eakin, C. M., Iglesias-Prieto, R., Muthinga, N., Bradbury, R. H., Dubi, A., Hatziolos, M. E. (2008). Coral Reeds Under Rapid Climate Change and Ocean Acidification. *Science*, *318*(December 2007), 1737–1743.

Hughes, T. A. (2006). Regulation of gene expression by alternative untranslated regions. *Trends in Genetics*, *22*(3), 3–6.

Jaiswal, B. S., & Conti, M. (2001). Identification and Functional Analysis of Splice Variants of the Germ Cell Soluble Adenylyl Cyclase. *The Journal of Biological Chemistry*, *276*(34), 31698–31708. https://doi.org/10.1074/jbc.M011698200

Kobayashi, M., Buck, J., & Levin, L. R. (2004). Conservation of functional domain structure in bicarbonate-regulated " soluble " adenylyl cyclases in bacteria and eukaryotes. *Dev Genes Evolution*, *214*, 503–509. https://doi.org/10.1007/s00427-004-0432-2

Liou, W., Geuze, H. J., & Slot, J. W. (1996). Improving structural integrity of cryosections for immunogold labeling. *Histochem Cell Biol*, *106*, 41–58.

Litvin, T. N., Kamenetsky, M., Zarifyan, A., Buck, J., & Levin, L. R. (2003). Kinetic properties

of “soluble” adenylyl cyclase. Synergism between calcium and bicarbonate. *The Journal of Biological Chemistry*, *278*(18), 15922–6. https://doi.org/10.1074/jbc.M212475200

Mayr, B., & Montminy, M. (2001). Transcriptional regulation by the phosphorylation-dependent factor CREB. *Nature Reviews. Molecular Cell bBology*, *2*(August), 599–609.

Moberg, F., & Folke, C. (1999). Ecological goods and services of coral reef ecosystems. *Ecological Economics*, *29*, 215–233.

Nomura, M., Beltrán, C., Darszon, A., & Vacquier, V. D. (2005). A soluble adenylyl cyclase from sea urchin spermatozoa. *Gene*, *353*(2), 231–8. https://doi.org/10.1016/j.gene.2005.04.034

Roa, J. N., & Tresguerres, M. (2016). Soluble adenylyl cyclase is an acid-base sensor in epithelial base-secreting cells, (44), 340–349. https://doi.org/10.1152/ajpcell.00089.2016

Romano, S. L., & Palumbi, S. R. (1996). Evolution of Scleractinian Corals Inferred from Molecular Systematics. *Science*, *271*(5249), 640–642.

Schmid, A., Sutto, Z., Nlend, M., Horvath, G., Schmid, N., Buck, J., Levin, L. R., Conner, G. E., Fregien, N., Salathe, M. (2007). Soluble Adenylyl Cyclase Is Localized to Cilia and Contributes to Ciliary Beat Frequency Regulation via Production of cAMP. *The Journal of General Physiology*, *130*(1), 99–109. https://doi.org/10.1085/jgp.200709784

Shinzato, C., Shoguchi, E., Kawashima, T., Hamada, M., Hisata, K., Tanaka, M., Fujie, M., Koyanagi, R., Ikuta, T., Fujiyama, A., Miller, D. J., Satoh, N. (2011). Using the Acropora digitifera genome to understand coral responses to environmental change. *Nature*, *476*(7360), 320–323. https://doi.org/10.1038/nature10249

Sievers, F., Wilm, A., Dineen, D., Gibson, T. J., Karplus, K., Li, W., Lopez, R., McWilliam, H., Remmert, M., Soding, J., Thompson, J. D., Higgins, D. G. (2011). Fast, scalable generation of high-quality protein multiple sequence alignments using Clustal Omega. *Molecular Systems Biology*, *7*(539). https://doi.org/10.1038/msb.2011.75

Steegborn, C., Litvin, T. N., Hess, K. C., Capper, A. B., Taussig, R., Buck, J., Levin, L. R., Wu, H. (2005a). A novel mechanism for adenylyl cyclase inhibition from the crystal structure of its complex with catechol estrogen. *The Journal of Biological Chemistry*, *280*(36), 31754–9. https://doi.org/10.1074/jbc.M507144200

Steegborn, C., Litvin, T. N., Levin, L. R., Buck, J., & Wu, H. (2005b). Bicarbonate activation of adenylyl cyclase via promotion of catalytic active site closure and metal recruitment. *Nature Structural & Molecular Biology*, *12*(1), 32–7. https://doi.org/10.1038/nsmb880

Stolarski, J., Kitahara, M. V, Miller, D. J., Cairns, S. D., Mazur, M., & Meibom, A. (2011). The ancient evolutionary origins of Scleractinia revealed by azooxanthellate corals The ancient evolutionary origins of Scleractinia revealed by azooxanthellate corals. *BMC Evolutionary Biology*, *316*(October), 1–10.

Taussig, R., & Gilman, A. (1995). Mammalian membrane-bound adenylyl cyclases. *Journal of Biological Chemistry*.

Tresguerres, M., Barott, K. L., Barron, M. E., Deheyn, D. D., Kline, D. I., & Linsmayer, L. B. (2017). Cell Biology of Reef-Building Corals: Ion Transport, Acid/ Base Regulation, and Energy Metabolism, 193–218. https://doi.org/10.1007/978-3-319-39617-0

Tresguerres, M., Barott, K. L., Barron, M. E., & Roa, J. N. (2014). Established and potential physiological roles of bicarbonate-sensing soluble adenylyl cyclase (sAC) in aquatic animals. *The Journal of Experimental Biology*, *217*, 663–72. https://doi.org/10.1242/jeb.086157

Tresguerres, M., Levin, L. R., & Buck, J. (2011). Intracellular cAMP signaling by soluble adenylyl cyclase. *Kidney International*, *79*(12), 1277–88. https://doi.org/10.1038/ki.2011.95

Tresguerres, M., Parks, S. K., Salazar, E., Levin, L. R., Goss, G. G., & Buck, J. (2010). Bicarbonate-sensing soluble adenylyl cyclase is an essential sensor for acid/base homeostasis. *Proceedings of the National Academy of Sciences of the United States of America*, *107*(1), 442–7. https://doi.org/10.1073/pnas.0911790107

Venn, A. A., Tambutté, E., Lotto, S., Zoccola, D., Allemand, D., & Tambutté, S. (2009). Imaging intracellular pH in a reef coral and symbiotic anemone. *Proceedings of the National Academy of Science*, *106*(39), 16574–16579.

Venn, A., Tambutté, E., Holcomb, M., Allemand, D., & Tambutte, S. (2011). Live Tissue Imaging Shows Reef Corals Elevate pH under Their Calcifying Tissue Relative to Seawater Live Tissue Imaging Shows Reef Corals Elevate pH under Their Calcifying Tissue Relative to Seawater. *Plos One*, *6*(5), 1–9. https://doi.org/10.1371/journal.pone.0020013

Wong, W., & Scott, J. D. (2004). AKAP signalling complexes: focal points in space ad time. *Nature Reviews. Molecular Cell Biology*, *5*(December), 959–970. https://doi.org/10.1038/nrm1527

Zaccolo, M., Di Benedetto, G., Lissandron, V., Mancuso, L., Terrin, A., & Zamparo, I. (2006). Restricted diffusion of a freely diffusible second messenger: mechanisms underlying compartmentalized cAMP signalling. *Biochemical Society Transactions*, *34*(Pt 4), 495–7. https://doi.org/10.1042/BST0340495

Zippin, J., Chen, Y., & Nahirney, P. (2003). Compartmentalization of bicarbonate-sensitive adenylyl cyclase in distinct signaling microdomains. *The FASEB Journal*, 82–84. https://doi.org/10.1096/fj.02

Zippin, J. H., Farrell, J., Huron, D., Kamenetsky, M., Hess, K. C., Fischman, D. A., Levin, L. R., Buck, J. (2004). Bicarbonate-responsive “soluble” adenylyl cyclase defines a nuclear cAMP microdomain. *The Journal of Cell Biology*, *164*(4), 527–34. https://doi.org/10.1083/jcb.200311119

CHAPTER 3: A Na^+/Ca^{2+} exchanger in vesicles in coral calcifying cells: revisiting calcification mechanisms

Abstract

The calcium carbonate skeletons of corals provide the underlying structure of coral reefs. Despite their ecological importance to marine ecosystems, very little is understood about the mechanisms behind coral calcification. In mammals, a Na^+/Ca^{2+} exchanger (NCX) is involved in calcium delivery to the site of bone calcification. To investigate whether NCX proteins have a similar role in corals, I cloned five NCXs from the coral *Acropora yongei* (ayNCX) and designed specific antibodies against one of them ($ayNCX_A$). Epifluorescence and confocal microscopy revealed strong $ayNCX_A$ immunoreactivity within the cytoplasm of calcifying cells, presumably in vesicles. We confirmed $ayNCX_A$ localization in intracellular vesicles by expression of recombinant, fluorescently tagged $ayNCX_A$ protein in sea urchin embryos and visualization using confocal microscopy. This is the first direct evidence for the presence of a Ca^{2+}-transporting protein in intracellular vesicles of a marine calcifying organism. Vesicular transport of Ca^{2+} to the site of calcification would help maintain low cytosolic [Ca^{2+}], which is essential for preventing intracellular calcium phosphate precipitation and impairment of crucial cellular functions that rely on Ca^{2+} signaling. Understanding the cellular mechanisms for delivering Ca^{2+} to the skeleton is essential for determining responses that supposedly could affect coral calcification, in particular ocean acidification.

Introduction

Coral reef ecosystems are valuable ecological (Knowlton et al., 2006) and economic resources (Spurgeon, 1992) centered around the calcium carbonate ($CaCO_3$) structures deposited by scleractinian corals. Despite the many challenges facing coral reefs today (Hughes et al., 2017;

Carpenter et al., 2008), very little is actually known about coral cell biology (reviewed in Tresguerres et al., 2017) and how these reef structures are produced at the cellular level. The aboral ectoderm (also known as the calicoblastic epithelium), is directly above the subcalicoblastic medium (SCM), where $CaCO_3$ precipitates for skeleton formation (reviewed in Allemand et al., 2011). Thus, the calicodermis is the tissue layer with the most direct role in skeleton calcification (Johnston, 1980).

Although the exact mechanisms behind coral calcification are currently unknown, they must concentrate Ca^{2+} and CO_3^{2-} ions to SCM. Current models regarding the transport of Ca^{2+} to the SCM propose paracellular transport as individual ions or within bulk transport of seawater, and transcellular transport through some combination of channel and transporter proteins (reviewed in Allemand et al., 2011). Additionally, $CaCO_3$ (amorphous or crystalline) may be transported inside vesicles (Hayes & Goreau, 1977), alone or complexed with calcium binding proteins such as coral acidic rich proteins (CARPs) (Mass et al., 2017). Importantly, those mechanisms are not mutually exclusive. CARPs, which have been immunolocalized in the calicoblastic epithelium, can spontaneously precipitate $CaCO_3$ out of solution *in vitro* (Mass et al., 2013; Mass et al., 2014).

The involvement of Ca^{2+} channels is supported by earlier findings where calcification in two coral species was inhibited by verapamil, an unspecific pharmacological antagonist of mammalian L-type calcium channels (Marshall, 1996; Tambutté et al., 1996). Ca^{2+} channels are predicted to be localized on the basolateral membrane of calicoblastic cells, allowing Ca^{2+} to passively enter the cells on the side distal from the skeleton (Tambutté et al., 1996). A subunit of a voltage-dependent Ca^{2+} channel has been cloned from the coral *Stylophora pistillata*, and was immunolocalized to the microvilli in apical membrane of ciliated support cells in the oral ectodermis and in cells in the calicoblastic epithelium (Zoccola et al., 1999). However, the Ca^{2+}

channel's specific subcellular localization in calicoblastic cells was not discussed, nor is it evident from the pictures provided.

Another Ca^{2+} transporter potentially involved in calcification is the plasma membrane Ca^{2+}-ATPase (PMCA), which is widely assumed to transport Ca^{2+} ions across the apical membrane of calicoblastic cells in exchange for H^+ from the SCM. This theoretical model is popular because H^+ removal from the site of calcification would have the added benefit of alkalizing the SCM, thus increasing the saturation state of aragonite (reviewed in Cohen & McConnaughey, 2003). There is ample evidence for the presence of PMCA in coral, including Ca^{2+}-ATPase activity in tissue homogenates of *Galaxea fascicularis* (Ip et al., 1991), inhibition of calcification by the unspecific inhibitor ruthenium red (Al-Horani et al., 2003; Allison et al., 2014; Marshall, 1996), and presence of PMCA mRNA throughout *S. pistillata* tissues (Zoccola et al., 2004). However, there is no direct evidence supporting the predicted presence of PMCA in the apical membrane of calcifying cells- even the inhibition of calcification by ruthenium red could be a side effect resulting from unspecific inhibition of Ca^{2+} uptake by mitochondria, or due to specific inhibition of PMCA, but in a different tissue layer. Furthermore a recent immunolocalization study reported strong PMCA signal consistent with cytoplasmic vesicles in *Acropora yongei* calcifying cells (Barott et al., 2015a).

A third potential mechanism for Ca^{2+} transport for coral calcification is *via* Na^+/Ca^{2+} exchange. Several Na^+/Ca^{2+} exchanger proteins exist; the better characterized are NCX1, NCX2 and NCX3 from vertebrate animals that export one Ca^{2+} ion in exchange for two or three Na^+ ions (reviewed in On et al., 2008; Quednau et al., 2004). Mammalian NCXs are generally located in the plasma membrane; however, Na^+/Ca^{2+} activity is also found in secretory vesicles (Krieger-Brauer & Gratzl, 1982; Thirion et al., 1999; Troadec,et al., 1998). Another mammalian Na^+/Ca^{2+}

exchanger, named NCLX because it can also transport Li^{2+}, is present in mitochondria (Palty et al., 2010).

NCXs play a general role in intracellular Ca^{2+} homeostasis in animal cells, and are also involved in specialized physiological functions such as muscle contractility, neurotransmitter release, transepithelial Ca^{2+} transport across kidney and intestine, Ca^{2+} removal from lens (reviewed in Blaustein & Lederer, 1999; Hoenderop et al., 2005) and osteoblast calcification (Akisaka et al., 1988; Sosnoski & Gay, 2008; Stains & Gay, 1998). NCXs have also been proposed to be involved in coral calcification (Davy et al., 2012; Marshall, 1996); however, direct experimental evidence is lacking.

Here, I cloned five NCX cDNAs from the coral *A. yongei*, and generated specific antibodies against one of them to determine its cellular and subcellular localization in coral. I found abundant NCX localization in intracellular vesicles in the calicoblastic epithelium, which I hypothesize allows coral cells to deliver Ca^{2+} to the SCM while avoiding harmful effects on cell viability.

Results

Coral NCX isoforms

We cloned five full-length transcripts encoding for putative NCX proteins from *A. yongei* (ayNCX). In addition, through BLAST searches in genomic and transcriptomic databases, I identified ortholog proteins in multiple other corals, including species from the Complex clade (*A. millepora, A. cervicornis, G. fascicularis, Porites australiensis, P. astreoides)* and the Robust clade *(Orbicella faveolata, Favia lizardensis, S. pistillata,* and *Pocillopora damicornis*) (Figure 3.1).

The relatedness of coral NCXs to NCXs from other organisms is shown in the phylogenetic tree in Figure 3.1. The vertebrate NCX proteins are more closely related to each other than they are to NCX proteins from invertebrates. Thus, established properties of mammalian NCX1, NCX2 and NCX3 such as subcellular localization and regulatory properties cannot be directly extrapolated to NCXs from invertebrates. To avoid confusion, I refer to coral NCXs as NCX_A and NCX_B, and to the *A. yongei* NCXs I cloned as $ayNCX_A$, $ayNCX_{B1}$, $ayNCX_{B2}$, $ayNCX_{B3}$, and $ayNCX_{B4}$.

$ayNCX_A$ has a predicted molecular weight of 101.7 kDa and is the most closely related to NCX proteins from vertebrates (Figure 3.1). The other four proteins, $ayNCX_{B1-4}$, have respective predicted molecular weights of 69.8 kDa, 61.7 kDa, 41.3 kDa, and 26.4 kDa, and branch together with NCX proteins from invertebrates exclusively (Figure 3.1). $ayNCX_{B1}$ and $ayNCX_{B2}$ are splice variants resulting from the mutually exclusive retention of two intronic sequences (Figure 3.2a). $ayNCX_{B3}$ contains a 2bp deletion compared to $ayNCX_{B1}$ and $ayNCX_{B2}$ that shifts the open reading frame and results in early termination. As such a small deletion would not result from alternative splicing, this sequence may represent a second allele of the NCX_B gene. Finally, $ayNCX_{B4}$, contains a unique ~1500 bp insert compared to $ayNCX_{B1-3}$ which contains an early stop codon, and thus $ayNCX_{B4}$ encodes for the smallest protein. This transcript has an alternative 5' splice junction, changing the 3' boundary of the first exon. Interestingly, besides the first exon encoding the start codon, and the last exon containing the reverse priming site, there are no shared exons between $ayNCX_{B4}$ and the other three $ayNCX_{B1-3}$ proteins.

Topology analysis predicts $ayNCX_A$ has 11 membrane-spanning helices, which is similar to earlier models for mammalian NCX1 (reviewed in Dipolo & Beauge, 2006; Philipson & Nicoll, 2000). $ayNCX_A$ also contains a peptide signal predicted (0.995 probability) to localize the protein to the secretory pathway (Emanuelsson et al., 2000). On the other hand, $ayNCX_{B1-4}$ only

have five predicted membrane-spanning helices, casting doubts on whether they are functional proteins, the putative ions they transport, and the mechanisms. Thus, the rest of the experiments focused on ayNCX$_A$.

Characterization of ayNCX$_A$ *in coral tissues*

Custom-made antibodies against an epitope present in ayNCX$_A$ and absent in ayNCX$_{B1-4}$ (Figure 3.2b) were made in rabbit. In Western blots with homogenized *A. yongei* tissue, the anti-ayNCX$_A$ antibodies revealed two major bands (Figure 3.3): a ~ 100kDa band that matches the predicted size of ayNCX$_A$ protein and a ~70kDa band that matches the size of a proteolytic product that is characteristic of mammalian NCX1 (Iwata et al., 1995; Philipson et al., 1988). Confirming the specificity of the anti-ayNCX$_A$ antibodies, both bands were absent in pre-absorbed and pre-immune controls (Figure 3.3).

In *A. yongei* histological sections, ayNCX$_A$ protein was detected in all four tissue layers (Figure 3.4a) (antibody specificity for immunofluorescence microscopy is shown in Figure 3.5). In the oral ectodermis, ayNCX$_A$ was most abundant in the seawater-facing apical membrane of ciliated support cells, while ayNCX$_A$ signal appeared cytoplasmic in the oral and aboral gastrodermis and in the calicoblastic epithelium (Figure 3.4a). ayNCX$_A$ protein abundance was highest in calicoblastic cells and desmocytes in the calicoblastic epithelium (Figure 3.4bc). Under higher magnification, ayNCX$_A$ had a punctate immunostaining pattern consistent with vesicles. However, calicoblastic cells are very thin (0.1-2 μm in height), are stacked on top of each other, and have numerous intracellular vesicles ranging from 80 to 500 nm in diameter (Figure 3.6). This convoluted morphology greatly complicates determining protein subcellular localization using immunofluorescence.

Heterologously expressed ayNCX$_A$ localizes in intracellular vesicles

To further investigate the subcellular localization of ayNCX$_A$, we expressed fluorescently-tagged ayNCX$_A$ in sea urchin embryos, an established system for heterologous expression of proteins (Gokirmak et al., 2014). ayNCX$_A$ fused to an mCherry or Cerulean tag in either the C- or N-terminus was widespread throughout the cytoplasm in embryos ages 16 to 72 days post fertilization (dpf). Tag type or position did not affect the subcellular localization of ayNCX$_A$, although N-tagged proteins resulted in higher background fluorescence. This is likely explained by incomplete/truncated N-tagged proteins, whereas only fully translated C-tagged proteins would contain the fluorescent protein (Figure 3.7). Higher magnification images of C-mCherry-ayNCX$_A$, the construct with the most robust fluorescence, revealed the signal was present in intracellular structures ~0.5-1 μm in diameter (Figure 3.8). This pattern resembled ABCC9, a sea urchin ATP-binding cassette protein with established localization in cytoplasmic vesicles (Gökirmak et al., 2012). Co-expression of C-cerulean-ayNCX$_A$ with C-mCherry-ABCC9 confirmed ayNCX$_A$ was indeed present in vesicles (Figure 3.9). Furthermore, C-cerulean-ayNCX$_A$ signal did not overlap with C-mCherry-ABCB6, a mitochondrial and golgi protein in humans (Krishnamurthy et al., 2006; Paterson et al., 2007; Tsuchida et al., 2008; reviewed in Zutzet al., 2009) which has similar localization when overexpressed in sea urchin (Gokirmak et al., 2014) (Figure 3.10).

Discussion

I cloned cDNAs encoding for five NCX proteins in the coral *A. yongei*: ayNCX$_A$ and ayNCX$_{B1-4}$. This is the first characterization of NCX proteins in coral. I focused on ayNCX$_A$, a ~102 kDa protein with 11 predicted transmembrane domains, due to its similarity in structure to vertebrate NCX proteins whose ion transport are well-characterized. Localization of ayNCX$_A$ in

intracellular vesicles in the calicoblastic epithelium provides evidence for a novel paracellular pathway for Ca^{2+} delivery to the site of calcification. Because ortholog proteins are present in nine other coral species from the Complex and Robust coral clade (which diverged from one another over 350 million years ago), the role of NCX_A in Ca^{2+} transport in corals is most likely both important and conserved.

Phylogenetic analysis groups coral NCX_A with NCX1 and NCX3 proteins from vertebrates, and NCX_B's with NCX proteins exclusively from invertebrates. This agrees with previous research suggesting that the three major NCX isoforms in vertebrates are the result of two genome duplication events, the first of which is predicted to have occurred after the divergence of chordates (On et al., 2008). Therefore, invertebrates have an ancestral gene similar to NCXs from vertebrates (in corals, it evolved to NCX_A), and the other genes annotated as NCX2 and NCX3 most likely arose from lineage-specific duplications that occurred after the evolution of chordates and independent of the duplication/evolution of vertebrate NCX2 and NCX3 proteins. Thus, designating invertebrate NCX proteins as NCX1, NCX2, or NCX3 is erroneous and misleading because they share little homology to vertebrate NCX proteins. In fact, some early annotations have changed. For example, what was previously identified as Urchin NCX1, XM_001184049, (On et al., 2008) has since been re-annotated as NCX3-like on NCBI. Furthermore, my own phylogenetic analysis (Figure 3.1) groups a tunicate protein predicted as an NCX2 isoform with NCKX proteins from bull and rat, suggesting that the tunicate protein has been incorrectly annotated as NCX (SLC8A) when in reality it may belong to a different gene family altogether (SLC24). This highlights some of the limitations of transcriptomic studies, especially when identifying proteins with multiple isoforms and splice variants that have not yet been characterized in the species in question.

Although I only cloned one ayNCX$_A$ sequence, two prominent protein bands were detected by Western blotting: one at 100 kDa that matches the ayNCX$_A$ predicted size, and a 70 kDa protein. This pattern matches mammalian NCXs, which also show a 70 kDa protein in Western blots that was determined to be an active proteolytic fragment derived from a larger 120 kDa protein (Iwata et al., 1995; Philipson et al., 1988). Furthermore, in chicken, the only NCX protein visible in Western blot is 70kDa in size, which the authors proposed is a truncated isoform of NCX, though they also consider the possibility that it is a proteolytic fragment (Stains & Gay, 1998). Thus, I conclude ayNCX$_A$ undergoes similar proteolysis, although I cannot rule an alternatively spliced mRNA not picked up in RT-PCR, or protein degradation.

Immunohistochemical staining of *A. yongei* tissue indicated ayNCX$_A$ is present in all four coral tissue layers. ayNCX$_A$ was most abundantly expressed in calicoblastic cells and desmocytes, suggesting a role in calcification. High magnification imaging revealed a punctate immunostaining consistent with intracellular vesicles; however, the small size and intricate morphology of those cells makes it difficult to rule out its presence in the cell membrane.

To circumvent this limitation, I expressed fluorescently tagged ayNCX$_A$ in sea urchin embryos, where protein subcellular localizations are more easily determined (Gökirmak et al., 2012). I used both N-terminal and C-terminal fluorescent tags (mCherry and Cerulean fluorescent protein) because tag position has been previously shown to sometimes impact localization (Gökirmak et al., 2012); however, all four recombinant ayNCX$_A$ proteins localized to vesicles. There was no localization of recombinant ayNCX$_A$ in the basolateral or apical plasma membrane, nor was there any localization in the mitochondria or Golgi apparatus. The findings in sea urchin embryos together with ayNCX$_A$ immunostaining in coral calicodermis tissue indicate ayNCX$_A$ is indeed present in vesicles. To my knowledge, this is the most convincing evidence of an ion-transporter localized in coral vesicles to date.

Vesicles have been observed in the calicodermis of multiple coral species, including *Pocillopora damicornis* (Johnston, 1980), *A. hebes* (Isa, 1986), *G. fascicularis* (Clode & Marshall, 2002), and *A. yongei* (Barott et al., 2015a). In *G. fascicularis*, vesicles were characterized into two major types based on diameter: 70 nm and 380 nm. However, the function(s) of those vesicles and their potential role in calcification remains controversial, as they sometimes have been described as lacking mineralized structures within, evidence of fusion with the cell membrane was not always observed (Clode & Marshall, 2002). These discrepancies are at least partially due to fixation artifacts (Clode & Marshall, 2002), but species-specific differences and variation in the part of the coral sampled (e.g. the tip vs. the side of a coral branch, which calcify at different rates) cannot be ruled out.

However, in *A. yongei*, vesicles in the process of fusing with the membrane have been observed (Barott et al., 2015a). Furthermore, the lack of visible, mineralized aragonite inside of vesicles does not preclude them from transporting Ca^{2+} ions, which has indeed been proposed based on findings of high [Ca^{2+}] in vesicles (Clode & Marshall, 2002). In fact, very recently, spectromicroscopy observations have identified amorphous $CaCO_3$ and small mineral crystals within the calicoblastic epithelium, which were predicted to be transported via vesicles to the SCM (Mass et al., 2017).

NCX is one way by which Ca^{2+} may enter and concentrate within vesicles. Using TEM microscopy, we identified vesicles in the calicoblastic epithelium of *A. yongei* ranging from 80 nm-500 nm in diameter (Figure 3.6). The size of these vesicles matches the size of the ayNCX_A punctate staining in calicoblastic cells, as well as the vesicles in urchin embryos containing recombinant coral ayNCX_A (Figure 3.8). Immunolocalization of ayNCX_A in *A. yongei* calicodermis tissue is also consistent with vesicular localization (Figure 3.4), and matches the immunolocalization pattern reported for PMCA in the same species (Barott et al., 2015a).

Interestingly, NCX and PMCA often colocalize in mammalian cells forming Ca^{2+}-concentration microdomains to maintain low intracellular [Ca^{2+}] (Blaustein et al., 2002; Brini & Carafoli, 2011; Castillo et al., 2007; Kwon et al., 2009).

What could be the significance of vesicular transport of Ca^{2+}? Intracellular concentrations of free Ca^{2+} must be ~20,000-fold less than extracellular concentrations because excess Ca^{2+} in the cytosol would precipitate phosphates and interfere with intracellular signaling pathways (reviewed in Clapham, 2007). Ca^{2+} signaling is involved in every aspect of a cell's life and death as it is able to bind to thousands of proteins to effect changes in localization, association, and function (Clapham, 2007). In the calicoblastic epithelium, [Ca^{2+}] is ~19 mmol kg^{-1} (Marshall et al., 2007), a concentration that would be lethal unless Ca^{2+} is sequestered in intracellular compartments.

We propose the following mechanism for Ca^{2+} transport in coral calicoblastic epithelium (Figure 3.11). First, Ca^{2+} enters the calicoblastic cells through Ca^{2+}-channels in the basolateral membrane (Tambutté et al., 1996; Zoccola et al., 1999). Ca^{2+} then is transported inside intracellular vesicles by NCX_A and PMCA. The Na^+/K^+-ATPase (NKA), which is abundant in the basolateral membrane of calicoblastic cells (Barott et al., 2015a), maintains a low cytosolic [Na^+] that helps drive NCX_A activity. Already contained within these vesicles are CARPs, collagen, and carbonic anhydrase (CA), which have all been identified in the skeleton protein matrix (Drake et al., 2013). Corals utilize CARPs to precipitate $CaCO_3$ (Mass et al., 2013) and it has recently been shown that they produce amorphous calcium carbonate while still within calicoblastic epithelium (Mass et al., 2017). Secretory signal peptides have been identified in three of the four known CARP proteins from *S. pistillata*, and the presence of an isoleucine-proline-valine (IPV)-like motif, which helps secrete acidic, Ca^{2+}-binding proteins from the endoplasmic reticulum in mammals (Marschall et al., 2012), is in two of these four CARP

proteins as well, providing additional evidence for CARPs in secretory vesicles. Meanwhile, metabolic CO_2 can diffuse into vesicles where CA, also localized there as a result of a secretory signal peptide, and can catalyze its reaction into H^+ and HCO_3^- ions (Bertucci et al., 2011; Drake et al., 2013). The H^+ ions are removed by PMCA in exchange for Ca^+, while the HCO_3^- provides an additional source of DIC for the CARPs to precipitate. In our model, Ca^{2+} ions, CARPs, structural proteins such as collagen, CA, and DIC are all located together in the vesicles, forming a Ca^{2+} delivery microdomain.

Calcification mechanisms involving vesicles have been proposed in foraminiferans, (Erez, 2003) and in coccolithophores (Outka & Williams, 1971; van der Wal et al., 1983; reviewed in Mackinder et al., 2010); however, the Ca^{2+}-transporting proteins involved are completely unknown.

By sequestering Ca^{2+} in vesicles and maintaining low intracellular [Ca^{2+}] corals are capable of avoiding the negative, sometimes toxic, effects of excess Ca^{2+} on signaling pathways. We propose a novel pathway for Ca^{2+} transport involving NCX, with PMCA and driven by NKA, in Ca^{2+} homeostasis and the transport of Ca^{2+} to the SCM for calcification. This mechanism improves our understanding of coral cell biology and calcification in marine organisms.

Methods

Corals

Colonies of *A. yongei* were provided by the Birch Aquarium at Scripps Institution of Oceanography (SIO). The corals were maintained in warmed (25 °C) flow through seawater and a 12:12 hour light:dark cycle in Hubbs Hall at SIO . Some corals that were decalcified for use with immunofluorescence microscopy were grown with simulated “moonlight” (4 hours) at the

beginning of the 12-hour dark period. There were 15 minutes of stimulated "sunrise" and "sunset" as well. These conditions were controlled by the preset M3 protocol programmed with Orbit Marine LED Fixture model 4103-B.

Cloning of NCX1 and NCX3 sequences from A. yongei

Total RNA was obtained from a ~3 cm coral fragment, which was flash frozen in liquid nitrogen and then crushed into a fine powder using a chilled mortar and pestle. The powder was homogenized with an electric homogenizer in 10 ml TRIzol Reagent (Invitrogen, Carlsbad, CA, USA) following the manufacturer's protocol with the following modifications: an overnight precipitation of the total RNA at -80 °C and an additional wash step the following day with 75% ethanol. The quality of the total RNA was assessed by incubating a small volume at 37 °C for 2 hours, and running the sample in an agarose gel to check for degradation. Total RNA was cleaned and concentrated using RNEasy Plus Mini (Qiagen, Hilden, Germany) according to the manufacturer's protocol. cDNA was synthesized using SuperScript III Reverse Transcriptase (Invitrogen) and oligo(dT) primers. RT-PCR was performed using primers designed against predicted *A. digitifera* NCX proteins identified by BLAST (primers provided in Table 3.1). For both ayNCX_A and NCX_B, the first round of PCR was performed using Phusion High Fidelity Taq polymerase (New England Biolabs, Ipswich, MA, USA). Obtaining the full-length ayNCX_A sequence required two additional rounds of PCR using Platinum Taq polymerase (Invitrogen), the final using a nested forward primer, before the band was gel-purified using a NucleoSpin kit (Macherey-Nagel, Düren, Germany) and TOPO-TA cloned into a PCR2.1 vector (Invitrogen). NCX3 required only one additional round of PCR with Platinum Taq before the PCR reaction was used directly in the TOPO-TA cloning reaction (Invitrogen). The PCR cycles, including anneal temperatures and extension times, are provided in (Table 3.2).

Nucleotide sequences were aligned (Figure 3.2a) using MUSCLE (http://www.ebi.ac.uk/Tools/msa/muscle/) (Edgar, 2004). Protein sequences were aligned (Figure 3.2b) using Clustal Omega (http://www.ebi.ac.uk/Tools/msa/clustalo/) (Sievers et al., 2011). Phylogenetic analysis was performed using the software package Phylogent with 500 bootstraps (http://www.phylogeny.fr/) (Dereeper et al., 2008); prediction of transmembrane helices was performed using TMHMM (http://www.cbs.dtu.dk/services/TMHMM-2.0) (Krogh et al., 2001; Sonnhammer et al., 1998). Prediction of subcellular localization was performed using TargetP 1.1 (http://www.cbs.dtu.dk/services/TargetP/) (Emanuelsson et al., 2000).

Antibodies

Custom polyclonal antibodies were developed in rabbit and affinity purified (GenScript USA, Inc). The peptide antigen sequence, KDEDGKSVLRTGEG, was designed using a predicted NCX protein sequence from the *A. digitifera* genome (Shinzato et al., 2011). Antibodies were validated for *A. yongei* for Western blotting on tissue homogenates (Figure 3.3), and by immunofluorescence on histological sections (Figure 3.4, 3.5).

Western blot

Coral fragments were flash frozen in liquid nitrogen and the tissue was removed from the skeleton using an airbrush containing 5 ml S22 buffer ([final]: 450 mM NaCl, 10 mM KCl, 58 mM $MgCl_2$, 10 mM $CaCl_2$, 100 mM Hepes) supplemented with Protease Inhibitor Cocktail (Sigma- Aldrich) and PhosStop (Roche Applied Science) as previously described (Barott et al., 2015a). While on ice, the coral slurry was passed through a 21g needle repeatedly to break up excess mucus. The homogenate was then sonicated for 3 x 10 second bursts (30 seconds rest between pulses) while on ice. The sonicated homogenate was then centrifuged at 500 g for 15 minutes at 4 °C to pellet out zooxanthellae. The remaining slurry was named “crude homogenate” The protein concentration in the crude homogenate was determined using the Bradford assay

(Bio-Rad). Crude homogenate samples were combined with 4x Laemmli buffer (BioRad) (1:3 vol:vol), the final mixed also 10% beta-mercaptoethanol. Samples were then heated at 72 °C for 15 minutes and 20 µg protein were loaded into a 10% polyacrylamide SDS-PAGE gel and run at 100 V for 75 minutes at 4 °C. Proteins were transferred from the gel onto a PVDF membrane using a TurboBlot machine (Bio-Rad) using the pre-programmed 30 minute "Standard Molecular Weight" protocol. PVDF membranes were blocked 1 hour in blocking buffer (5% powdered fat-free milk in Tris-Buffered Saline + 0.1% Tween detergent (TBS-T), on a shaker at room temperature. The PDVF membrane was then incubated overnight on a shaker at 4 °C with primary antibody (0.151 µg ml^{-1}; 1:100 dilution from the stock), primary antibody with 400x excess peptide on a molar basis ('pre-absorption control'), or pre-Immune Serum (0.151 µg ml^{-1}) diluted in blocking buffer. PVDF membranes were then washed 3 times in TBS-T for 10 minutes each and then incubated 1 hour on a shaker at room temperature, with secondary antibody (goat anti-rabbit-HRP diluted 1:10,000, Bio-Rad). PVDF membranes were washed 3 times in TBST-for 10 minutes, then bands were developed using ECL Prime Western Blot Detection Kit (GE Healthcare, USA) and imaged using a Bio-Rad Chemidoc Imaging system.

Immunohistochemistry

Coral fragments were fixed and decalcified as previously described (Barott & Tresguerres, 2015; Barott et al., 2015a, 2015b). 1 cm coral fragments were fixed in S22 buffer (pH 7.8) with 3% paraformaldehyde at 4 °C overnight. The samples were then decalcified in Ca^{2+}-free S22 buffer with 0.5 M EDTA (pH 7.8), shaking at 4 °C. The decalcification buffer was replaced daily until the skeleton was dissolved (~14-21 days depending on the size of the fragment). Following decalcification, the tissue was dehydrated and embedded in paraffin wax. Wax blocks were sectioned into 7-10 µm thick sections and placed on glass microscope slides. Sections were incubated on the slides overnight at 30 °C, and stored the next day at 4 °C until

ready for use. Tissue sections were rehydrated, blocked for 1 hour in blocking buffer (phosphate buffered solution with normal goal serum and keyhole limpet hemocyanin solution) and incubated with coral NCX antibody (1.51 μg ml^{-1} coral NCX antibody with pre-adsorbed peptide in excess (4.55 μg ml^{-1} pre-adsorbed peptide diluted), or with pre-immune serum (2.36 μg ml^{-1}) overnight at 4 °C. "Secondary-only" control images were incubated overnight with blocking buffer containing no antibody. The next day, following 3, 5 minute washes in PBS with Triton-X (0.2%), sections were incubated for 1 hour at room temperature with secondary antibody (goat anti-rabbit-Alexa Fluor555, 4 μg ml^{-1}; Invitrogen) followed by a 5 minute incubation at room temperature with Hoechst (1 μg ml^{-1}) to stain DNA. Slides were imaged using a fluorescence microscope (Zeiss AxioObserver) or confocal microscope (Zeiss LSM 700). Control images were taken with the same exposure settings used for imaging the corresponding NCX antibody-treated section.

Recombinant NCX expression in sea urchin embryos

Four plasmids encoding fluorescent proteins (mCherry or Cerulean fluorescent protein, located either at the N- or C- terminus of a cloning site) were provided by the Hamdoun lab at SIO: pCS2+8NmCherry pCS2+8CmCherry, pCS2+8NCerulean, pCS2+8CCerulean (Gökirmak et al., 2012). 800 ng of each plasmid was digested by two restriction enzyme digests (N-tags: Eco-RI, then Xhol; C-tags: ClaI, then SpeI, New England Biolabs) and the linear plasmids were purified using a NucleoSpin Kit (Macherey-Nagel) from a 1% agarose gel and stored at -20 °C. Primers were designed for use with Gibson Cloning/Assembly. Primers were 48 bp long and approximately half of each primer sequence was complementary to NCX_A while the other half was complementary to the cloning vector at the site of restriction enzyme digest (Table 3.3). PCR was performed with the two primer sets (one for N-fluorescent protein plasmids, the other for C-fluorescent protein plasmids) using a PCR2.1 vector containing the NCX_A sequence

(NCX1b9mc11) as template and Phusion Taq polymerase (New England Biolabs) and bands were gel purified and stored at -20 °C. The PCR cycles used are provided (Table 3.4).

Amplified NCX_A was cloned into the plasmids by In-Fusion Cloning (Clontech), with a 3:1 molar ratio of insert:vector (86.25 ng insert:50 ng vector). Cloning was performed by a 15 minute incubation at 50 °C and then held at 4 °C until plasmids were transformed into Top 10 *E. coli* (Invitrogen) or Stellar Competent Cells (Clontech) for propagation. Colonies were screened via colony PCR and successful constructs were identified and fully sequenced (Table 3.3) to confirm the ORF was uninterrupted. 20 ng of each were transformed into Top 10 *E. coli* to propagate. 10 μg of each plasmid underwent restriction digest by NotI and linearized plasmid was gel-purified and stored at -20 °C. ~800 ng linearized plasmid DNA was transcribed *in vitro* using the SP6 mMessage mMachine kit (Ambion) according to the manufacturer's suggested protocol, and mRNA was run in an agarose gel to ensure no degradation occurred. mRNA was diluted to a concentration of 2 μg μl^{-1} (except N-mCherry tagged NCX, which was diluted to 500 ng μl^{-1} due to lower yield) and aliquoted into 1 or 2 μl aliquots for long-term storage in -80 °C. For the colocalization experiments, mRNAs encoding C-mCherry *Sp*-ABCC9 and *Sp*-ABCB6 (Gokirmak et al., 2014) were also prepared with the SP6 mMessage mMachine kit (Ambion) according to the manufacturer's protocol and diluted to 2 μg μl^{-1} stocks stored at -80 °C as previously described (Campanale & Hamdoun, 2012). *Sp*-ABCC9 and *Sp*-ABCB6 mRNA was then diluted to 500 ng μl^{-1} and mixed with 100 ng μl^{-1} mCerulean NCX.

Adult *Strongylocentrotus purpuratus* were collected in San Diego, California, and held in 11 ºC (± 1 °C) in flowing seawater aquaria. Animals were spawned by intra-coelomic injection of 0.55 M KCl. Eggs were collected in natural seawater, filtered through a 120 μm mesh and washed twice in 0.22 micron filtered seawater (FSW) and kept at 14 °C. Sperm was collected dry in 1.5 ml tubes and stored at 4 °C. Unfertilized *S. purpuratus* eggs were prepared for injection as

previously described (Lepage & Gache, 2004) stuck to 35 mm petri dishes (Fisher Scientific) coated with 0.25% protamine sulfate and fertilized. One-cell zygotes were then injected at between 2-5% egg volume with the mRNA mixture described above. Ampicillin (Sigma Aldrich, St. Louis, MO) at 100 μg ml^{-1} in FSW was added to the injection plate. Embryos were then cultured at 15 °C (±1 °C) for between 16 and 48 hours. At the times described above injected *S. purpuratus* embryos were mounted on 1.5 coverglass (VWR, Radnor, PA) and imaged on either a Zeiss LSM 700 (Jena, Germany) or a Leica Sp8 (Wetzlar, Germany) confocal microscope. Captured images were then processed using ImageJ to adjust brightness and contrast.

Acknowledgements

Chapter 3, in part, is currently being prepared for submission for publication of the material, as it may appear in the following citation: Barron, M. E., Thies, A. B., Espinosa, J. A., Barott, K. L., Hamdoun, A., Tresguerres, M. A Na^+/Ca^{2+} exchanger in vesicles in coral calcifying cells: revisiting calcification mechanisms. The dissertation author was the primary investigator and primary author of this material.

I would like to thank Dr. Jonathan Matalonga Borrel for his advice designing the restriction enzyme digest and primers necessary for cloning ayNCX_A into pCS2/fluorescent protein plasmids.

Figures

Figure 3.1: Phylogenetic tree of ayNCX$_A$ (A.yongeiNCXA) (highlighted blue) and ayNCX$_{B1-4}$ (A.yongeiNCXB1-4)(highlighted green) with other NCX and NCX-like proteins. The following accession numbers were used for obtaining either predicted transcripts, mRNA, or protein sequences. **Coral NCX proteins** (highlighted grey): *Acropora digitifera* (A.digitiferaNCXA: XP_015752015.1, A.digitiferaNCXB: XP_015772900.1)[1], *Acropora millepora* NCX (A.milleporaNCXA: JT007757.1, A.milleporaNCXB: JT003571.1), *Acropora cervicornis* (A.cervicornisNCXA: GASU01080071.1, A.cervicornisNCXB: GASU01087165.1), *Orbicella faveolata* (O.faveolataNCXA: XM_020750226.1, O.faveolataNCXB: XP_020626605.1), *Galaxea fascicularis* (G.fascicularisNCXA: GFAZ01129628), *Porites australiensis* (P.australiensisNCXA: FX462417.1), *Porites astreoides* (P.astreoidesNCXA: GEHP01352486), *Favia lizardensis* (F.lizardensisNCXA: GDZU01041167), *Pocillopora damicornis* (P.damicornisNCXA: GEFF01028265), *Stylophora pistillata* (S.pistillataNCXA: GARY01000181.1 – this sequence was edited to fix frameshift errors that split the protein into three incomplete NCX proteins). All coral sequences were designated A or B based on their homology to ayNCX proteins. **Invertebrate NCX proteins:** *Exaiptasia pallida* (AnenomeNCX1: XP_020915137.1, AnenomeNCX2: XM_021049204.1, AnenomeNCX3: XP_020912295.1), *Strongylocentrotus purpuratus* (UrchinNCX2: XM_011685576.1, UrchinNCX3: XM_011663639.1- this sequence was originally annotated as an NCX1 protein in (On et al., 2008)), *Crassostrea gigas* (OysterNCX1: XP_011444293.1, OysterNCX2: XM_011445979.2, OysterNCX3: XM_020074533.1), *Doryteuthis opalescens* (SquidNCX: AAB52920.1)[2], *Drosophila melanogaster* (FlyCalx: AAB63464.1) [2], **Chordate NCX proteins:** , *Ciona intestinalis* (TunicateNCX1: XM_002126723.4, TunicateNCX2: XM_002129316.4, TunicateNCX3: XM_002122937.3) *Danio rerio* (ZebrafishNCX1: NM_001037102.1, ZebrafishNCX3: XM_005156997.4), *Callorhinchus milii* (ElephantFishNCX1: XM_007893988.1, ElephantFishNCX3: XM_007893267.1), *Squalus acanthias* (DogfishNCX1: DQ068478.1)[3], *Gallus* (ChickenNCX1: AJ012579.1, ChickenNCX3: AJ012580.1)[4], *Rattus norvegicus* (RatNCX2: P48768.1, RatNCX3: P70549.1) [2], *Mus musculus* (MouseNCX1: AF004666.1, MouseNCX3: NM_080440.3)[5], *Canis sp*. (DogNCX1: AAA62766.1) [2], *Homo sapiens* (HumanNCX1: NM_021097.2, HumanNCX2: NM_015063.2- the original accession number cited in paper, XM_0038970, no longer exists, HumanNCX3: NM_033262.4)[6] **NCKX proteins:** *Bos taurus* (BullNCKX1: Q28139.2- was 108825 in reference but number has been updated) [2], *Rattus norvegicus* (RatNCKX2: AAC19405.1)[2] **Other:** *Saccharomyces cerevisiae* (YeastVX1: Q99385.1) [2], *Homo sapiens* (HumanNCLX: NP_079235.2)

NCBI BLAST was used to identify most sequences. Others provided in papers are referenced as follows: [1](Shinzato et al., 2011), [2](Philipson & Nicoll, 2000), [3](On et al., 2008), [4](Stains et al., 2002), [5](Sosnoski & Gay, 2008), [6](Quednau et al., 2004).

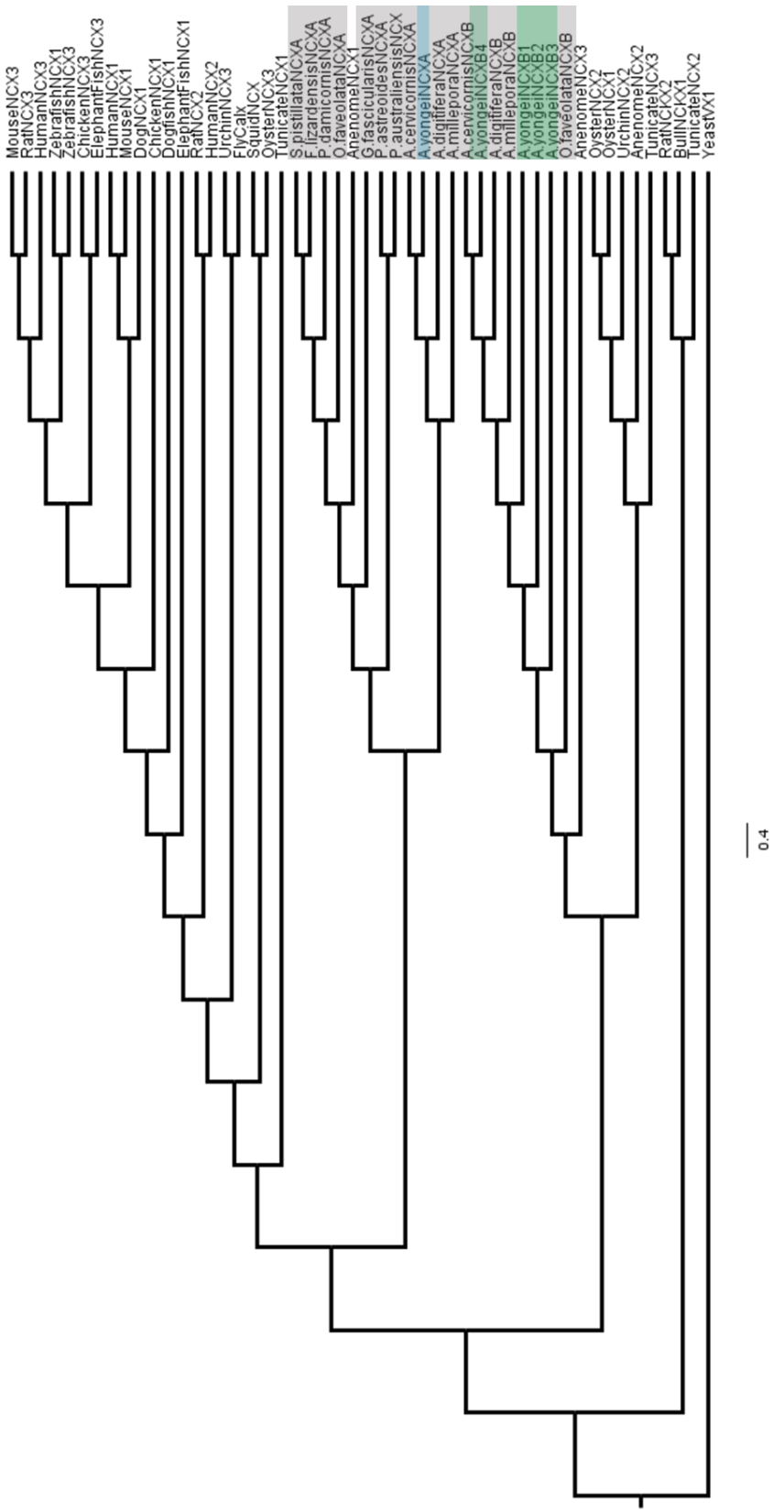
MouseNCX3
RatNCX3
HumanNCX3
ZebrafishNCX1
ZebrafishNCX3
ChickenNCX3
ElephantFishNCX3
HumanNCX1
MouseNCX1
DogNCX1
ChickenNCX1
DogfishNCX1
ElephantFishNCX1
RatNCX2
HumanNCX2
UrchinNCX3
FlyCalx
SquidNCX
OysterNCX3
TunicateNCX1
S.pistillataNCXA
F.lizardensisNCXA
P.damicornisNCXA
O.faveolataNCXA
AnenomeNCX1
G.fascicularisNCXA
P.astreoidesNCXA
P.australiensisNCX
A.cervicornisNCXA
A.yongeiNCXA
A.digitiferaNCXA
A.milleporaNCXA
A.cervicornisNCXB
A.yongeiNCXB4
A.digitiferaNCXB
A.milleporaNCXB
A.yongeiNCXB1
A.yongeiNCXB2
A.yongeiNCXB3
O.faveolataNCXB
AnenomeNCX3
OysterNCX2
OysterNCX1
UrchinNCX2
AnenomeNCX2
TunicateNCX3
RatNCX2
BullNCX1
TunicateNCX2
YeastVX1
0.4

A)

```
ayNCXB1         AAGTTTTGTTGCCGATGCCTAGTCTGATGTAACAGACAAAACATATGGGATGCCTTTGCT
ayNCXB2         AAGTTTTGTTGCCGATGCCTAGTCTGATGTAACAGACAAAACATATGGGATGCCTTTGCT
                ************************************************************

ayNCXB1         CTGCATTGATTTTTGATCGGTCGAACTGGATATGACTATGACTGACAAATGTTCTGAAGG
ayNCXB2         CTGCATTGATTTTTGATCGGTCGAACTGGATATGACTATGACTGACAAATGTTCTGAAGG
                ************************************************************

ayNCXB1         GACACTCTTGCTTCCATTTTTGGATGAATCTGAATGGATTGAAGAGCTCAGGATTTTTAT
ayNCXB2         GACACTCTTGCTTCCATTTTTGGATGAATCTGAATGGATTGAAGAGCTCAGGATTTTTAT
                ************************************************************

ayNCXB1         CTATCTTGTAGCGCTGTTATGGTGTTTTATGGGAGTTGCTATAATCGCAGACGTATTTAT
ayNCXB2         CTATCTTGTAGCGCTGTTATGGTGTTTTATGGGAGTTGCTATAATCGCAGACGTATTTAT
                ************************************************************

ayNCXB1         GTGTGCTATCGAAACCATAACAAGCAAAACAAAGCAAGTGAAAGTGGCAAGACAAGATAG
ayNCXB2         GTGTGCTATCGAAACCATAACAAGCAAAACAAAGCAAGTGAAAGTGGCAAGACAAGATAG
                ************************************************************

ayNCXB1         CGACCAAGTTGACTTGGTTGAAATTCGCATATGGAATGACACAGTGGCGAACCTAACTTT
ayNCXB2         CGACCAAGTTGACTTGGTTGAAATTCGCATATGGAATGACACAGTGGCGAACCTAACTTT
                ************************************************************

ayNCXB1         GATGGCACTGGGATCATCAGCCCCTGAAATTTTGCTGGCCATCATTGAGATCACTATTTT
ayNCXB2         GATGGCACTGGGATCATCAGCCCCTGAAATTTTGCTGGCCATCATTGAGATCACTATTTT
                ************************************************************

ayNCXB1         GAACAAATTTAATGCAGGCGAACTCGGCCCAAGCACTATCGTCGGTTCTGCGGCTTTCAA
ayNCXB2         GAACAGATTTAATGCAGGCGAACTCGGCCCAAGCACTATCGTCGGTTCTGCGGCTTTCAA
                ***** ********************************************************

ayNCXB1         CCTTCTTGTTATAACTGGAGTATGTATAATGACCGTTCCAGCTCACGAACAGCGAAGAAT
ayNCXB2         CCTTCTTGTTATAACTGGAGTATGTATAATGACCGTTCCAGCTCACGAACAGCGAAGAAT
                ************************************************************

ayNCXB1         CAAGTCTGTCAAAGTGTTCGCTGTGACGGCTTCTTTCTCCGTTCTGGCTTACGTTTGGCT
ayNCXB2         CAAGTCTGTCAAAGTGTTCGCTGTGACGGCTTCTTTCTCCGTTCTGGCTTACGTTTGGCT
                ************************************************************
```

Figure 3.2: Alignment of ayNCX$_B$ sequences. A) Alignment of ayNCX$_{B1}$ and ayNCX$_{B2}$ PCR products. Start codons (highlighted green) indicate the beginning of the protein-coding sequence. Both sequences are nearly identical, except for some SNPs (highlighted grey) and where they contain two mutually exclusive intronic sequences (ayNCXB1 highlighted blue, ayNCXB2 highlighted yellow). Each exon contains a unique stop codon (highlighted red). As a result of these stop codons, ayNCXB2 encodes a smaller protein than NCXB1. B) Alignment of all four ayNCX$_B$ proteins with the epitope region used to generate polyclonal coral NCX antibodies. The first methionine of each protein sequence is indicated (highlighted green), as well as the location of the last amino acid (highlighted red). ayNCX$_{B1}$ and ayNC$_{B2}$ contain a slightly homologous region, but only 4/14 amino acids (28.6%) are conserved (highlighted black). For comparison, 13/14 (92.9%) amino acids are conserved in ayNCX$_A$. All four ayNCXB isoforms have distinct C-terminal sequences, which we have indicated for ayNCX$_{B2}$ (highlighted yellow), ayNCX$_{B3}$ (highlighted purple), and ayNCX$_{B4}$ (highlighted pink). No sequence is highlighted for ayNCX$_{B1}$ because it is the longest.

```
ayNCXB1         GTTTTTTGCCCTCACTGTGAGCTCTAAAAATGAGATAGAACTTTGGGAAGCAATTTTAAC
ayNCXB2         GTTTTTTGCCCTCACTGTGAGCTCTAAAAATGAGATAGAACTTTGGGAAGCAATTTTAAC
                ************************************************************

ayNCXB1         CTTTCTGTTGTTTCCAGTTCTTGTTGTTATCGCTTATATCGCGGACAAAGATTACTGTTC
ayNCXB2         CTTTCTGTTGTTTCCAGTTCTTGTTGTTATCGCTTATATCGCGGACAAAGATTACTGTTC
                ************************************************************

ayNCXB1         TGGAAAAATATCCCCGCAAGACCCTGGAGTCCTCGAACTCGCTGAAGGTTCAAAGGTCCT
ayNCXB2         TGGAAAAATATCCCCGCAAGACCCTGGAGTCCTCGAACTCGCTGAAGGTTCAAAGGTCCT
                ************************************************************

ayNCXB1         GAAAACACCATCACATGATCCTGAGGTTGAGAGCTTCATAAAGGAAGTCAGCAGAAATCC
ayNCXB2         GAAAACACCATCACATGATCCTGAGGTTGAGAGCTTCATAAAGGAAGTCAGCAGAAATCC
                ************************************************************

ayNCXB1         TAATTTGACAGAAGATGAGGCTGCTGTGCTTGTAGCTGCCCACATTAAGTCTAAACAACC
ayNCXB2         TAATTTGACAGAAGATGAGGCTGCTGTGCTTGTAGCTGCCCACATTAAGTCTAAACAACC
                ************************************************************

ayNCXB1         AAAAAACTACGGATACTATCGCGTTGGTGCAATACGAGACCTTGGTGGTAGTCACAAACT
ayNCXB2         AAAAAACTACGGATACTATCGCGTTGGTGCAATACGAGACCTTGGTGGTAGTCACAAACT
                ************************************************************

ayNCXB1         GACACCAAACATGGATCCACAATTAAGACTGATCTACGAGGAGCTGTCTGAAGTTGGTTT
ayNCXB2         GACACCAAACATGGATCCACAATTAAGACTGATCTACGAGGAGCTGTCTGAAGTTGGTTT
                ************************************************************

ayNCXB1         TTCTTCGTCAGGAGCTTCGGCAATCATGAACCATGCCCTTGGAGGGAAAGTTCAACCTGC
ayNCXB2         TTCTTCGTCAGGAGCTTCGGCAATCATGAACCATGCCCTTGGAGGGAAAGTTCAACCTGC
                ************************************************************

ayNCXB1         TCGCGTGGAATTTGCTGCTCCGAAATGCGCTGTACTTGAAAGTGATAAACTTGTGAGGAT
ayNCXB2         TCGCGTGGAATTTGCTGCTCCGAAATGCGCTGTACTTGAAAGTGATAAACTTGTGAGGAT
                ************************************************************

ayNCXB1         TGGAGTCACGAGAACTGGCAACACTAAAATCCCCACAACTGTCAATTATGAAACCATCAA
ayNCXB2         TGGAGTCACGAAAACTGGCAACACTAAAATCCCCACAACTGTCAATTATGAAACCATCAA
                *********** ************************************************

ayNCXB1         TGGCACAGCAATGGCAGGCTCGGACTATGAGGCCAGGAAAGATGTGCTTGTCTTCAAACC
ayNCXB2         TGGCACAGCAATGGCAGGCTCGGACTATGAGGCCAGGAAAGATGTGCTTGTCTTCAAACC
                ************************************************************

ayNCXB1         AGGAGAAACTTTGAAACACATCGATATCACCATTATTGATGATGATGAGTGGGAGGAAAA
ayNCXB2         AGGAGAAACTTTGAAACACGTCGATATCACCATTATTGATGATGATGAGTGGGAGGAAAA
                ****************** ****************************************

ayNCXB1         TGAAGTCTTCTTCATTAAACTGTCGAGATTTGATTACAAAGATGATTCCGTTGAAATTGG
ayNCXB2         TGAAGTCTTCTTCATTAAACTGTCGAGATTTGATTACAAAGATGATTCCGTTGAAATTGG
                ************************************************************

ayNCXB1         AGGACAGAGTGTTACTGAAGTGACAATTATCAATGACGATGAGCCTGGAATCTTCTCGCT
ayNCXB2         AGGACAGAGTGTTACTGAAGTGACAATTATCAATGACGATGAGCCTGGAATCTTCTCGCT
                ************************************************************

ayNCXB1         AGAGAACCCAAGCTTTGTGATCAAAGAGAGTATTGGCAAAGCGTCCTTCAAGGTAGAGCG
ayNCXB2         AGAGAACCCAAGCTTTGTGATCAAAGAGAGTATTGGCAAAGCGTCCTTCAAGGTAGAGCG
                ************************************************************
```

Figure 3.2: Alignment of ayNCX$_B$ sequences *continued.*

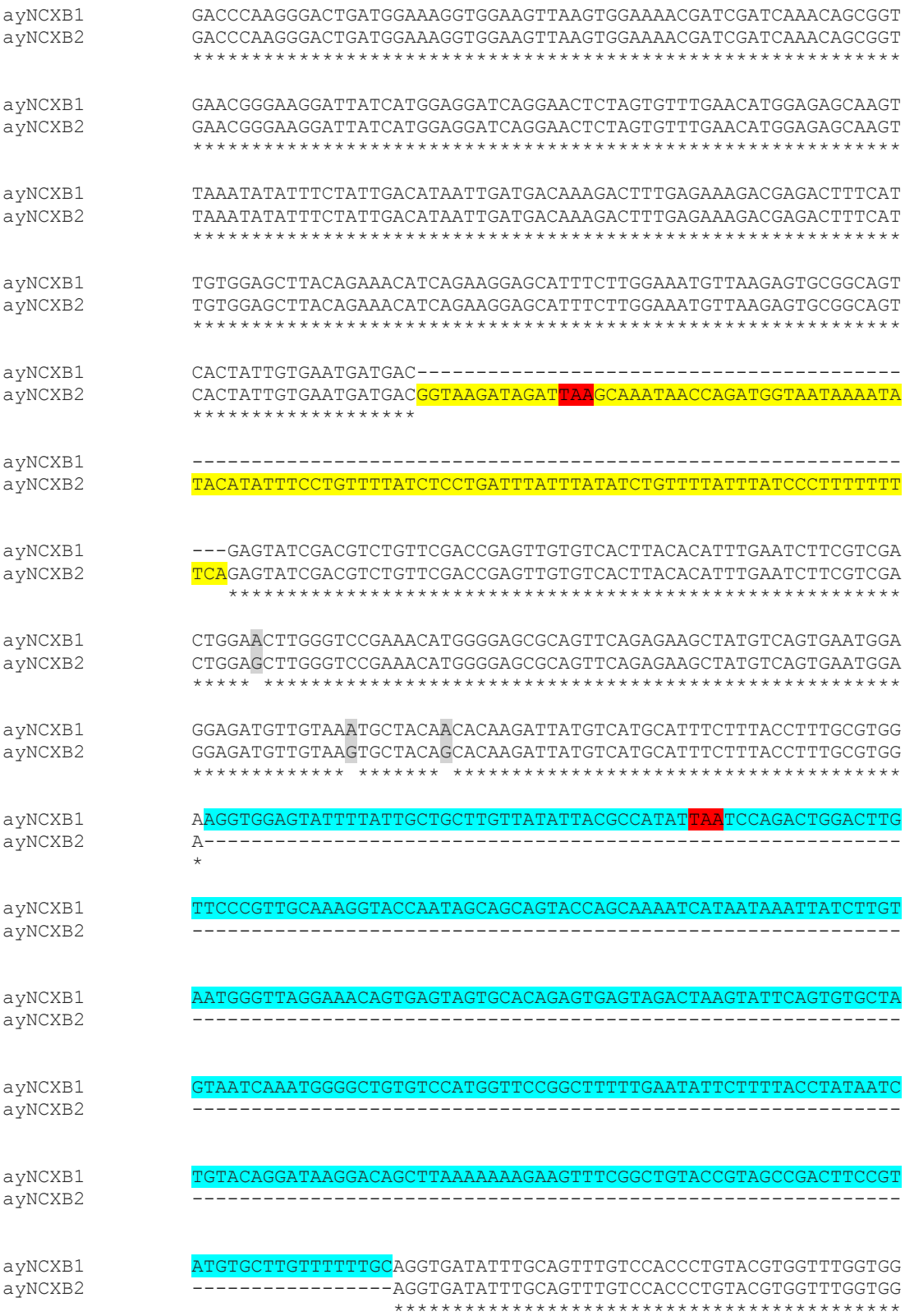

Figure 3.2: Alignment of ayNCX$_B$ sequences *continued.*

```
ayNCXB1         CTGGTTGACATTTTGTGTTGCTCTGGGAATGATTGGACTTCTTACTGTTATTGTTGGAGA
ayNCXB2         CTGGTTGACATTTTGTGTTGCTCTGGGAATGATTGGACTTCTTACTGTTATTGTTGGAGA
                ************************************************************

ayNCXB1         CCTGGCAACTATATTTGGTTGCCTGATTGGACTCAAGGCGGAAGTGACTGCCATTACCTT
ayNCXB2         CCTGGCAACTATATTTGGTTGCCTGATTGGACTCAAGGCGGAAGTGACTGCCATTACCTT
                ************************************************************

ayNCXB1         TGTTGCACTCGGCACCAGTCTCCCAGACTTGTTTGCCAGTAAATGCGCAGCTGTTAGTGA
ayNCXB2         TGTTGCACTCGGCACCAGTCTCCCAGACTTGTTTGCCAGTAAATGCGCAGCTGTTAGTGA
                ************************************************************

ayNCXB1         GAAACACGCAGACGCAGCTGTCGGCAACGTCACTGGAAGTAACTCAGTTAATGTGTTTCT
ayNCXB2         GAAACACGCAGACGCAGCTGTCGGCAACGTCACTGGAAGTAACTCAGTTAATGTGTTTCT
                ************************************************************

ayNCXB1         GGGCCTTGGAACCCCTTGGTTAATAGCGTGCATTTATCATACAGTCAAGGGAACAAAATT
ayNCXB2         GGGCCTTGGAACCCCTTGGTTAATAGCGTGCATTTATCATACAGTCAAGGGAACAAAATT
                ************************************************************

ayNCXB1         CATAGTTGAAGCTGGAACACTGTCAATAAGTGTGATAACGTACAGCATCTGTGCTATTGT
ayNCXB2         CATAGTTGAAGCTGGAACACTGTCAATAAGTGTGATAACGTACAGCATCTGTGCTATTGT
                ************************************************************

ayNCXB1         CTGTATGGTACTCTTGGTGGTGCGACGAAACAGCAAGTTTATGGGTCGCGCCGAGCTTGG
ayNCXB2         CTGTATGGTACTCTTGGTGGTGCGACGAAACAGCAAGTTTATGGGTCGCGCCGAGCTTGG
                ************************************************************

ayNCXB1         AGGACCCAGTGGACCGAAATATTTCTCAGGCAGTTTTCTGATCTTCTTGTGGCTCCTTTA
ayNCXB2         AGGACCCAGTGGACCGAAATATTTCTCAGGCAGTTTTCTGATCTTCTTGTGGCTCCTTTA
                ************************************************************

ayNCXB1         CGTTTTAATCTCATCGTTGGTATCATACGAAATTATCACCTTTTAGAGTATTTACAACTA
ayNCXB2         CGTTTTAATCTCATCGTTGGTATCATACGAAATTATCACCTTTTAGAGTATTTACAACTA
                ************************************************************

ayNCXB1         TTTTCCC
ayNCXB2         TTTTCCC
                *******
```

B)

```
epitope         ------------------------------------------------------------
ayNCXB4         MTMTDKCSEGTLLLPFLDESEWIEELRIFIYLVALLWCFMGVAIIADVFMCAIETITSKT
ayNCXB3         MTMTDKCSEGTLLLPFLDESEWIEELRIFIYLVALLWCFMGIAIIADVFMCAIETITSKT
ayNCXB1         MTMTDKCSEGTLLLPFLDESEWIEELRIFIYLVALLWCFMGVAIIADVFMCAIETITSKT
ayNCXB2         MTMTDKCSEGTLLLPFLDESEWIEELRIFIYLVALLWCFMGVAIIADVFMCAIETITSKT


epitope         ------------------------------------------------------------
ayNCXB4         KQVKVARQDSDQVDLVEIRIWNDTVANLTLMALGSSAPEILLAIIEITILNKFNAGELGP
ayNCXB3         KQVKVARQDSDQVDLVEIRIWNDTVANLTLMALGSSAPEILLAIIEITILNKFNAGELGP
ayNCXB1         KQVKVARQDSDQVDLVEIRIWNDTVANLTLMALGSSAPEILLAIIEITILNKFNAGELGP
ayNCXB2         KQVKVARQDSDQVDLVEIRIWNDTVANLTLMALGSSAPEILLAIIEITILNRFNAGELGP


epitope         ------------------------------------------------------------
ayNCXB4         STIVGSAAFNLLVITGVCIMTVPAHEQRRIKSVKVFAVTASFSVLAYVWLFFALTVSSKN
ayNCXB3         STIVGSAAFNLLVIAGVCIMTVPAHEQRRIKSVKVFAVTASFSVLAYVWLFFALTVSSKN
ayNCXB1         STIVGSAAFNLLVITGVCIMTVPAHEQRRIKSVKVFAVTASFSVLAYVWLFFALTVSSKN
ayNCXB2         STIVGSAAFNLLVITGVCIMTVPAHEQRRIKSVKVFAVTASFSVLAYVWLFFALTVSSKN
```

Figure 3.2: Alignment of ayNCX$_B$ sequences *continued.*

```
epitope      ------------------------------------------------------------
ayNCXB4      EIELWEAILTFLLFPVLVVIAYIADKDYCSGKISPQDPGVLELGTCYKYRAFCVTF-QV-
ayNCXB3      EIELWEAILTFLLFPVLVVIAYIADKDYCSGKISPQDPGVLELAEGSKVLKTPSHDPEVE
ayNCXB1      EIELWEAILTFLLFPVLVVIAYIADKDYCSGKISPQDPGVLELAEGSKVLKTPSHDPEVE
ayNCXB2      EIELWEAILTFLLFPVLVVIAYIADKDYCSGKISPQDPGVLELAEGSKVLKTPSHDPEVE

epitope      ------------------------------------------------------------
ayNCXB4      ------------------------------------------------------------
ayNCXB3      SFIKEVSRNPNLTEDEAAVLVAAHIKSKQPKNYGYYRVGAIRDLGGSHKLTPNMDPQLRL
ayNCXB1      SFIKEVSRNPNLTEDEAAVLVAAHIKSKQPKNYGYYRVGAIRDLGGSHKLTPNMDPQLRL
ayNCXB2      SFIKEVSRNPNLTEDEAAVLVAAHIKSKQPKNYGYYRVGAIRDLGGSHKLTPNMDPQLRL

epitope      ------------------------------------------------------------
ayNCXB4      ------------------------------------------------------------
ayNCXB3      IYEELSEVGFSSSGASAIMNHALGGKVQPARVEFAAPKCAVLESDKLVRIGVTRTGNTKI
ayNCXB1      IYEELSEVGFSSSGASAIMNHALGGKVQPARVEFAAPKCAVLESDKLVRIGVTRTGNTKI
ayNCXB2      IYEELSEVGFSSSGASAIMNHALGGKVQPARVEFAAPKCAVLESDKLVRIGVTKTGNTKI

epitope      ------------------------------------------------------------
ayNCXB4      ------------------------------------------------------------
ayNCXB3      PTTVNYETINGSNGRLGL--------------------------------------------
ayNCXB1      PTTVNYETINGTAMAGSDYEARKDVLVFKPGETLKHIDITIIDDDEWEENEVFFIKLSRF
ayNCXB2      PTTVNYETINGTAMAGSDYEARKDVLVFKPGETLKHVDITIIDDDEWEENEVFFIKLSRF

epitope      ------------------------------------------------------------
ayNCXB4      ------------------------------------------------------------
ayNCXB3      ------------------------------------------------------------
ayNCXB1      DYKDDSVEIGGQSVTEVTIINDDEPGIFSLENPSFVIKESIGKASFKVERTQGTDGKVEV
ayNCXB2      DYKDDSVEIGGQSVTEVTIINDDEPGIFSLENPSFVIKESIGKASFKVERTQGTDGKVEV

epitope      ---------------KDEDGKSVLRTGEG-------------------------------
ayNCXB4      ------------------------------------------------------------
ayNCXB3      ------------------------------------------------------------
ayNCXB1      KWKTIDQTAVNGKDYHGGSGTLVFEHGEQVKYISIDIIDDKDFEKDETFIVELTETSEGA
ayNCXB2      KWKTIDQTAVNGKDYHGGSGTLVFEHGEQVKYISIDIIDDKDFEKDETFIVELTETSEGA

epitope      ------------------------------------------------------------
ayNCXB4      ------------------------------------------------------------
ayNCXB3      ------------------------------------------------------------
ayNCXB1      FLGNVKSAAVTIVNDDEYRRLFDRVVSLTHLNLRRLELGSETWGAQFREAMSVNGGDVVN
ayNCXB2      FLGNVKSAAVTIVNDDGKID------------------------------------------

epitope      ----------------------------
ayNCXB4      ----------------------------
ayNCXB3      ----------------------------
ayNCXB1      ATTQDYVMHFFTFAWKVEYFIAACYITPY
ayNCXB2      ----------------------------
```

Figure 3.2: Alignment of ayNCX$_B$ sequences *continued*.

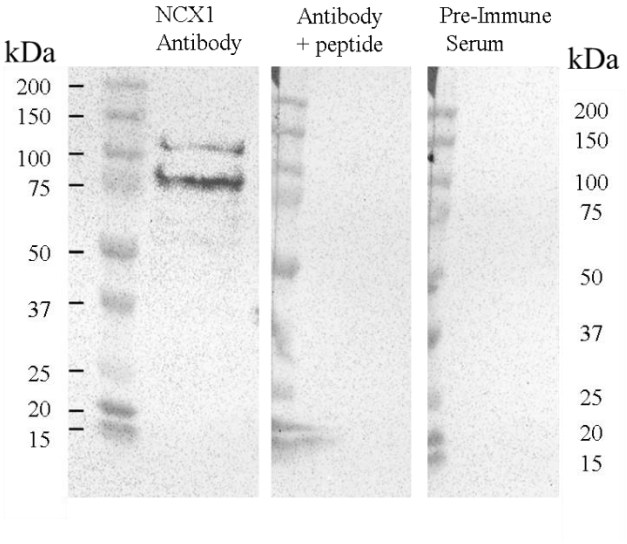

Figure 3.3: Validation of coral NCX antibody. A) The NCX antibody recognizes a ~100 kDa and a ~75 kDa protein in homogenized *A. yongei* tissue. B) Both bands are eliminated when the antibody is pre-adsorbed with the epitope peptide overnight. C) Both bands are eliminated when the membrane is incubated with the pre-immune serum. All three wells contain the same amount of protein; all three images were taken at the same exposure.

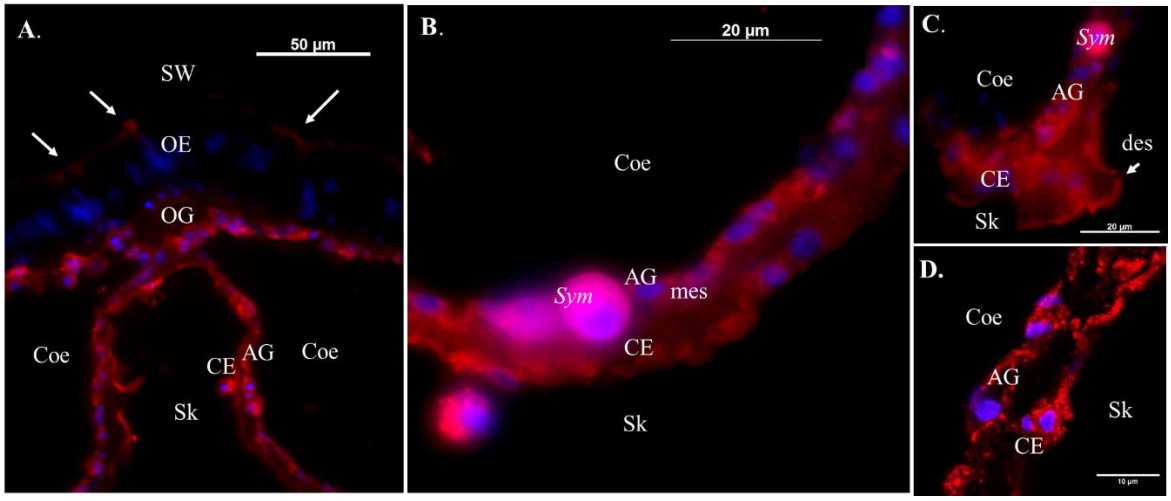

Figure 3.4: Immunofluorescence microscopy of *A. yongei* tissue. A) NCX (red fluorescence) is present in all four tissue layers. It is found in the apical membrane (white arrows) of the oral ectodermis, and in the cytoplasm of oral gastrodermis, aboral gastrodermis and the calicoblastic epithelium. B) At higher magnification, vesicle staining is visible in the both aboral layers, with no clear staining in the basolateral or apical membranes of either tissue C) A desmocyte (white arrow, labeled des) has a higher abundance of NCX protein near the apical membrane facing the skeleton. D) Confocal microscopy provides higher resolution of the vesicle staining pattern visible in the calicoblastic epithelium. Nuclei are stained by Hoechst (blue). Abbreviations: SW- Seawater, Coe- Coelenteron, Sk- Skeleton, *Sym*.- *Symbiodinium* (algae), OE- Oral Ectodermis, OG- Oral Gastrodermis, AG- Aboral Gastrodermis, CE- Calicoblastic Epithelium, des- desmocyte.

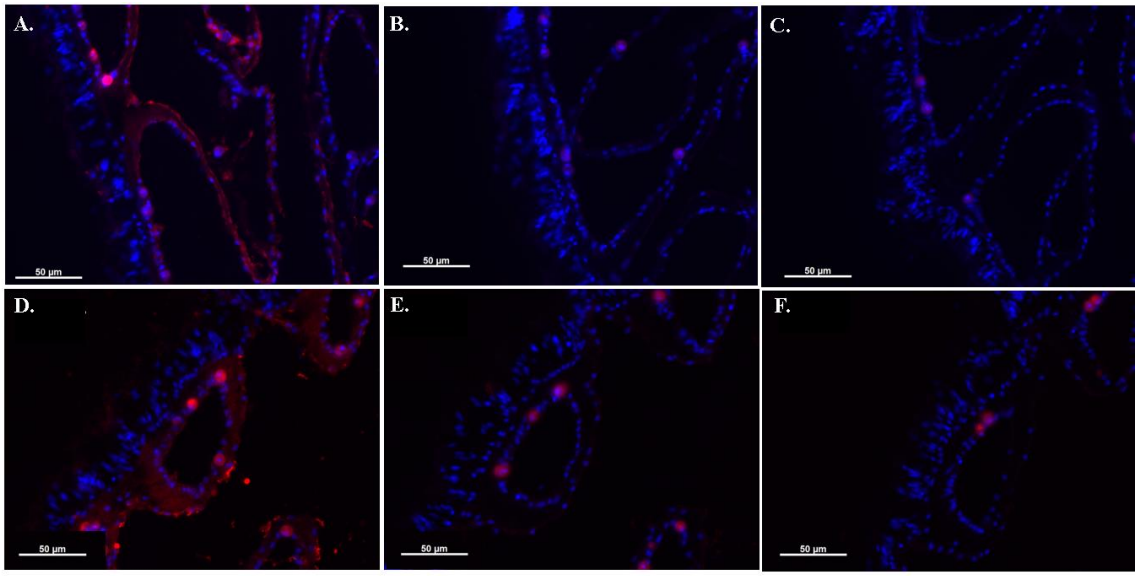

Figure 3.5: Immunofluorescence microscopy controls indicate the NCX antibody (red fluorescence) is specific. *A. yongei* tissue stained with A) NCX antibody B) NCX antibody pre-adsorbed overnight with peptide and C) no primary antibody (secondary antibody only) imaged at the same exposure time. *A. yongei* tissue stained with D) NCX antibody E) pre-immune serum and F) no primary antibody (secondary antibody only) imaged at the same exposure time. Nuclei were stained with Hoechst (blue fluorescence).

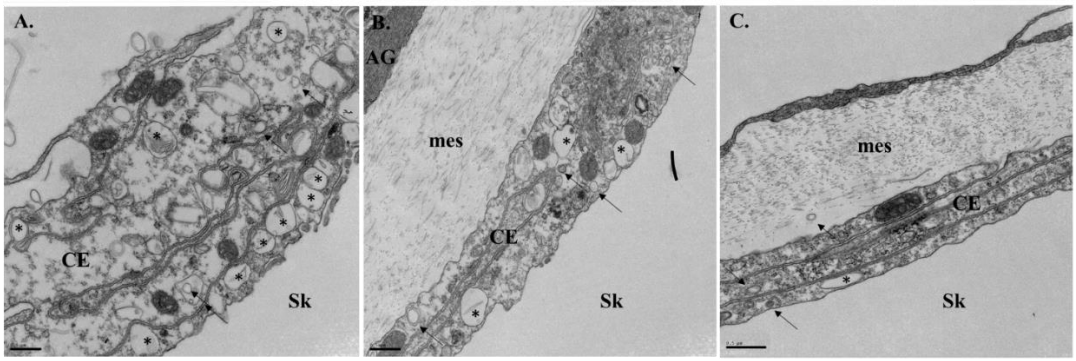

Figure 3.6: Transmission electron microscopy (TEM) of the calicoblastic epithelium in *A. yongei*. A-C) Vesicles of a variety of sizes are visible in the calicoblastic epithelium. Larger vesicles are indicated by a black asterisk (*), smaller vesicles are indicated by black arrows. Scale bar is 500 nm.

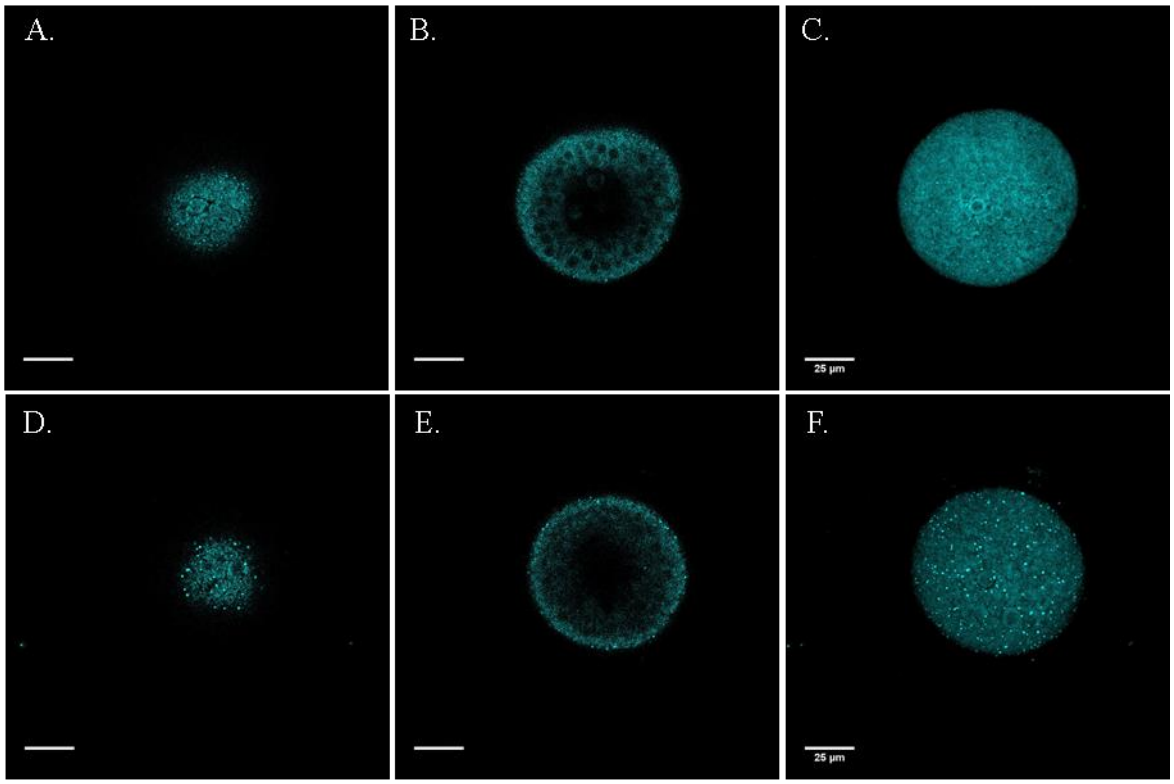

Figure 3.7: Sea urchin embryos expressing coral ayNCX$_A$ tagged with fluorescent protein. A-C) ayNCX$_A$ with Cerulean fluorescent protein (CFP) at the N-terminus. A) shows a single z-stack at the base of the embryo, B) shows a z-stack through the middle of the embryo, and C) is a z-project of all z-stacks. D-F) ayNCX$_A$ with Cerulean fluorescent protein (CFP) at the C-terminus. G-I) ayNCX$_A$ with mCherry fluorescent protein at the N-terminus. J-L) ayNCX$_A$ with mCherry fluorescent protein at the C-terminus. Embryos expressing CFP-tagged ayNCX$_A$ were imaged 16 hpf, embryos expressing mCherry-tagged ayNCX$_A$ were imaged 24 hpf.

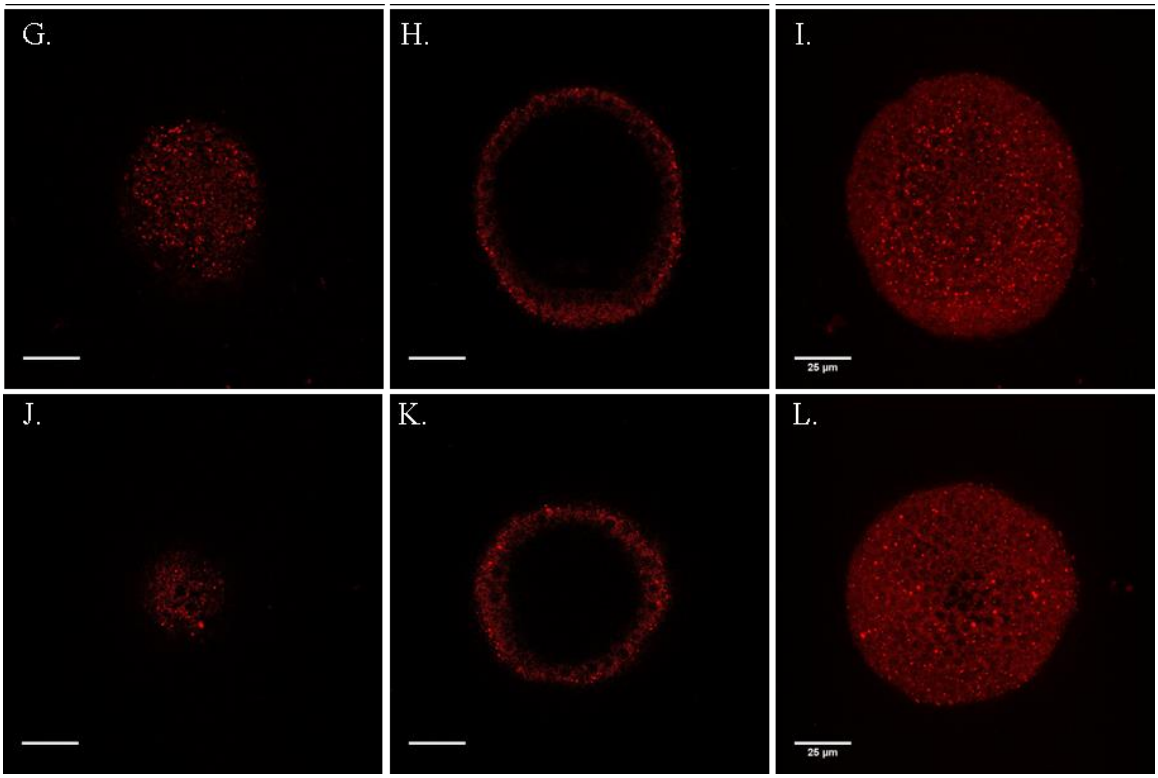

Figure 3.7: Sea urchin embryos expressing coral ayNCX$_A$ tagged with fluorescent protein *continued.*

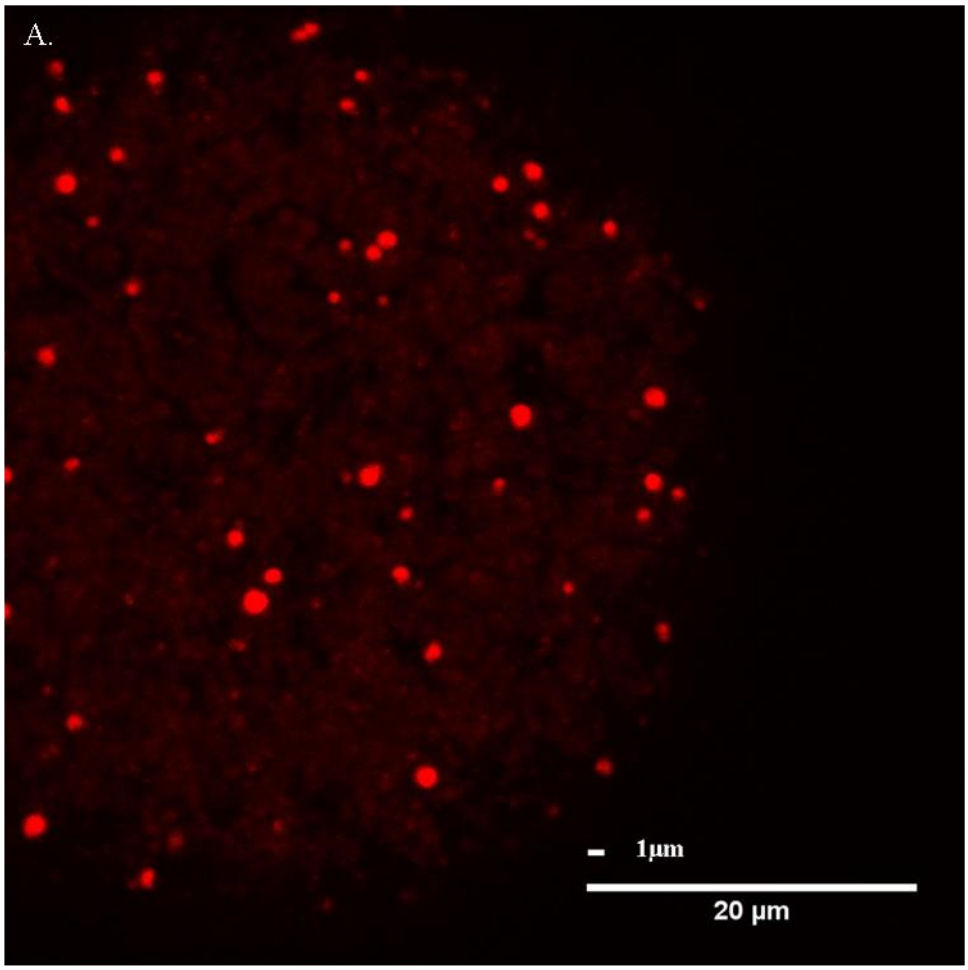

Figure 3.8: Sea urchin embryo expressing C-mCherry-ayNCX$_A$ (red fluorescence) A) z-project of the embryo imaged at high magnification indicates that vesicles containing ayNCX$_A$ are less than 1µm in diameter. B) a single z-plane from the base of the embryo C) the DIC image of the same plane and D) the two images merged. E) a single z-plane from the middle of the embryo, F) the DIC image from the same plane and G) the two images merged.

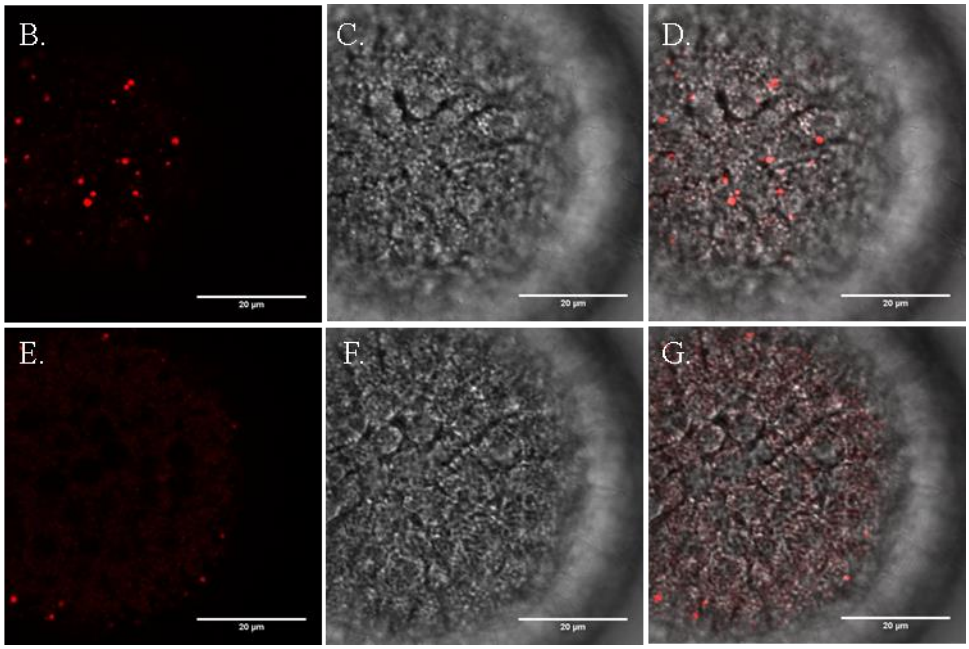

Figure 3.8: Sea urchin embryo expressing C-mCherry-ayNCX$_A$ (red fluorescence) *continued.*

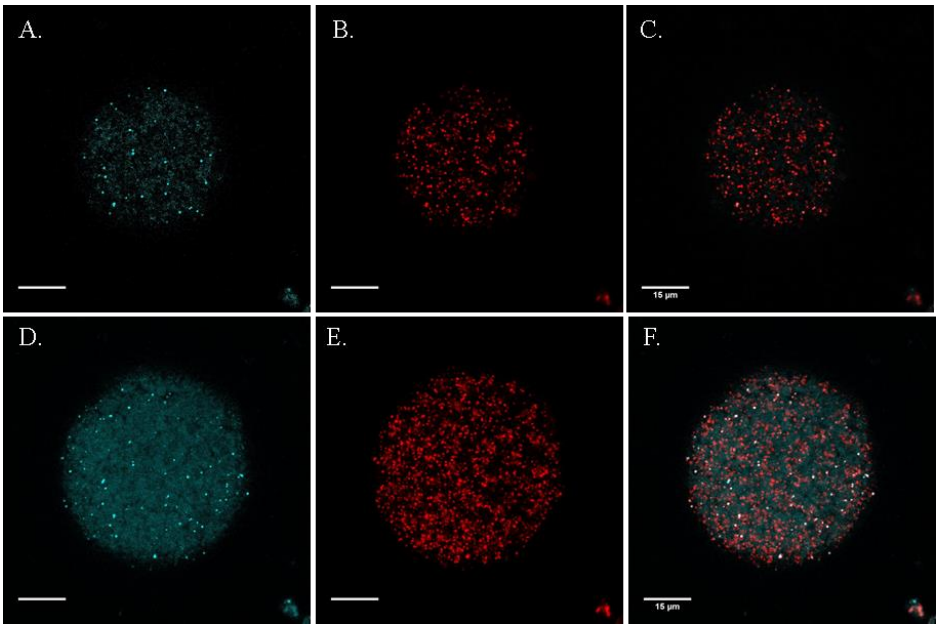

Figure 3.9: Sea urchin embryo expressing C-CFP-ayNCX_A and C-mCherry-ABCC9, an urchin protein localized in vesicles. A-C) a single z-plane from the base of the urchin embryo showing A) CFP-tagged ayNCX_A, B) mCherry-tagged ABCC9, and C) the two images merged. D-F) a z-project of all z-planes showing D) CFP-tagged ayNCX_A, E) mCherry-tagged ABCC9, and F) the two images merged. G) The merge, enlarged, shows the colocalization of the two proteins (appears white).

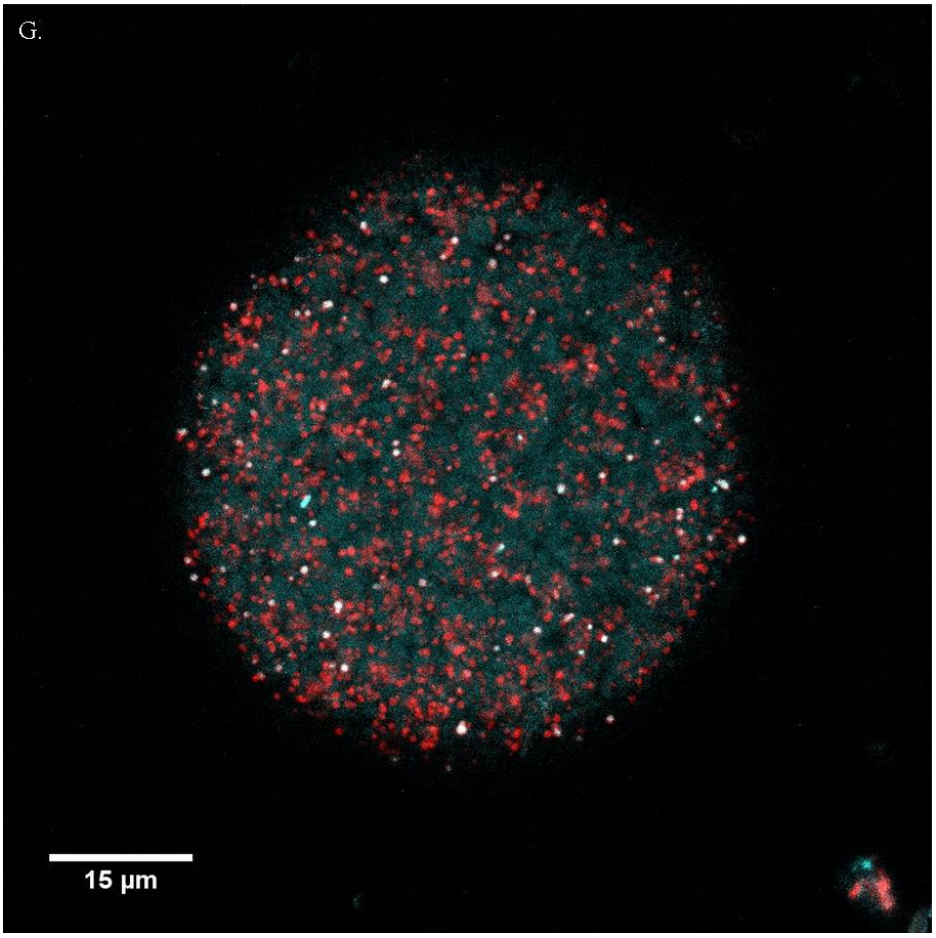

Figure 3.9: Sea urchin embryo expressing C-CFP-ayNCX_A and C-mCherry-ABCC9, an urchin protein localized in vesicles *continued.*

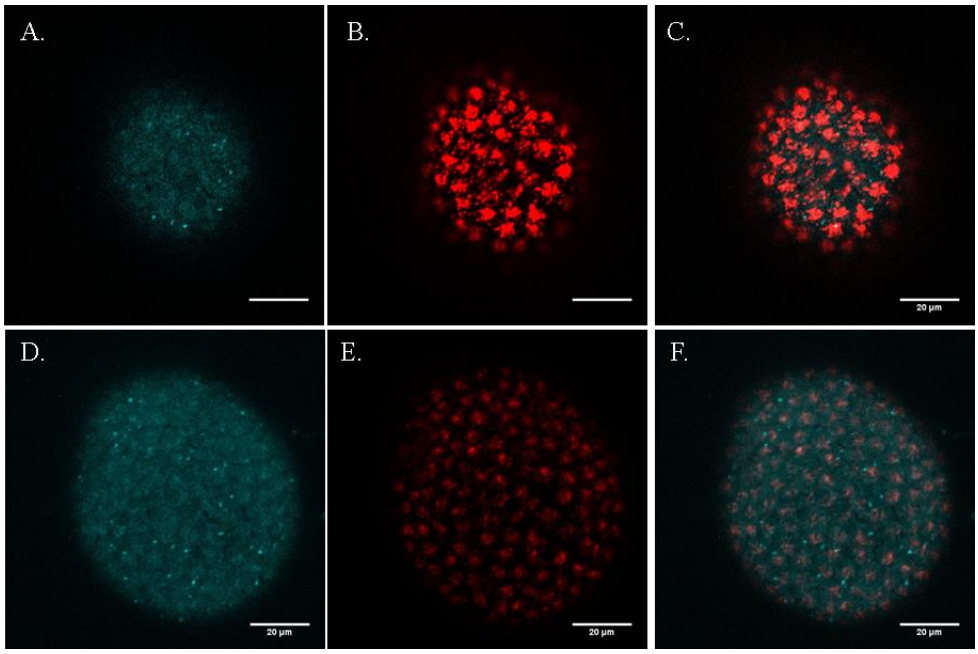

Figure 3.10: Sea urchin embryo expressing C-CFP-ayNCX$_A$ and C-mCherry-ABCB6, an urchin protein localized in the mitochondria. A-C) a single z-plane from the base of the urchin embryo showing A) CFP-tagged ayNCX$_A$, B) mCherry-tagged ABCB6, and C) the two images merged. D-F) a z-project of all z-planes showing D) CFP-tagged ayNCX$_A$, E) mCherry-tagged ABCB6, and F) the two images merged. G) The merge, enlarged, shows there is no colocalization of the two proteins (would appear white).

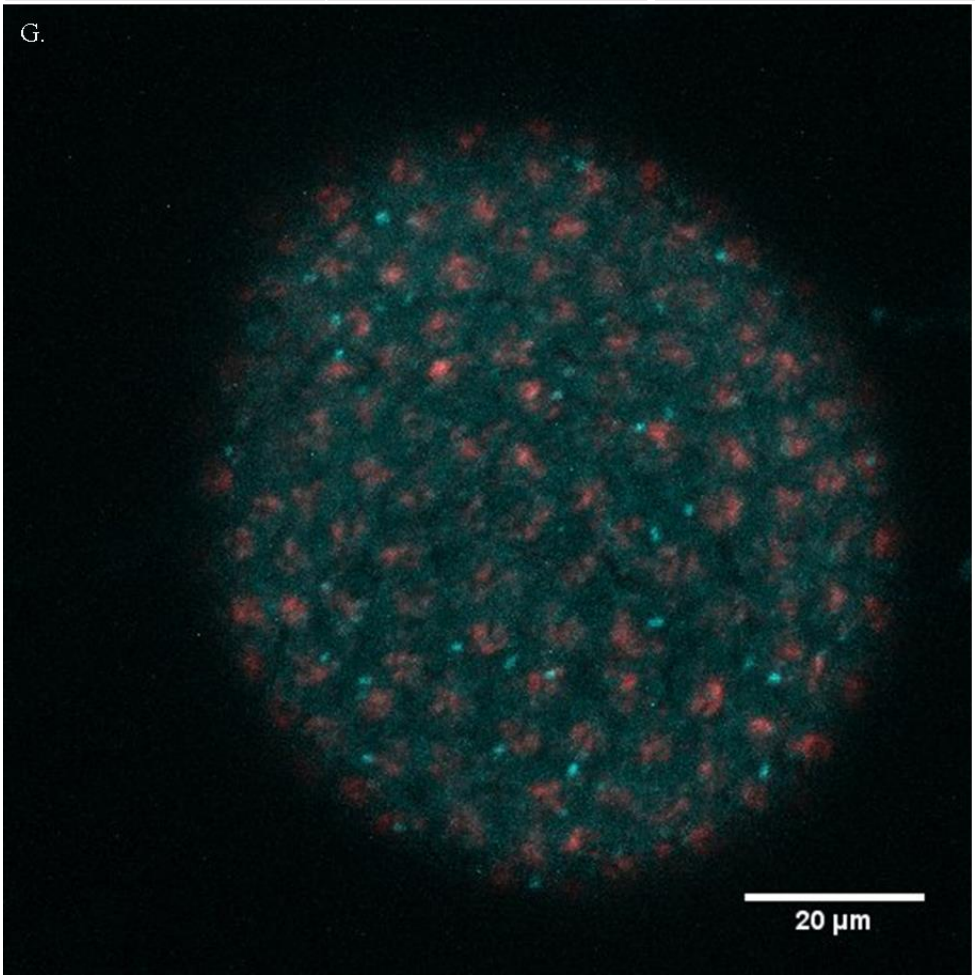

Figure 3.10: Sea urchin embryo expressing C-CFP-ayNCX$_A$ and C-mCherry-ABCB6, an urchin protein localized in the mitochondria *continued*.

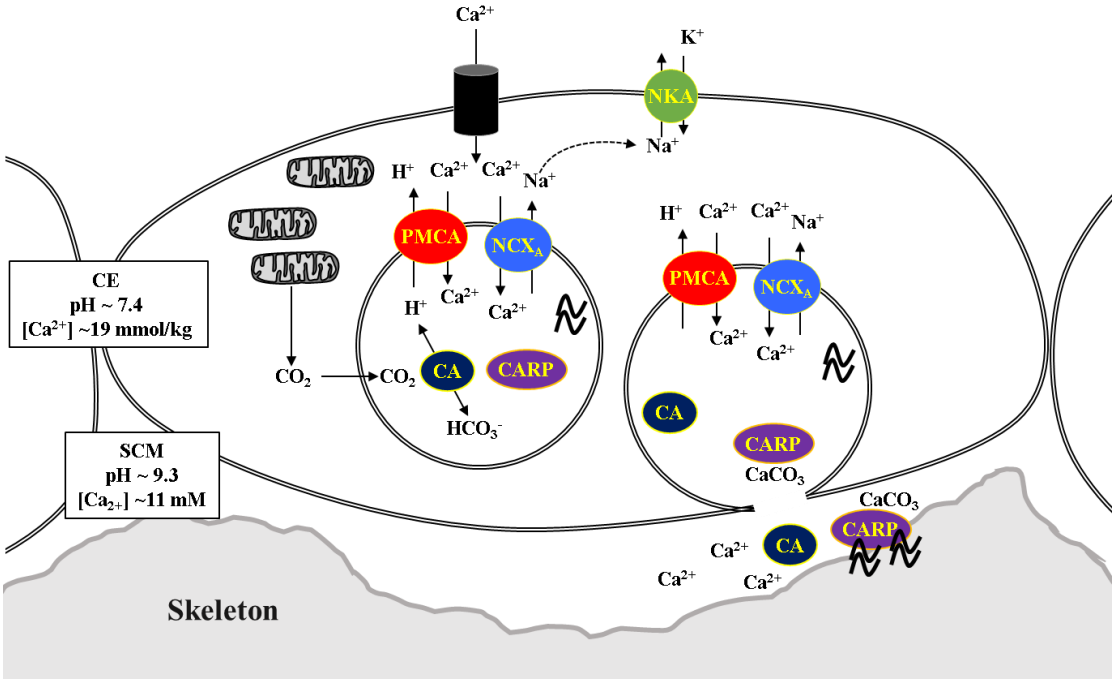

Figure 3.11: Mechanism of Ca^{2+} through a cell from the calicoblastic epithelium. The Ca^{2+}-Channel in the basolateral membrane (black cylinder) moves Ca^{2+} ions into the cell. It enters into vesicles through two transporters: Plasma Membrane Ca^{2+}-ATPase (PMCA) (red oval) and Na^{+}/Ca^{+} Exchanger (NCX) (blue oval). The Na+ that is removed from the vesicle exits the cell via Na^{+}/K^{+}-ATPase (NKA) (green circle) located in the basolateral membrane. The vesicles also contain collagen (curvy lines), Coral Acid-Rich Proteins (CARPs)(purple oval) and Carbonic Anhydrase (CA)(navy oval) (Bertucci et al., 2011; Drake et al., 2013; Mass et al., 2013). The Ca^{2+}-enriched vesicles merge with the apical membrane of the cell and releases Ca^{2+} and contents to the Subcalicoblastic Medium (SCM), where the Ca^{2+} and proteins are incorporated into the skeleton and its organic matrix. pHi of the calicoblastic cell has been determined for the coral *S. pistillata* (Venn et al., 2011) [Ca^{2+}] values within the calicoblastic cell are from G. *fascicularis*, a Complex coral like *A. yongei* (Marshall et al. 2007). pH and [Ca^{2+}] values for the SCM are also from G. *fascicularis* (Al-Horani et al., 2003).

Table 3.1: $NCX_{A/B}$: PCR primers

NCX1 = NCX_A, NCX3 = NCX_B

PCR Primer	Sequence 5' → 3'
NCX1flFWD1	TCTTTAGCTCTAACCGTTCATCG
NCX1flREV1	CTGCTTAAATAACCAGCCCAAAT
NCX1flFWD2	AAGCGACTAACCATGTCCTG
NCX3flFWD1	TTCGTAAGACACACATCCTCTG
NCX3flREV1	AAATAACGCGCAACTTGAGAAA
NCX3flFWD2	CTTGGCGTTCTAGAGAGGTAAAT
Sequencing Primer	**Sequence 5' → 3'**
NCX1seqF1	TCGCTTTATGTCCGCGATAG
NCX1seqF2	GGCTCTCCTAACCTTTCTGTTC
NCX1seqR1	AGGAAGACATTCACGGAGTTG
NCX1flREV2	CAACCCTCGCATACTTAAATTGG
NCX1epFWD1	GAGATGCAGGATATCGAGTATGAA
NCX1epREV1	GCCTGATGTAGCAATATGTTTGT
NCX1epFWD2	GGGCGGTGATCCGAATAATA
NCX1epREV2	CCTGGCCTGATGTAGCAATA
NCX3seqF1	CAAGTGAAAGTGGCAAGACAAG
NCX3seqF2	TCTTTCTCCGTTCTGGCTTAC
NCX3seqF3	GCTTGTAGCTGCCCACATTA
NCX3seqR1	CCGAGTGCAACAAAGGTAATG
NCX3seqR2	GGTCGAACAGACGTCAATACTC
NCX3seqR1a	CCACTTGATTGACGGTGTCTT A
NCX3seqF3a	CAGGATAAACGACACAGCAGATA
NCX3seqF4a	CACACCCACCAACTGTGAATA

Table 3.2: $NCX_{A/B}$: PCR protocols

NCX_A	Primer Pair	Template	Polym.	Cycles
Round 1	NCX1flFWD1/ NCX1flREV1	1x cDNA	Phusion	98° 30s, [98° 10s, 66° 30s, 72° 90s] x35, 72° 10min, 4° hold
Round 2	NCX1flFWD1/ NCX1flREV1	Gel plug	Platinum	94° 60s, [94° 30s, 54° 30s, 72° 180s] x35, 72° 10min, 4° hold
Round 3	NCX1flFWD2/ NCX1flREV1	Gel-pure. PCR band	Platinum	94° 60s, [94° 30s, 54° 30s, 72° 180s] x35, 72° 10min, 4° hold *band was gel-purified and TOPO-TA cloned into PCR2.1 vector
NCX_3				
Round 1	NCX3flFWD1/ NCX3flREV1	1x cDNA	Phusion	98° 30s, [98° 10s, 65° 30s, 72° 90s] x35, 72° 10min, 4° hold
Round 2	NCX3flFWD2/ NCX3flREV1	Gel plug	Platinum	94° 60s, [94° 30s, 54° 30s, 72° 180s] x35, 72° 10min, 4° hold *PCR reaction (4uL) was TOPO-TA cloned into PCR2.1 vector

Table 3.3: NCX_A cloning with fluorescent protein: PCR primers

The underlined portions of sequences align with the Fluorescent Protein-containing plasmid.

PCR Primer	**Sequence 5' → 3'**
N_NCX1_FWD	CGGCGGCATGGACGAGCTGTACAAGATGTCCTGTGTACAAAGGCTGGT
N_NCX1_REV	ACTCACTATAGTTCTAGAGGCTCGACTAAAAGCCTGGCCTGATGTAGC
C_NCX1_FWD	CTACTTGTTCTTTTTGCAGGATCCAATGTCCTGTGTACAAAGGCTGGT
C_NCX1_REV	TGTTATCCTCCTCGCCCTTGCTCACCATAAAGCCTGGCCTGATGTAGC
Sequencing Primer	**Sequence 5' → 3'**
SP6	ATTTAGGTGACACTATAG
FP_FWD	ATGGTGAGCAAGGGCGA
FP_REV	CTTGTACAGCTCGTCCATGC
Plasmid_REV	ATTGGCGCCGCGGCCGCGAATTAAAAAA
MidCerFWD	ACGACGGCAACTACAAGAC
MidCerREV	GTCGTCCTTGAAGAAGATGGT
MidCherryFWD	AGGACGGCGAGTTCATCTA
MidCherryREV	CGCAGCTTCACCTTGTAGAT
NCX1start	ATGTCCTGTGTACAAAGGCTG
NCX1seqR2	TGAGGATGCTTCTGTCGTATTT
NCX1seqF4	GTGGGTACATCATCCTGGAAAG

Table 3.4: NCX_A cloning with fluorescent protein: PCR protocols

Plasmid	**Primer Pair**	**Template**	**Polym.**	**Cycles**
N-FP	N_NCX1_FWD/ N_NCX1_REV	34.7ng/ul plasmid DNA NCX1b9mc11	Phusion	98° 30s, [98° 10s, 69° 30s, 72° 90s] x35, 72° 10min, 4° hold
C-FP	C_NCX1_FWD/ C_NCX1_REV	34.7ng/ul plasmid DNA NCX1b9mc11	Phusion	98° 30s, [98° 10s, 65° 30s, 72° 90s] x35, 72° 10min, 4° hold

References

Akisaka, T., Yamamot, T., & Gay, C. V. (1988). Ultracytochemical Investigation of Calcium-Activated Adenosine Triphosphate (CA++-ATPase) in Chick Tibia, *3*(1), 19–25.

Al-Horani, F. A., Al-Moghrabi, S. M., & de Beer, D. (2003). The mechanism of calcification and its relation to photosynthesis and respiration in the scleractinian coral Galaxea fascicularis. *Marine Biology*, *142*, 419–426. https://doi.org/10.1007/s00227-002-0981-8

Allemand, D., Tambutté, É., Zoccola, D., & Tambutté, S. (2011). *Coral Calcification, Cells to Reefs*. *Coral Reefs: An Ecosystem in Transition*. https://doi.org/10.1007/978-94-007-0114-4

Allison, N., Cohen, I., Finch, A. A., Erez, J., Tudhope, A. W., & Edinburg, I. M. F. (2014). Corals concentrate dissolved inorganic carbon to facilitate calcification. *Nature Communications*, *5*(5741), 1–6. https://doi.org/10.1038/ncomms6741

Barott, K. L., Perez, S. O., Linsmayer, L. B., & Tresguerres, M. (2015a). Differential localization of ion transporters suggests distinct cellular mechanisms for calcification and photosynthesis between two coral species. *American Journal of Physiology - Regulatory, Integrative and Comparative Physiology*, *309*(3), R235–R246. https://doi.org/10.1152/ajpregu.00052.2015

Barott, K. L., & Tresguerres, M. (2015). Immunolocalization of Proteins in Corals: the V-type H+-ATPase Proton Pump. *Bio-Protocol*, *5*(17), 1–10.

Barott, K. L., Venn, A. A., Perez, S. O., Tambutté, S., & Tresguerres, M. (2015b). Coral host cells acidify symbiotic algal microenvironment to promote photosynthesis, *112*(2). https://doi.org/10.1073/pnas.1413483112

Bertucci, A., Tambutté, S., Supuran, C. T., Allemand, D., & Zoccola, D. (2011). A New Coral Carbonic Anhydrase in Stylophora pistillata. *Marine Biotechnology*, *13*, 992–1002. https://doi.org/10.1007/s10126-011-9363-x

Blaustein, M. P., Juhaszova, M., Golovina, V. A., Church, P. J., & Stanley, E. F. (2002). Na/Ca Exchanger and PMCA Localization in Neurons and Strocytes Functional Implications. *Annals of the New York Academy of Science*, *976*, 356–366.

Blaustein, M. P., & Lederer, W. J. (1999). Sodium/Calcium Exchange: Its Physiological Implications. *Physiological Reviews*, *79*(3), 763–854.

Brini, M., & Carafoli, E. (2011). The Plasma Membrane Ca 2 þ ATPase and the Plasma Membrane Sodium Calcium Exchanger Cooperate in the Regulation of Cell Calcium. *Cold Spring Harbor Perspectives in Biology*, *3*(2), a004168.

Campanale, J. P., & Hamdoun, A. (2012). Programmed reduction of ABC transporter activity in sea urchin germline progenitors Programmed reduction of ABC transporter activity in sea urchin germline progenitors. *Development*, *139*, 783–792. https://doi.org/10.1242/dev.098830

Carpenter, K. E., Abrar, M., Aeby, G., Aronson, R. B., Banks, S., Bruckner, A., Chiriboga, A., Cortes, J.., Delbeek, J. C., Devanntier, L., Edgar, G. J., Edwards, A. J., Fenner, D., Guzman,

H. M., Hoeksema, B. W., Hodgson, G., Johan, O., Licuanan, W. Y., Livingstone, S. R., Lovell, E. R., Moore, J. A., Obura, D. O., Ochavillo, D., Polidoro, B. A., Precht, W. F., Quibilan, M. C., Reboton, C., Richards, Z. T., Rogers, A. D., Sanciangco, J., Sheppard, A., Sheppard, C., Smith, J., Stuart, S., Turak, E., Veron, J. E., Wallace, C., Weil, E., Wood, E. (2008). One-Third of Reef-Building Corals Face Elevated Extinction Risk from Climate Change and Local Impacts. *Science*, *321*(580), 560–563. https://doi.org/10.1126/science.1159196

Castillo, K., Delgado, R., & Bacigalupo, J. (2007). Plasma membrane Ca2+-ATPase in the cilia of olfactory receptor neurons: possible role in Ca2+ clearance. *European Journal of Neuroscience*, *26*, 2524–2531. https://doi.org/10.1111/j.1460-9568.2007.05863.x

Clapham, D. E. (2007). Calcium Signaling. *Cell*, *131*(6), 1047–1058. https://doi.org/10.1016/j.cell.2007.11.028

Clode, P. L., & Marshall, A. T. (2002). Low temperature FESEM of the calcifying interface of a scleractinian coral. *Tissue & Cell*, *34*(3), 187–198. https://doi.org/10.1016/S0040-8166(02)00031-9

Cohen, A. L., & McConnaughey, T. A. (2003). Geochemical Perspectives on Coral Mineralization. *Reviews in Mineralogy and Geochemistry*, *54*, 151–187.

Davy, S. K., Allemand, D., & Weis, V. M. (2012). Cell Biology of Cnidarian-Dinoflagellate Symbiosis. *Microbiology and Molecular Biology Reviews*, *76*(2), 229–261. https://doi.org/10.1128/MMBR.05014-11

Dereeper, A., Guignon, V., Blanc, G., Audic, S., Buffet, S., Chevenet, F., Dufayard, J. F., Guindon, S., Lefort, V., Lescot, M., Claverie, J. M., Gascuel, O. (2008). Phylogeny .fr: robust phylogenetic analysis for the non-specialist. *Nucleic Acids Research*, *36*(Web Server Issue), 465–469. https://doi.org/10.1093/nar/gkn180

Dipolo, R., & Beauge, L. (2006). Sodium/Calcium Exchanger: Influence of Metabolic Regulation on Ion Carrier Interactions. *Physiological Reviews*, *86*(1), 155–203. https://doi.org/10.1152/physrev.00018.2005.

Drake, J. L., Mass, T., Haramaty, L., Zelzion, E., Bhattacharya, D., & Falkowski, P. G. (2013). Proteomic analysis of skeletal organic matrix from the stony coral Stylophora pistillata. *Proceedings of National Academy of Science*, *110*(10), 3788–3793. https://doi.org/10.1073/pnas.

Economic Values of Coral Reefs, Mangroves, and Seagrasses, A Global Compilation. (2008). *Conservation International*.

Edgar, R. C. (2004). MUSCLE: multiple sequence alignment with high accuracy and high throughput. *Nucle*, *32*(5), 1792–1797. https://doi.org/10.1093/nar/gkh340

Emanuelsson, O., Nielsen, H., Brunak, S., & von Heijne, G. (2000). Predicting Subcellular Localization of Proteins Based on their N-terminal Amino Acid Sequence. *Journal of Molecular Biology*, *300*, 1005–1016. https://doi.org/10.1006/jmbi.2000.3903

Erez, J. (2003). The Source of Ions for Biomineralization in Foraminifera and Their Implications

for Paleoceanographic Proxies. *Reviews in Mineralogy and Geochemistry*, *54*(1), 115–149. https://doi.org/10.2113/0540115

Gökirmak, T., Campanale, J. P., Shipp, L. E., Moy, G. W., Tao, H., & Hamdoun, A. (2012). Localization and substrate selectivity of sea urchin multidrug (MDR) efflux transporters. *Journal of Biological Chemistry*, *287*(52), 43876–43883. https://doi.org/10.1074/jbc.M112.424879

Gokirmak, T., Shipp, L. E., Campanale, J. P., Nicklisch, S. C. T., & Hamdoun, A. (2014). Transport in technicolor: Mapping ATP-binding cassette transporters in sea urchin embryos. *Molecular Reproduction and Development*, *81*(9), 778–793. https://doi.org/10.1002/mrd.22357.Transport

Hayes, R. L., & Goreau, N. I. (1977). Intracellular crystal-bearing vesicles in the epidermis of scleractinian corals, Astrangia dane (agassiz) and Porites Porites (pallas). *The Biological Bulletin*, *152*, 26–40.

Hoenderop, J. G. J., Nilius, B., & Bindels, R. J. M. (2005). Calcium Absorption Across Epithelia. *Physiological Reviews*, *85*, 373–422. https://doi.org/10.1152/physrev.00003.2004.

Hughes, T. P., Barnes, M. L., Bellwood, D. R., Cinner, J. E., Cumming, G. S., Jackson, J. B. C., Kleypas, J., van de Leemput, I. A., Lough, J. M., Morrison, T. H., Palumbi, S. R., van Nes, E. H., Scheffer, M. (2017). Coral reefs in the Anthropocene. *Nature*, *546*, 82–90. https://doi.org/10.1038/nature22901

Ip, Y. K., Lim, A. L. L., & Lim, R. W. L. (1991). Some properties of calcium-activated adenosine triphosphate from the hermatypic coral Galaxea fascicularis. *Marine Biology*, *111*, 191–197.

Isa, Y. (1986). An electron microscope study on the mineralization of the skeleton of the staghorn coral Acropora hebes. *Marine Biology*, *93*, 91–101.

Iwata, T., Galli, C., Dainese, P., Guerini, D., & Carafoli, E. (1995). The 70 kD component of the heart sarcolemmal preparation is the C-terminal portion of the protein. *Cell Calcium*, *17*, 263–269.

Johnston, I. S. (1980). The Ultrastructure of Skeletogenesis in Hermatypic Corals. *International Review of Cytology*, *67*, 171–214.

Khananshvili, D. (2013). The SLC8 gene family of sodium – calcium exchangers (NCX) – Structure, function, and regulation in health and disease. *Molecular Aspects of Medicine*, *34*(2–3), 220–235. https://doi.org/10.1016/j.mam.2012.07.003

Knowlton, N., Brainard, R. E., Fisher, R., Moews, M., Plaisance, L., & Caley, M. J. (2006). Coral Reef Biodiversity. *Life in the World's Oceans: Diversity, Distribution, and Abundance*, 65–77.

Krieger-brauer, H., & Gratzl, M. (1982). Uptake of Ca2+ by isolated secretory vesicles from adrenal medulla. *Biochimica et Biophysica Acta*, *691*, 61–70.

Krishnamurthy, P. C., Du, G., Fukuda, Y., Sun, D., Sampath, J., Mercer, K. E., Wang, J., Sosa-Pineda, B., Murti, K. G., Schuetz, J. D. (2006). Identification of a mammalian mitochondrial

porphyrin transporter. *Nature*, *443*(October), 3–7. https://doi.org/10.1038/nature05125

Krogh, A., Larsson, B., von Heijne, G., & Sonnhammer, E. L. L. (2001). Predicting Transmembrane Protein Topology with a Hidden Markov Model : Application to Complete Genomes. *Journal of Molecular Biology*, *305*, 567–580. https://doi.org/10.1006/jmbi.2000.4315

Kwon, H. J., Koo, J. H., Zufall, F., Leinders-zufall, T., & Margolis, F. L. (2009). Ca2+ Extrusion by NCX Is Compromised in Olfactory Sensory Neurons of OMP -/- Mice. *Plos One*, *4*(1), e4260. https://doi.org/10.1371/journal.pone.0004260

Lepage, T., & Gache, C. (2004). Expression of Exogenous mRNAs to Study Gene Function in the Sea Urchin Embryo. *Methods in Cell Biology*, *74*, 677–697.

Mackinder, L., Wheeler, G., Schroeder, D., Riebesell, U., Brownlee, C. (2010). Molecular Mechanisms Underlying Calcification in Coccolithophores. *Geomicrobiology Journal*, *27*(6–7), 585–595. https://doi.org/10.1080/01490451003703014

Marschall, Z. Von, Mok, S., Phillips, M. D., Mcknight, D. A., & Fisher, L. W. (2012). Rough Endoplasmic Reticulum Trafficking Errors by Different Classes of Mutant Dentin Sialophosphoprotein (DSPP) Cause Dominant Negative Effects in Both Dentinogenesis Imperfecta and Dentin Dysplasia by Entrapping Normal DSPP. *Journal of Bone and Mineral Research*, *27*(6), 1309–1321. https://doi.org/10.1002/jbmr.1573

Marshall, A. T. (1996). Calcification in hermatypic and ahermatypic corals. *Science*, *271*, 637–639.

Marshall, A. T., Clode, P. L., Russell, R., Prince, K., & Stern, R. (2007). Electron and ion microprobe analysis of calcium distribution and transport in coral tissues. *The Journal of Experimental Biology*, *210*, 2453–2463. https://doi.org/10.1242/jeb.003343

Mass, T., Drake, J. L., Haramaty, L., Kim, J. D., Zelzion, E., & Bhattacharya, D., Falkowski, P. G. (2013). Cloning and Characterization of Four Novel Coral Acid-Rich Proteins that Precipitate Carbonates In Vitro. *Current Biology*, *23*(12), 1126–1131. https://doi.org/10.1016/j.cub.2013.05.007

Mass, T., Drake, J. L., Peters, E. C., Jiang, W., & Falkowski, P. G. (2014). Immunolocalization of skeletal matrix proteins in tissue and mineral of the coral Stylophora pistillata. *Proceedings of the National Academy of Science*, (28), 1–6. https://doi.org/10.1073/pnas.1408621111

Mass, T., Giuffre, A. J., Sun, C. Y., Stifler, C. A., Frazier, M. J., Neder, M., Tamura, N., Stan, C. V., Marcus, M. A., Gilbert, P. U. P. A. (2017). Amorphous calcium carbonate particles form coral skeletons. *Proceedings of National Academy of Science*, (31). https://doi.org/10.1073/pnas.1707890114

On, C., Marshall, C. R., Chen, N., Moyes, C. D., & Tibbits, G. F. (2008). Gene Structure Evolution of the Na+-Ca2+ Exchanger (NCX) Family. *BMC Evolutionary Biology*, *8*(1), 127. https://doi.org/10.1186/1471-2148-8-127

Outka, D. E., & Williams, D. C. (1971). Sequential Coccolith Morphogenesis in Hymenomonas carterae. *Journal of Eukaryotic Microbiology*, *18*(2), 285–297.

Palty, R., Silverman, W. F., Hersh, M., Caporale, T., Sensi, S. L., Parnis, J., Nolte, C., Fishman, D., Shoshan-Barmatz, V., Herrmann, S., Khananshvili, D., Sekler, I. (2010). NCLX is an essential component of mitochondrial. *Proceedings of National Academy of Science*, *107*(1), 436–441. https://doi.org/10.1073/pnas.0908099107

Paterson, J. K., Shukla, S., Black, C. M., Tachiwada, T., Garfield, S., Wincovitch, S., Ernst, D. N., Agadir, A., Li, X., Ambudkar, S. V., Szakacs, G., Akiyama, S., Gottesman, M. M. (2007). Human ABCB6 Localizes to Both the Outer Mitochondrial Membrane and the Plasma Membrane. *Biochemistry*, *46*, 9443–9452. https://doi.org/10.1021/bi700015m

Philipson, K. D., Longoni, S., & Ward, R. (1988). Purification of the cardiac Na+-Ca2+ exchange protein. *Biochimica et Biophysica Acta - Biomembranes*, *945*, 298–306.

Philipson, K. D., & Nicoll, D. A. (2000). Sodium-Calcium Exchange: A Molecular Perspective. *Annual Reviews in Physiology*, *62*, 111–133.

Puverel, S., Tambutté, É., Zoccola, D., Domart-Coulon, I., Bouchot, A., Lotto, S., Allemand, D., Tambutté, S. (2005). Antibodies against the organic matrix in scleractinians : a new tool to study coral biomineralization. *Coral Reefs*, *24*, 149–156. https://doi.org/10.1007/s00338-004-0456-0

Quednau, B. D., Nicoll, D. A., & Philipson, K. D. (2004). The sodium / calcium exchanger family — SLC8. *Pflugers Archive - European Journal of Physiology*, *7943*, 543–548. https://doi.org/10.1007/s00424-003-1065-4

Shinzato, C., Shoguchi, E., Kawashima, T., Hamada, M., Hisata, K., Tanaka, M., Fujie, M., Fujiwara, M., Koyanagi, R., Ikuta, T., Fujiyama, A., Miller, D. J., Satoh, N. (2011). Using the Acropora digitifera genome to understand coral responses to environmental change. *Nature*, *476*(7360), 320–323. https://doi.org/10.1038/nature10249

Sievers, F., Wilm, A., Dineen, D., Gibson, T. J., Karplus, K., Li, W., Lopez, R., McWilliam, H., Remmert, M., Soding, J., Thompson, J.D., Higgins, D. G. (2011). Fast, scalable generation of high-quality protein multiple sequence alignments using Clustal Omega. *Molecular Systems Biology*, *7*(539). https://doi.org/10.1038/msb.2011.75

Sonnhammer, E. L. L., von Heijne, G., & Krogh, A. (1998). A hidden Markov model for predicting transmembrane helices in protein sequences. In *Proceedings of the Sixth International Conference on Intelligent Systems for Molecular Biology* (pp. 175–182).

Sosnoski, D. M., & Gay, C. V. (2008). NCX3 is a major functional isoform of the sodium-calcium exchanger in osteoblasts. *Journal of Cellular Biochemistry*, *103*(4), 1101–1110. https://doi.org/10.1002/jcb.21483

Spurgeon, J. P. G. (1992). The Economic Valuation of Coral Reefs. *Marine Polltution Bulletin*, *24*(11).

Stains, J. P., & Gay, C. V. (1998). Asymmetric Distribution of Functional Sodium-Calcium Exchanger in Primary Osteoblasts, *13*(12), 1862–1869.

Tambutté, É., Allemand, D., Mueller, E., & Jaubert, J. (1996). A compartmental approach to the mechanism of calcification in hermatypic corals. *The Journal of Experimental Biology*, *199*,

1029–1041.

Thirion, S., Troadec, J.-D., Pivovarova, N. B., Pagnotta, S., Andres, S. B., Leapman, R. D., & Nicaise, G. (1999). Stimulus – secretion coupling in neurohypophysial nerve endings: A role for intravesicular sodium? *Proceedings of the National Academy of Science*, *96*(March), 3206–3210.

Tresguerres, M., Barott, K. L., Barron, M. E., Deheyn, D. D., Kline, D. I., & Linsmayer, L. B. (2017). Cell Biology of Reef-Building Corals: Ion Transport, Acid/ Base Regulation, and Energy Metabolism, 193–218. https://doi.org/10.1007/978-3-319-39617-0

Troadec, J.-D., Thirion, S., Laugier, J., & Nicaise, G. (1998). Calcium-induced calcium increase in secretory vesicles of permeabilized rat neurohypophysial nerve terminals. *Biology of the Cell*, *90*, 339–347.

Tsuchida, M., Emi, Y., Kida, Y., & Sakaguchi, M. (2008). Human ABC transporter isoform B6 (ABCB6) localizes primarily in the Golgi apparatus, *369*, 369–375. https://doi.org/10.1016/j.bbrc.2008.02.027

van der Wal, P., de Jong, E. W., Westbroek, P., de Bruijn, W. D., & Mulder-Stapel, A. A. (1983). Polysaccharide Localization , Coccolith Formation , and Golgi Dynamics in the Coccolithophorid Hymenomonas carterae. *Journal of Ultrastructure Research*, *85*, 139–158.

Zoccola, D., Tambutté, E., Kulhanek, E., Puverel, S., Scimeca, J. C., Allemand, D., & Tambutté, S. (2004). Molecular cloning and localization of a PMCA P-type calcium ATPase from the coral Stylophora pistillata. *Biochimica et Biophysica Acta - Biomembranes*, *1663*(1–2), 117–126. https://doi.org/10.1016/j.bbamem.2004.02.010

Zoccola, D., Tambutté, E., Sénégas-Balas, F., Michiels, J.-F., Failla, J.-P., Jaubert, J., & Allemand, D. (1999). Cloning of a calcium channel α1 subunit from the reef-building coral, Stylophora pistillata. *Gene*, *227*(2), 157–167. https://doi.org/10.1016/S0378-1119(98)00602-7

Zutz, A., Gompf, S., Schägger, H., & Tampé, R. (2009). Biochimica et Biophysica Acta Mitochondrial ABC proteins in health and disease. *Biochimica et Biophysica Acta - Bioenergetics*, *1787*(6), 681–690. https://doi.org/10.1016/j.bbabio.2009.02.009

DISCUSSION

Soluble adenylyl cyclase in two coral species

The sequences and localization results for soluble adenylyl cyclase (sAC) in *P. damicornis* and *A. yongei* species show high homology with each other. In terms of alternative splicing, a similar reliance on alternative promoters and exon splicing occurs at the beginning of transcripts, and at least one identified splice variant from each (pdsAC5UTR2 and pdsAC5UTR3 with aysAC5UTR1) are comparable with nearly identical N-terminal amino acid sequences. I obtained a full-length sAC mRNA transcript encoding for a ~212 kDa in *P. damicornis*, and another mRNA transcript encoding for a ~68 kDa protein in *A.* yongei. However, Western blotting reveals that both coral species most abundantly express a ~90 kDa sAC protein, and a complete transcript of this size was not identified in either coral species, although a 3'RACE product that was obtained is predicted to encode a 94 kDa protein. As mentioned previously in Chapters 2 and 3, these discrepancies between the transcripts identified and the proteins recognized by the custom coral sAC antibodies are most likely due to low mRNA abundance.

sAC proteins in both coral species show similar localization patterns. In both *A. yongei* and in *P. damicornis*, sAC is abundantly expressed in the calicoblastic epithelium, suggesting a role in pHi regulation of the calcifying cells. Furthermore, both coral species show sAC expressed through all four tissues, implying sAC is responsible for sensing and regulating pHi in response to acid/base disturbances that are diverse in origin. The HCO_3^--stimulated cAMP production I measured in *A. yongei* is also comparable to HCO_3^--stimulated cAMP production in *P. damicornis*, and these results were published together to emphasize their significance as the highest rates of cAMP production ever recorded in the literature (Barott et al., 2013). Both corals have half maximal stimulation (EC_{50}) at ~10 mM HCO_3^-. However, since cAMP production was measured in homogenized tissues, it is impossible to tease apart the potential contributions of

different sAC splice variants. Still, the similarities in sequence, relative abundance of protein isoforms, localization patterns, and HCO_3^- stimulated activity in these two corals species which diverged ~300-450 million years ago suggests an essential role for sAC in corals and further supports findings across phyla suggesting that sAC is an evolutionarily conserved pH sensor (Buck et al., 1999; Chen et al., 2000).

Soluble adenylyl cyclase and Na^+/Ca^{2+} exchanger

In Chapter 3, I proposed a mechanism for calcification of the coral skeleton that included vesicular transport as the primary method of Ca^{2+} delivery to the subcalicoblastic medium (SCM) (Figure 3.11). These vesicles are predicted to concentrate Ca^{2+} via plasma membrane Ca^{2+}-ATPase (PMCA) and Na^+/Ca^{2+} Exchanger (NCX) localized in the vesicle membrane. By concentrating Ca^{2+} in a subcellular compartment, Ca^{2+} is sequestered from the cytoplasm of the calicoblastic cells where it could otherwise accumulate in toxic concentrations. The process of calcification is most effective in basic pH conditions, and is thus sensitive to changes in pH. However, the link between day/light conditions and observed increases in the rate of calcification has not yet been determined, though presumably it is linked to photosynthetic activity by *Symbiodinium* in nearby gastrodermis tissue.

I propose that sAC could be involved in my calcification mechanism (Chapter 3, Figure 3.11). During the day, photosynthesis would remove CO_2 from the coral's tissues, shifting the carbonate equilibrium equation to increase the $[HCO_3^-]$. A dramatic, ~50x increase in $[HCO_3^-]$ in tissues is observed during the day/light conditions in *S. pistillata.* sAC, which is stimulated by HCO_3^-, would then produce cAMP that could trigger numerous physiological responses. cAMP could activate Protein Kinase A (PKA) to phosphorylate target proteins, resulting in their translocation through the cell. If PKA were to phosphorylate PMCA and increase its abundance

in the proposed Ca^{2+}-concentrating vesicles, the effect on calcification would be two-fold. First, increased PMCA in the vesicle membrane would increase the $[Ca^{2+}]$ in the vesicles and thus increase the $[Ca^{2+}]$ in the SCM post-transport. This would increase the saturation state of aragonite. Second, the simultaneous increase in the rate of H^+ ion removal from the vesicles by PMCA would increase the pH within the vesicle, creating a microdomain containing more basic conditions. If the vesicles also transport dissolved inorganic carbon as predicted by our mechanism, removal of H^+ ions would result in increased conversion of CO_2 (that has passively diffused into the vesicle) into HCO_3^- by carbonic anhydrase (CA). HCO_3^- and CO_3^{2-} could then begin forming amorphous $CaCO_3$ crystals, aided by the coral acid-rich proteins (CARPS) also predicted to be present in the vesicles, while the vesicle moves across the cell. In this modified mechanism, sAC is the link between photosynthesis and light-enhanced calcification.

Limitations of working with corals

As mentioned briefly in the discussion sections of Chapters 1 and 2, sAC mRNAs in animals are generally low in abundance except in the testes (Buck et al., 1999; Geng et al., 2005; Tresguerres et al 2010). However, all RNA extractions in corals were improved by scaling up the total RNA extraction protocol to use at least 10 ml of Trizol Reagent, so successfully obtaining enough RNA from gametes would require access to a large number of spawning corals. RNA extractions could also use samples from tissues during different times during the day (RNA extractions were never performed at night or in the dark) or even during different seasons. Since sAC senses and regulates pH, corals could also be exposed experimentally to more acidic or alkaline sea water for acute or extended exposures before performing the RNA extraction, to see if changes in pHe potentially increase the abundance of any specific sAC transcripts. However, it would be unsurprising if there was no change in mRNA abundance, as sAC mRNA expression

does not seem to change in response to acid/base stress. Perhaps one or all of these additional experiments could prove successful in generating cDNA containing the transcript encoding the 94 kDa indicated by Western blotting techniques.

Another difficult aspect of studying cell biology in corals is tight association of all four coral tissues and their proximity to the calcium carbonate skeleton. While it is possible, through centrifugation, to enrich samples for a particular cell type (gastrodermal cells for example), there will always be at least some contamination. Minimal contamination may be acceptable for protein work or some enzymatic activity assays, but complicates attempts at studying tissue-specific RNA expression. Instead, localizing sAC proteins to specific tissues is best achieved by immunofluorescence microscopy. Even then, these types of studies are not straightforward in coral: they have endogenous green fluorescent protein, which limits the use of green secondary antibodies, and chlorophyll in the symbiotic algae have red auto-fluorescence. Those endogenous florescence signals sometimes make it difficult to identify the signal from the primary antibody and fluorescently-labeled secondary antibodies. However, those limitations can be overcome by optimizing specificity and strength of the primary antibody to achieve an acceptable signal-to-noise ratio.

The subcellular localization of proteins in coral tissues is relatively easy to identify in the three upper most coral tissue layers: the oral ectodermis, oral gastrodermis, and aboral gastrodermis. However, due to the thin shape and "stacked" nature of the calicoblastic cells that make up the calicoblastic epithelium, it is very difficult to identify individual cells and cell membranes. Furthermore, distinguishing between the apical and basolateral membrane in calicoblastic cells is only possible in sections that have been sliced at a specific angle (these sections are obtained by luck). Attempts at improving resolution by using transmission electron microscopy have not been successful for the calicoblastic epithelium because preservation of

ultrastructural features requires a harsh fixation protocol that affects the epitopes on proteins, making them unrecognizable by the antibodies. Conversely, milder fixation protocols maintain antigenicity but do not preserve the ultrastructure of the calicoblastic epithelium.

My inability to confidently determine the subcellular localization of NCX protein in coral calicoblastic epithelium is what prompted the experiments expressing recombinant coral sAC in sea urchin embryos. While these experiments provided very helpful information about protein targeting to a specific subcellular localization (vesicles), the results alone cannot be used to make assumptions about the physiological roles of the protein in corals. Similarly, colocalization techniques in coral tissue, which are useful for proposing pathways and microdomains, if created in sea urchins by injections with multiple mRNAs, may not accurately reflect the relationship between coral proteins in their native tissue.

Final thoughts

Despite these limitations and the difficulties in working with corals, research investigating coral cell biology and physiology is improving. A growing number of genomic and transcriptomic data bases are becoming available, facilitating molecular techniques like RT-PCR and fluorescent *in situ* hybridization and epitope selection for designing custom antibodies. As research techniques in corals are optimized and shared, the types of experiments that can be performed in corals will expand as well. The research contained in this dissertation makes a significant contribution to our current understanding of cellular and molecular mechanisms for acid/base sensing and calcification in corals.

References

Barott, K. L., Helman, Y., Haramaty, L., Barron, M. E., Hess, K. C., Buck, J., Levin, L. R., Tresguerres, M. (2013). High adenylyl cylcase activity and in vivo cAMP fluctuations in corals suggest central physiological role. *Scientific Reports*, *3*(1379). https://doi.org/10.1038/srep01379

Buck, J., Sinclair, M. L., Schapal, L., Cann, M. J., & Levin, L. R. (1999). Cytosolic adenylyl cyclase defines a unique signaling molecule in mammals. *Proceedings of the National Academy of Sciences of the United States of America*, *96*(1), 79–84.

Chen, Y., Cann, M. J., Litvin, T. N., Iourgenko, V., Sinclair, M. L., Levin, L. R., & Buck, J. (2000). Soluble adenylyl cyclase as an evolutionarily conserved bicarbonate sensor. *Science (New York, N.Y.)*, *289*(5479), 625–8.

Geng, W., Wang, Z., Zhang, J., Reed, B. Y., Pak, C. Y. C., & Moe, O. W. (2005). Cloning and characterization of the human soluble adenylyl cyclase. *American Journal of Physiology Cell Physiology*, *288*, 1305–1316. https://doi.org/10.1152/ajpcell.00584.2004.